INVESTIGATING GROUNDWATER AND SURFACE WATER INTERACTIONS IN THE UTHUKELA CATCHMENT, KWAZULU-NATAL, SOUTH AFRICA

By

MUTONDI TSHIKORORO

Submitted in fulfilment of the requirements of

Master of Science

in Hydrology

Centre of Water Resources Research

School of Agriculture, Earth, and Environmental Sciences

University of KwaZulu-Natal

Pietermaritzburg

South Africa

05 February 2025

Supervisor: Prof. S Kebede Gurmessa

PREFACE

The research contained in this dissertation/thesis was completed by the candidate while based in the Discipline of Hydrology, School of Agricultural, Earth and Environmental Sciences of the College of Agriculture, Engineering and Science, University of KwaZulu-Natal, Pietermaritzburg, South Africa. The research was financially supported by the Water Research Commission (WRC).

The contents of this work have not been submitted in any form to another university, and except where the work of others is acknowledged in the text, the results reported are due to investigations by the candidate.

Signed: Supervisor

Date: 05 February 2025

DECLARATION PLAGIARISM

I, Tshikororo Mutondi, declare that:

(i) The research reported in this thesis, except where otherwise indicated or acknowledged, is my original work;

(ii) This thesis has not been submitted in full or in part for any degree or examination to any other university;

(iii) This thesis does not contain other persons' data, pictures, graphs or other information unless specifically acknowledged as being sourced from other persons;

(iv) This thesis does not contain other persons' writing unless specifically acknowledged as being sourced from other researchers. Where other written sources have been quoted, then:

a) Their words have been re-written, but the general information attributed to them has been referenced;

b) There their exact words have been used, their writing has been placed inside quotation marks, and referenced;

(v) Where I have used material for which publications followed, I have indicated in detail my role in the work;

(vi) This thesis is primarily a collection of material prepared by myself, published as journal articles, or presented as a poster or oral presentation at conferences. In some cases, additional material has been included;

(vii) This thesis does not contain text, graphics or tables copied and pasted from the Internet, unless specifically acknowledged, and the source being detailed in the thesis and in the References sections.

Signed:……...

Date: 05/02/2025

Supervisor:……

Date 05/02/2025

ABSTRACT

Groundwater-surface water (GW-SW) interactions are not fully explored in South Africa. This study investigated the interaction between GW-SW in the uThukela Catchment, located in KwaZulu Natal, South Africa. Understanding the complex interactions of the GW-SW is very important for water resources and water quality management, thus making it essential to investigate the factors that control these interactions. The widely referred factors include topography, geology (lineament and dykes), climate and land use.

The research employed stable isotopes of oxygen-18 ($\delta^{18}O$) and deuterium ($\delta^{2}H$), piezometric analysis, baseflow analysis, in situ measurements of radioactive radon isotope (^{222}Rn), and hydrochemical parameter of Temperature, pH and electrical conductivity (EC). Rainfall $\delta^{18}O$ and $\delta^{2}H$ were sampled across altitudinal transect and precipiation gradient at five locations; Catchment 6 (1921 masl, 1273 mm), Mike Pass (1621 masl, 1236 mm), Winterton (1103 masl, 833 mm), Pietermarzitburg (627 masl, 825 mm), and Eshowe (522 masl, 800 mm). The $\delta^{18}O$ and $\delta^{2}H$ revealed a weak altitude effect limiting its use to trace regional scale movement of groundwaters.The role of groundwater was investigated across three spatial scales: hillslope, catchment, and regional. A total of 470 samples were collected and analysed during the dry and wet seasons. These included 39 groundwater samples, 28 wetland samples, 363 surface water samples, and 40 spring samples. At the hillslope scale, stable isotope data and EC measurements indicate that groundwater plays a dominant role in runoff generation both during rainfall events and periods of no rainfall. At the catchment scale, stable isotopes and EC measurements shows mountain front aquifers are recharged from losing streams. Additionally, at the regional scale, ^{222}Rn and baseflow analysis indicate substantial groundwater contributions to streamflow in the upper uThukela Catchment. However, there is no clear evidence of deep regional groundwater flow.

.**Keywords: ^{222}Rn, baseflow, hydrochemistry, nested scale, piezometric analysis, stable water isotopes, and uThukela Catchment**

ACKNOWLEDGMENTS

First and foremost, I would like to express my heartfelt gratitude to Almighty God, who made it possible for me to complete my Master's degree in just one year and six months. Indeed, it is through His favour and grace that all things are possible.

I would like to extend my deepest thanks to my late aunt, Mrs Ntavhanyeni Magret Muthelo, whose inspiration and motivation instilled in me the importance of perseverance. She always reminded me that education is the key to unlocking a world of opportunities in life. Her memory lives on in my heart.

I am also grateful to the Water Research Commission (WRC) for funding this research. Their support enabled me to travel and collect data that was crucial for my work.

I would like to acknowledge the South African Environmental Observation Network (SAEON) and Mr. Ross Stockil from Glen Farm, whose contributions to the sampling process were invaluable.

My sincere appreciation goes to my supervisor, Prof. Seifu Kebede. This research would not have been possible without his insightful guidance and unwavering support. I am particularly grateful for the skills and knowledge he imparted to me and for his patience throughout this journey.

I would also like to thank Mr. Vivek Naiken for his technical guidance and for teaching me essential skills I applied in my research.

A special thanks to Ms Thobeka Mpungose and Mr Thabang Phori for their assistance and for sharing their expertise in this field. Their support was instrumental in helping me navigate this research, and I am truly grateful.

I would also like to express my appreciation to the Centre of Water Resource Research staff and students. Their contributions were highly valued.

Lastly, I would like to acknowledge my grandmother, mother, and sisters for their unwavering support and prayers. Your encouragement has meant the world to me.

TABLE OF CONTENTS

PREFACE ii

DECLARATION PLAGIARISM iii

ABSTRACT i

ACKNOWLEDGMENTS ii

ABBREVIATIONS, ACRONYMS AND UNITS viii

LIST OF TABLES x

LIST OF FIGURES xi

1. CHAPTER ONE: INTRODUCTION AND BACKGROUND 1

1.1 Introduction 1

1.2 Background of the study 3

1.3 Research aim and objectives 5

1.4 Significance of study 5

1.5 Thesis structure 5

2. CHAPTER TWO: LITERATURE REVIEW 8

2.1 Introduction 8

2.2 Stable isotopes 9

2.2.1 Rainfall isotopic characteristics 10

2.2.1.1 Amount effect 11

2.2.1.2 Altitude effect 11

2.2.1.3 Seasonality effect 12

2.2.1.4 Continentality effect 14

2.2.1.5 Interannual variation 14

2.2.2 Meteoric water line 14

2.2.3 Deuterium excess 16
2.2.4 Isotopic composition of surface water 17
2.2.5 Isotopic composition of groundwater 17
2.2.2 Case studies: Stable isotope use in South Africa 18
2.3. Factors affecting the connection of GW-SW interactions. 21
2.3.1 Geology 21
2.3.1.1 Lithology 21
2.3.1.2 Lineaments 22
2.3.1.3 Dykes 22
2.3.2 Topography 23
2.3.3 Land use 23
2.4 Groundwater recharge, discharge and lateral groundwater flow 24
2.4.1 Groundwater recharge 24
2.4.2 Groundwater discharge 25
2.4.3 Lateral groundwater flow 26
2.5 Contributions of extreme rainfall patterns in groundwater recharge 27
2.5.1 El Nino Southern Oscillation 28
2.5.2 Tropical storms 28
2.6 Subsurface path flows 29
2.6.1 Overland flow 29
2.6.2 Subsurface lateral flow 30
2.6.3 Bedrock flow 31
2.7 Case studies of GW-SW interaction at a global scale 31
2.8 Case studies of GW-SW interaction in South Africa 34

2.9 Synthesis of literature 39
3. CHAPTER THREE: DESCRIPTION OF THE STUDY AREA 42
3.1 Introduction 42
3.2 Location of study area 42
3.3 Geology 43
3.4 Lineaments 45
3.5 Topography 46
3.6 Rainfall 47
3.7 Climate 48
3.8 Land use 48
4. CHAPTER FOUR: MATERIALS AND METHODS 50
4.1 Introduction 50
4.2 Sampling procedure and analysis 50
4.2.1 Field sampling 50
4.2.2 Rainwater collection 52
4.2.3 Event-based sampling 54
4.1.2 Stable isotopes 55
4.1.3 Stable isotope data analysis 56
4.1.4 Radon 58
4.1.5 Radon analysis 59
4.1.4 Hydrochemistry 60
4.1.5 Baseflow separation 60
4.1.6 Piezoemtric analysis 61
5. CHAPTER 5: RESULTS 63

5.1 Introduction 63

5.2 Rainfall isotopic composition 63

5.2.1 D-excess 64

5.2.2 Local Meteoric Water Line (LMWL) 65

5.2.3 Rainfall Isotope Effects 66

5.2.3.1 Amount effect 66

5.2.3.2 Altitude effect 70

5.2.3.3 Continentality effect 71

5.2.3.4 Seasonality effect 72

5.3 GW-SW interaction at multiple scales 73

5.3.1 Regional scale 73

5.3.1.1 Radon 73

5.3.1.2 Baseflow separation 74

5.1.3.3 Piezometric analysis 75

5.1.3.4 Isotope composition (δ^2H and $\delta^{18}O$) for regional-scale groundwater and surface water 76

5.3.2 Catchment scale 77

5.3.2.1 Isotope composition of δ^2H and $\delta^{18}O$ for Winterton rainfall and mountain valley boreholes and streams. 77

5.3.2.2 Electrical conductivity of boreholes and rivers in the Mountain valley 78

5.3.3 Hillslope scale 80

5.3.3.1 EC comparison for seven catchments at Cathedral Peak 80

5.3.3.2 EC comparison of dry and wet seasons at the seven catchments 85

5.3.3.3 $\delta^{18}O$ comparison for seven catchments at Cathedral Peak 85

5.3.3.4 Isotope comparison of δ^2H and $\delta^{18}O$ for Cathedral Peak 90

5.3.3.5 Isotope comparison of δ^2H and $\delta^{18}O$ for catchment 6,7 and 9 during dry and wet season 91

5.3.3.6 Catchment 6 event-based sampling EC 92

5.3.3.7 Catchment 6 event-based sampling for δ^2H and $\delta^{18}O$ 94

5.3.3.8 Catchment 6 second event-based sampling (EC) 95

5.3.3.9 Catchment 6 second event-based sampling (δ^2H and $\delta^{18}O$) 97

6. CHAPTER 6: DISCUSSION 99

6.1 Introduction 99

6.2.1 Characterising rainfall isotope signals 99

6.2.2 GW-SW interactions 103

6.2.2.1 Regional scale 103

6.2.2.2 Catchment scale 104

6.2.2.3 Hillslope scale 106

6.2.2.4 Conceptual model 111

7. CHAPTER 7: CONCLUSION AND RECOMMENDATIONS 113

7.1 Conclusion 113

7.2 Recommendations 114

8. REFERENCES 116

ABBREVIATIONS, ACRONYMS AND UNITS

^{222}Rn	222-Radon
^{14}C	Carbon-14
cm	Centimeter
Cl^-	Chloride Ion
°	Degrees
δ	Delta
δ^2H	Delta Deuterium
$\delta^{18}O$	Delta Oxygen-18
δ^3H	Delta Tritium
DWS	Department Of Water And Sanitation
^2H	Deuterium
d-excess	Deuterium Excess
EC	Electrical Conductivity
Fe^{2+}	Ferrous Ion
GMWL	Global Meteoric Water Line
GW-SW	Groundwater-Surface Water
GW and SW	Groundwater and Surface Water
ITCZ	Inter Tropical Convergence Zone
IAEA	International Atomic Energy Agency
IAE	Inverse Altitude Effect
km	Kilometre
LULC	Land Use/Land Cover

Lat	Latitude
L	Litres
LMWL	Local Meteoric Water Line
Long	Longitude
MAP	Mean Annual Precipitation
masl	Meters Above Sea Level
µS/cm	Micro Siemens Per Centimeter
mL	Millilitres
mm	Millimetre
n	Number Of Samples
^{16}O	Oxygen-16
^{17}O	Oxygen-17
^{18}O	Oxygen-18
‰	Per Mill
%	Percentage
^{1}H	Protoium
Na^{+}	Sodium Ion
^{3}H	Tritium
UCT	University Of Cape Town
VSMOW	Vienna Standard Mean Ocean Water

LIST OF TABLES

Table 2.1: Summary of case studies on stable isotopes in South Africa 19

Table 2.2: Case studies of GW-SW interaction at a global scale 33

Table 2.3: Case studies of GW-SW interaction in South Africa 36

Table 5.1: Summary of rainfall isotope data from five sampling stations 63

Table 5.2: Minimum, maximum and mean values for d-excess for five different stations in the uThukela Catchment 64

LIST OF FIGURES

Figure 2.1: Altitude effect on precipitation for the eastern slopes of the Andes Mountain range (Vogel et al., 1975; Samie, 2020). 12

Figure 2.2: Seasonal influence on the $\delta^{18}O$ and $\delta^{2}H$ relation for average monthly precipitation in the northern hemisphere (data from the GNIP network) (Samie, 2020). 13

Figure 2.3: Meteoric water Line (Zega et al., 2020) 16

Figure 2.4: Lateral groundwater flow (Kebede, 2023) 27

Figure 3.1: Location of study area 42

Figure 3.2: Geological map of the uThukela Catchment (source: Council for Geoscience) 43

Figure 3.3: Lineaments of uThukela Catchment (source: Council for Geoscience) 45

Figure 3.4: Topography of uThukela Catchment (source: Shuttle Radar Tropical Mission (STRM) 90m) 46

Figure 3.5: Mean Annual Precipitation for uThukela Catchment (source: Pegram DVD Backup. (2024). Retrieved from \pmb-cloud10\data\TRANSFER\Richard\Pegram_DVD) 47

Figure 3.6: LULC in uThukela Catchment (source: South African National Land Cover (SANLC) 2018) 48

Figure 4.1: Field sampling map 50

Figure 4.2: Installed rainfall stations at uThukela Catchment (source: STRM 90m) 52

Figure 4.3: Palmex Rain Sampler (RS-1D) 53

Figure 4.4: Event-based sampling points 54

Figure 4.5: Isco Sampler 55

Figure 4.6: Isotope analysing equipment 58

Figure 4.7: Big bottle system set up (Durridge Company Inc, 2022) 59

Figure 4.8: Drainage station for baseflow separation 61

Figure 4.9: Monitoring boreholes and weather stations used for piezometric analysis 62

Figure 5.1: LMWL for all 5 stations and the GMWL 66

Figure 5.2: Amount effect for all five stations: (a) Winterton, (b) Eshowe, (c) Mike Pass, (d) Catchment 6, (e) Pietermaritzburg 69

Figure 5.3: Change in $\delta^{18}O$ with elevation 70

Figure 5.4: $\delta^{18}O$ vs Distance from the coast 72

Figure 5.5: Seasonal variation of d-excess of Pietermaritzburg for three years (March 2022 to January 2024) 72

Figure 5.6: uThukela ^{222}Rn Concentration in Bq/m^3 74

Figure 5.7: BFI index for uThukela 75

Figure 5.8: Monthly time series of groundwater level vs daily rainfall for selected boreholes 76

Figure 5.9: δ^2H and $\delta^{18}O$ for Mike Pass LMWL, Shu Shu thermal springs and uThukela surface water 77

Figure 5.10: Winterton LMWL, Mike Pass LMWL, and δ^2H and $\delta^{18}O$ for boreholes and streams at the Mountain valley 78

Figure 5.11: Illustrates EC measurements of boreholes and streams in the Mountain Valley during dry and wet season 79

Figure 5.12: Comparison of EC between upstream and downstream of catchments 2,3,4,5,6,7 and 9 84

Figure 5.13: EC of Cathedral Peak catchments dry and wet season 85

Figure 5.14: Comparison of $\delta^{18}O$ upstream and downstream of catchment 2,3,4,5,6,7 and 9 89

Figure 5.15: δ^2H and $\delta^{18}O$ for Cathedral Peak from February 2022 to July 2024 90

Figure 5.16: Isotope comparison of the wet and dry seasons for catchment 6,7 and 9 92

Figure 5.17: EC for event-based sampling at Catchment 6 from the 12 to 14 Dec 93

Figure 5.18: Isotope composition for event-based sampling at catchment 6 from 12 to 14 December 95

Figure 5.19: EC for event-based sampling at Catchment 6 from 11 to 12 April 96

Figure 5.20: Isotope composition for event-based sampling at Catchment 6 (April 11-12, 2024) 98

Figure 6.1: Air moisture trajectory of the uThukela 101

Figure 6.2: Image showing the landscape of the catchment scale (source: Google Earth Pro) 106

Figure 6.3: Landscape terrain of catchment 3 (source: Google Earth Pro) 107

Figure 6.4: Catchment 6 and 7 plateau (source: Google Earth Pro) 108

Figure 6.5: Schematic diagram of groundwater ridging in hillslope riparian zone (Zang et al., 2018) 109

Figure 6.6: GW-SW interaction at Catchment 6, shaded numbers are EC (µS/cm) collected on the 12th of December 2023. 110

Figure 6.7: Conceptual Model of GW-SW interactions at uThukela Catchment 112

CHAPTER ONE: INTRODUCTION AND BACKGROUND

1.1 Introduction

In recent years, there has been a shift in understanding of GW-SW interactions; they have both been considered separate entities and have been investigated individually. The physical, chemical, and biological properties of surface water and groundwater are indeed different, but both surface water and groundwater should be considered a single resource as surface water is hydraulically connected to groundwater (Sophocleous, 2002; Bertrand *et al.*, 2014). Surface water bodies are integral parts of groundwater flow systems; the interactions of streams, lakes and wetlands with groundwater are mainly governed by the positions of the surface water bodies with respect to groundwater flow systems, geological properties and their climatic settings (Sophocleous, 2002). The relationship between groundwater and surface water (GW and SW) interactions is strongly influenced by the elevation of the water table relative to the elevation of the stream's bed (Baker *et al.*, 2000). Streams, lakes, and wetlands can gain water from groundwater, lose water to groundwater, or engage in both processes at different sites and different seasons of the year.

To fully understand the interaction between GW-SW, factors such as topography, land use, linameants, dykes geology, and climate must be examined. Climate change influences processes in the hydrological cycle, influencing the interaction of GW-SW both indirectly and indirectly. It influences deeper percolation, soil infiltration and mostly groundwater recharge (Banerjee and Ganguly, 2023). Climate change is known to alter various components of the hydrological cycle, including temperature, precipitation intensity, seasonality, and evapotranspiration (Trenberth, 1999). In some regions, climate change has been associated with increased rainfall intensity or total rainfall, which can enhance groundwater recharge where geological and land use conditions permit (Mileham *et al.*, 2009; Owuor *et al.*, 2016). Increased temperatures result in higher evaporative demand over land, which limits the amount of water available to replenish groundwater (Hughes *et al.*, 2021). Increased variability in precipitation, temperature, and evapotranspiration projected under various climate change scenarios can affect groundwater recharge and storage, as well as alter the mechanisms and seasonality of GW–SW interactions and groundwater quality (Green, 2016; Costa *et al.*, 2021).

Identifying the locations and understanding the directions of GW-SW interactions is vital for effective environmental and water management. Water and chemicals are constantly being exchanged between the surface and subsurface of the land (Hemond and Fechner, 2022). Groundwater discharges into the surface, providing baseflow for streams, while surface water seeps into the ground and recharges the aquifer. The exchange of water and chemicals between GW-SW affects their quality and quantity, making it essential to assess these interactions. Understanding the interactions between GW-SW is essential for managing issues related to water resources, such as the combined utilisation of GW-SW resources, the evaluation and control of surface water contamination caused by groundwater and vice versa, and the assessment and mitigation of losses and delays in the release of water from surface water resources (Winter, 2000; Khan and Khan, 2019).

Several approaches are available to determine the mechanism of GW-SW interactions. These approaches include; pumping test (Zhu *et al.*, 2020), heat tracer method (Kalbus *et al.*, 2006), incremental streamflow (Huntington and Niswonger, 2012), and environmental isotopes (Baskaran *et al.*, 2009). Furthermore, environmental isotopes (stable and radioactive) in conjunction with conventional hydrochemistry (Liu and Yamanaka, 2012), baseflow separation (Partington *et al.*, 2012) and piezometric analysis (Kebede *et al.*, 2017) have been used in several studies. According to Paces and Wurster (2014), stable isotopes such as $\delta^{2}H$ and $\delta^{18}O$ can be used to provide an estimate of recharge by tracing the origin, pathway, and behaviour of water. Additionally, Vreča and Kern (2020) stated that $\delta^{2}H$ and $\delta^{18}O$ are ideal tracers to provide insight into GW-SW interaction because the components of water molecules remain unchanged except in situations of water phase shift or isotopic fractionation in the hydrological cycle. The difference between the isotopic composition of water molecules in different water bodies, such as wetlands, streams, rainfall, and groundwater can be used to quantify the interaction between GW-SW. In other studies, GW-SW interactions have been assessed using radioactive isotopes such as ^{222}Rn (Qin *et al.*, 2021; Peel *et al.*, 2022; Li *et al.*, 2023). Radon is a gas used as a tracer to assess groundwater discharge. Radon concentration is more present in groundwater than in surface water because of its production in rocks but not in water (Skeppström and Olofsson, 2007). Since radon concentration is higher in groundwater than in surface water, the detection of radon concentration in surface water can be used to assess and quantify GW-SW exchange (Peel *et al.*, 2022).

A study in New Zealand by Guggenmos *et al.* (2011) assessed GW-SW interactions by using hydrochemistry (Electric conductivity (EC), temperature, pH, total dissolved solids (TDS)), the method assumed that a change in one or any of the parameters in a pathway of surface water is caused by the interaction with groundwater. Moreover, Baalousha (2016) demonstrated that baseflow separation depicts groundwater discharge into streams, which is useful in assessing groundwater contribution to streamflow.

1.2 Background of the study

The uThukela River is located in South Africa in the province of KwaZulu-Natal. It is the largest river in the province and one of the most significant rivers in the country. Stretching approximately 502 kilometers, with many of its tributaries originating from the Mont-aux-Sources of the Drakensberg Mountains and flowing toward the Indian Ocean, the uThukela River plays an important role for rural and urban communities within its boundaries (PLAN, 2015). The river provides water for irrigation in the agricultural sector to help farmers sustain crops and their livelihood. Additionally, the uThukela River serves as a water source for various industries in the uThukela Catchment, including food processing, tyre production, and textile in Ladysmith. Moreover, the uThukela River is crucial in maintaining the ecological balance of the uThukela Catchment and its surrounding areas. Therefore, the uThukela River plays a significant role in South Africa's economy.

Few hydrological studies have been done on the uThukela catchment. The studies highlighted that the uThukela Catchment is a basin under water stress in terms of quantity and quality. For example, a study by Ntanganedzeni *et al.* (2018) illustrated that geochemical processes have led to the degradation of groundwater quality in the uThukela catchment, especially in the coastal and river regions. UMgeni-UThukela Water (2021) indicated that since 2018-2021 uThukela River has been showing unsatisfactory water quality results. The Cathedral Peak, located in the Northern Drakensberg within the uThukela Catchment, plays a vital role as a water source for the uThukela River. The Cathedral Peak comprises of ten instrumented catchments, with the Cathedral Peak research catchments offering an ideal setting for various research initiatives. These catchments are highly instrumented, with discharge-measuring weirs, eddy covariance towers, cosmic ray probes, and piezometers that were installed in the late 1940s and 1950s (Toucher *et al.*, 2020). Their

remote, high-altitude location and long historical record make them ideal for long-term monitoring and research. The Cathedral Peak research catchments provide valuable insights into various aspects of research. For instance, a study conducted by Kuenene *et al.* (2013) provided insight into the relationship between soil properties and soil water regime in the Cathedral Peak VI catchment. Another study by Harrison *et al.* (2022) provided insights into the significance of Cathedral Peak's soil and geology in generating groundwater and affecting streamflow. Previous research in the uThukela Catchment has mostly focused on rainfall patterns (Chabalala *et al.*, 2019), groundwater recharge (Ndlovu and Demlie, 2018), and water quality (Wade *et al.*, 2021), with little attention focused on GW-SW interaction in this catchment.

Therefore, there is a significant gap in knowledge on the interaction of these entities. To address this significant gap, this study used different techniques, such as environmental tracers (δ^2H, $\delta^{18}O$, ^{222}Rn, and hydrochemistry), baseflow and piezometric analysis to investigate the origin, interaction, and movement of water within the uThukela Catchment. Through the use of the techniques mentioned above, this study aims to gain a comprehensive understanding of the role of groundwater in three spatial scales: hillslope, catchment and regional scale. At the hillslope scale, samples were collected from Cathedral Peak at the nine catchments to understand the role of groundwater in streamflow generation. At the catchment scale, the investigation centred on the role of intermediate groundwater flow in recharging mountain valley aquifers, which originates from the mountains and discharges into the valleys. At the regional scale, the study examined the role of regional groundwater flow and groundwater discharging into the stream networks along the uThukela Catchment.

This focus is crucial because the role of groundwater in streamflow generation has been under-investigated in this area. Additionally, this investigation aims to determine the role of groundwater in the catchment's water balance. This is significant because the water balance of a catchment is a crucial element of its overall hydrological system, and understanding groundwater's contribution to this balance is vital for effective water resource management. Additionally, a conceptual model of GW-SW interaction has been developed, considering key factors that influence these interactions, such as geology, climate, topography, lineaments, dykes, and land use. This model facilitates the interpretation and understanding of groundwater's role in the recharge and discharge processes within the hydrological system.

1.3 Research aim and objectives

This research aims to develop a conceptual model of GW-SW interactions in the uThukela Catchment.

The Specific objectives are:

- To characterise rainfall isotopes
- To assess the connection between GW and SW (locating recharge and discharge) along the uThukela River by assessing the role of geology (lithology, dykes and lineamnets), topography, and land use.
- To identify the mechanism of groundwater discharge in the uThukela River.

1.4 Significance of study

Geology, topography, vegetation, and lithology play an important role in controlling the interaction of GW-SW because all these factors directly and indirectly influence the recharge and discharge of GW-SW regimes. While the influence of geology, topography, vegetation, and lithology on GW-SW interaction is well documented globally, limited research has explored how these factors influence such interactions within the unique hydrogeological context of the uThukela Catchment in South Africa. Therefore, this study is significant in that:

- Conceptual model shall serve as the basis for future numerical model development.
- The understanding of GW–SW interaction will serve as a foundation for evaluating the vulnerability of surface water systems under the impacts of future climate change and anthropogenic activities.

1.5 Thesis structure

Chapter 1

This chapter presents an introduction to the proposal. It provides an overview of the mechanisms contributing to GW-SW interactions, such as geology, topography, and climate. It also highlights a gap in knowledge on GW-SW interactions in South Africa. It also gives an overview of the various techniques used in previous studies to investigate the movement, recharge, and discharge of water between GW-SW. This chapter also contains the study's aim, objectives, and significance.

Chapter 2

This chapter synthesises previous global and local studies on the interactions GW-SW. It presents a detailed overview of the isotopic characteristics of rainfall and examines how these isotopic compositions vary in relation to rainfall effects. Additionally, it discusses various mechanisms and characteristics influencing the discharge and recharge of GW-SW, including geological features, topography, lineaments, dykes, and land use practices.

Furthermore, the chapter elaborates on groundwater recharge and discharge processes, detailing the dynamics of groundwater movement. It highlights the mechanisms affecting groundwater recharge, such as the El Niño Southern Oscillation and tropical cyclones. The chapter also addresses the movement of groundwater and the hydrological dynamics of hillslopes. Lastly, it provides a comprehensive synthesis of the existing literature on these topics.

Chapter 3

This chapter presents the description of the study site, geology, climate, dykes, lineaments, topography, rainfall and land use/land cover.

Chapter 4

The chapter presents these methods that were applied: Stable isotopes, radon, baseflow separation, hydrochemistry and piezometric analysis.

Chapter 5

This chapter presents the findings of this study, interpreting the results obtained from the aforementioned methods across the three spatial scales: hillslope, catchment, and regional.

Chapter 6

This chapter provides a comprehensive discussion of the results obtained from this study. It concludes with the development of a hydrogeological conceptual model for the study site, which

offers a simplified yet quantified description that encompasses all aspects of the local hydrology and hydrogeology.

Chapter 7

This chapter summarises the study's conclusions and offers recommendations for future research, followed by a comprehensive list of references.

CHAPTER TWO: LITERATURE REVIEW

2.1 Introduction

While there are many hydrogeological studies in South Africa, various researchers have identified that there is still limited knowledge of GW-SW interactions (Parsons, 2004; Moseki, 2013; Mahlangu *et al.*, 2020). The limitation results from a lack of knowledge about the geology, climate, and land use variables that control GW-SW interactions. GW-SW interaction also depends on the hydraulic head difference between surface waters and groundwater. Literature from across the world and South Africa has identified climate as the primary determinant of the water-table depth and surface-water stage, making it the main driving force behind GW-SW interactions (Yang *et al.*, 2021). Furthermore, climate change has been shown to influence GW-SW interactions by increasing groundwater recharge and replenishing both resources (Al Atawneh *et al.*, 2021).

Aquifers in South Africa are mostly predominated by fractured sedimentary rocks, covering 54.6% of the land area in the country (Levy and Xu, 2011). Groundwater flows through basement rocks, granite, extrusive and fractured sedimentary rocks through secondary porosity created by weathering, faults, and fractures (Le Maitre and Colvin, 2008). These aquifers' groundwater flow to surface water is typically restricted to certain areas near significant faults, fractures, and dykes (Schneeberger *et al.*, 2018). Sedimentary aquifers may have more extensive discharge zones and linear contact zones between sandstones and interbedded shale layers or beneath less permeable formations, and their discharge rates may be higher than those of other aquifer types because of their occasionally higher permeability (Levy and Xu, 2011). However, the link between GW-SW is still complex and requires more site-specific studies as it is fundamental for water resource management and local sustainability. This study examined past literature to better understand the link between GW-SW interactions. The following topics provide a thorough review of the literature from both global and local sources to enhance the understanding of the processes governing GW-SW interactions. These topics include rainfall characteristics, the connectivity between groundwater and surface water, the mechanisms that regulate groundwater recharge, groundwater movement and dynamics at hillslope and case studies examining various techniques related to GW-SW interactions

2.2 Stable isotopes

Stable isotopes (δ^2H and $\delta^{18}O$) are commonly used for a wide range of studies in hydrology, such as identifying sources of GW-SW flow, movement of water through landscapes, residence time (McDonnell *et al.*, 1999; Rodgers *et al.*, 2005; Chizhova *et al.*, 2022), quantifying surface-atmosphere water exchange and GW-SW interactions (Ala-aho *et al.*, 2015; Kirchner and Allen, 2019), source of groundwater recharge and researching runoff generation (Trinh *et al.*, 2017; Chizhova *et al.*, 2022). Thus, stable isotope tracers can be utilised to generate quantitative information on water resources and to improve our understanding of the hydrological cycle and its processes.

Stable isotopes undergo variation during chemical processes and phase changes. For instance, water in an open body such as a stream, lake, or dam, the lighter isotopes (δ^1H and $\delta^{16}O$) would evaporate easily into the water vapour phase, while the heavier isotopes (δ^2H and $\delta^{18}O$) would remain within the stream/lake. However, the opposite happens during condensation, as heavy isotopes condense easily during the liquid phase. The fundamental idea is that during evaporation, lighter isotopes are enriched in vapour, as opposed to the loss of heavy isotopes from vapour first during condensation (Ngubo, 2019). This process is called 'fractionation' (or natural distillation) and continues with rainfall. This fractionation process can also be influenced by latitude, continentality, temperature and humidity. Furthermore, the isotopic variation in atmospheric precipitation would indicate past and present climate changes within the precipitation that recharges both GW-SW (Qin *et al.*, 2021).

This illustrates the variation of isotope ratio caused by evaporation and condensation; a plot of stable isotopes ($\delta^{18}O$ versus δ^2H) is done for the meteoric water known as the Global Meteoric Water Line (GMWL). Craig (1961) first developed the GMWL, which identified a linear correlation between $\delta^{18}O$ and δ^2H in global precipitation samples. The GMWL has since been frequently employed in environmental geochemistry and hydrogeology to trace water masses and to understand the relationship between the isotopic composition of meteoric waters (Putman *et al.*, 2019). Craig (1961) developed an equation for the GMWL as shown in equation 2.1:

$$\delta^2 H = 8 \times \delta^{18} O + 10 \text{ ‰} \quad \text{2-1}$$

The GMWL is characterised by s=8 and d=10. The "s" represents the slope, which is controlled by average temperature and occurrence of secondary evaporation during rainout. The "d" is known as deuterium-excess (d-excess), and it is mainly influenced by temperature, humidity and sea surface temperature in moisture sources. The GMWL is a global reference representing annual relationships between isotopes in meteoric water. However, to determine and understand the changes in local precipitation in a specific area, the Local Meteoric Water Line (LMWL) must be determined. Through the LMWL, local humidity, local climate and tracing of climate change can be studied (Tyler *et al.*, 1996; Putman *et al.*, 2019). Additionally, LMWL can trace the origin of groundwater and groundwater recharge and identify sources of water that contribute to runoff generation.

2.2.1 Rainfall isotopic characteristics

Rainwater is formed when water vapour in the atmosphere condenses due to evaporation of water and land surfaces. As water evaporates and condenses, isotopic fractionation occurs, leading to a depletion of heavy isotopes in the vapour phase and an enrichment of heavy isotopes in the liquid phase (Ingraham, 1998; Deshpande *et al.*, 2013). The stable isotope composition of rainwater is primarily controlled by temperature, which affects the amount of condensation. The isotopic composition of precipitation can reveal valuable information about the type of precipitation, its origin and pathway, as well as the history of the moisture source (Ingraham, 1998).

Various climatic parameters such as amount, altitude, continentality, seasonality, and interannual variation can influence the isotopic composition of precipitation. Understanding the isotopic composition of precipitation is essential for comprehending the hydrological cycle and gaining insight into the type of precipitation that recharges water systems, such as groundwater and surface water.

2.2.1.1 Amount effect

Amount effect refers to the relationship between the amount of rainfall and stable isotopes (δ^2H and $\delta^{18}O$) found in precipitation. The amount effect is a phenomenon that describes the correlation between the isotopic composition of rainfall and the amount of rainfall. In particular, it is observed that heavy isotopes are depleted in rainfall, and this depletion is more noticeable in heavier rainfall events (Allen *et al.*, 2017). This implies that the heavier the rainfall, the more depleted it is in heavy isotopes. According to Dansgaard (1964), there is a depletion of heavy isotopes in rainy months and an enrichment of isotopes in months in sparse rains. In other words, the higher the volume of rainfall, the lower the δ^2H and $\delta^{18}O$ content and vice versa. For instance, the exceptionally powerful tropical rains that occur during the passage of the Intertropical Convergence Zone (ITCZ), which are characterised by soaring clouds and powerful downdrafts, may be significantly depleted in heavy isotopes by as much as 15‰. Precipitation from thunderstorms, which typically produce intense but short-lived rainfall, shows isotope depletion patterns consistent with the amount effect, although the depletion is often less pronounced compared to prolonged heavy rainfall events (Sun *et al.*, 2022).

Various South African studies have shown that heavy isotopes are depleted due to the rainfall amount effect. For example, a study by Leketa and Abiye (2020) in Johannesburg found evidence of the amount effect. The study showed that the high amount of rainfall observed corresponded well with the depletion of δ^2H and $\delta^{18}O$, while the low rainfall corresponded with the enrichment of δ^2H and $\delta^{18}O$. Additionally, a study in Thohoyandou by Durowoju *et al.* (2019b) demonstrated that during periods of heavy rain, isotopic values were more depleted, whereas more enriched isotopic values were obtained during periods of light rain, and this was due to the amount effect.

2.2.1.2 Altitude effect

The altitude effect, sometimes known as the ‘elevation effect’, refers to the change in the isotopic composition of precipitation with increasing altitude. As the altitude increases, the more the depletion of δ^2H and $\delta^{18}O$ (**Figure *2.1***). The altitude effect is temperature-related, and condensation is caused by low temperature due to increased altitude. The effect of altitude occurs as air masses are lifted orographically, causing them to cool and preferentially precipitate heavier isotopes at lower elevations. As the air mass continues to rise, the remaining moisture becomes progressively

depleted in heavy isotopes, resulting in more isotopically light (depleted) precipitation at higher altitudes. Many studies that demonstrate the effect of altitude on the isotopic composition of precipitation have been done (Niewodnizański *et al.*, 1981; Kern *et al.*, 2014; Kong and Pang, 2016; Jiao *et al.*, 2020), and it was found that altitude effects vary from -0.15 to -0.5‰/100m for ^{18}O and -1 to -4‰/100m for ^{2}H (Clark and Fritz, 2013). The altitude effect is vital in hydrogeology, as it distinguishes groundwaters recharged at high altitudes from those recharged at low altitudes.

However, some studies have discovered that there is an increase of heavy isotopes with an increase in altitude in certain regions, in contradiction with the expected altitude effect. Researchers have discovered the "Inverse altitude effect" (IAE) , in which $\delta^{2}H$ and $\delta^{18}O$ increase with an increase in altitude. For example, a study by Jing *et al.* (2022) found IAE in North Africa and Asia drylands where the heavy isotopes increase with an increase in altitude.

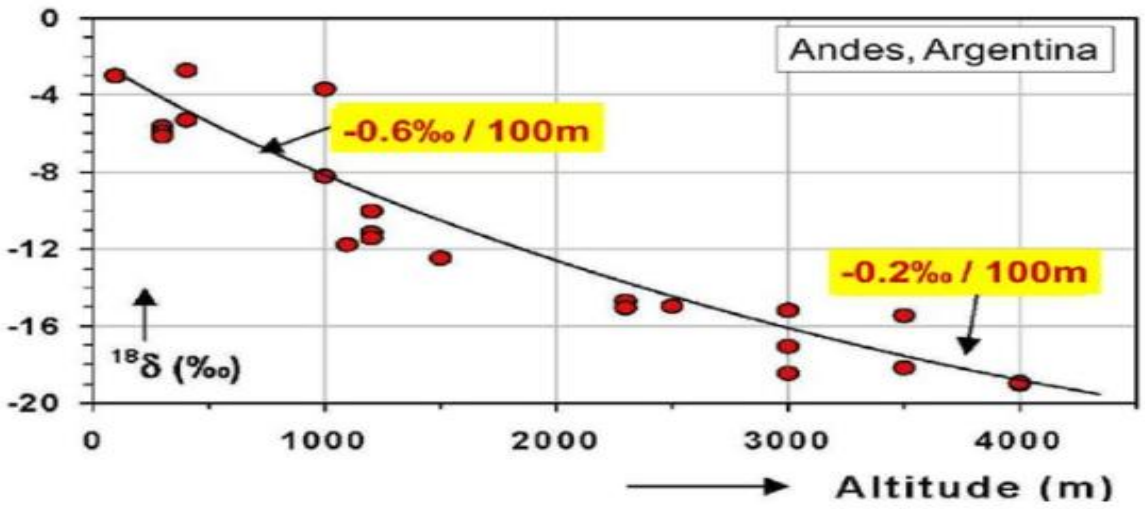

Figure 2.1: Altitude effect on precipitation for the eastern slopes of the Andes Mountain range (Vogel *et al.*, 1975; Samie, 2020).

2.2.1.3 Seasonality effect

Seasonal variation in isotopic characteristics refers to changes in isotopic composition due to seasonal variation. Seasonal variation of heavy isotopes is closely related to longitudinal migration of the atmospheric circulation system. The ITCZ movement in the tropics produces wet and dry

seasons, which, when combined with the amount effect, cause fluctuations in the seasonal abundance of heavy isotopes (Cluett *et al.*, 2021).

In contrast, the temperature effect is a major contributor to seasonal changes in the mid-latitudes, although shifts in atmospheric circulation can also impact the trajectory of moisture transport and the origin of precipitation in specific sites. In subtropical to mid-latitudes, there is a seasonal pattern because convective rainfall tends to occur more frequently during the summer months, when the land surface is heated, whereas frontal storms are more common during the winter season (Wu *et al.*, 2020).

In South Africa, a study by Braun *et al.* (2017) found that heavy isotopes correlate with seasonal variation; the heavy isotopes were highest (enriched) between January and April (summer) and lowest (depleted) in June and July (winter). At a global scale, Otte *et al.* (2017) observed seasonal patterns of isotopic composition; the findings demonstrated that the lowest values were experienced during the wet season, and the highest was experienced during the dry season. **Figure 2.2** shows the seasonal variation of various cities in the Northern Hemisphere; during the wet season, the values were at their lowest and they were at their highest during the dry season.

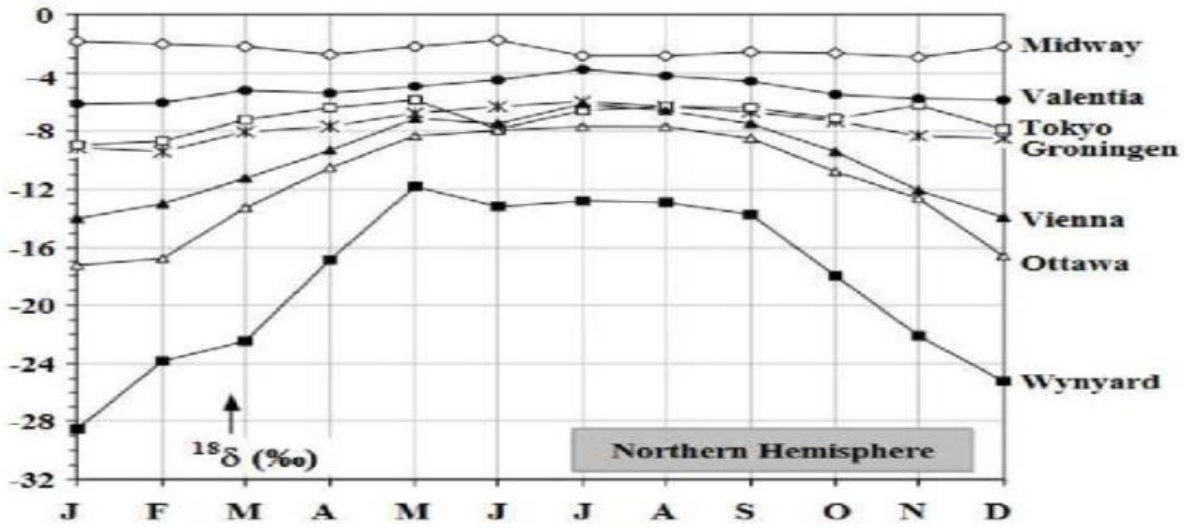

Figure 2.2: Seasonal influence on the $\delta^{18}O$ and $\delta^{2}H$ relation for average monthly precipitation in the northern hemisphere (data from the GNIP network) (Samie, 2020).

2.2.1.4 Continentality effect

The continentality effect in terms of isotopic rainfall characteristics describes the loss of heavy isotopes as precipitation gradually moves inland from the coast. The depletion occurs as precipitation moves from the ocean and when air is losing moisture as it travels inalnd, and the depletion varies from area to area. The continentality effect is strongly related to the temperature effect, topography, and climate (Chidambaram *et al.*, 2009).

A study by Kern *et al.* (2020) in the Adriatic-Pannonian region in Central and Southeast Europe discovered a seasonal 'continental effect' where ^{18}O had a decrease of -2.4‰/100 km, and ^{2}H had -20‰/100 km. This was from the Adriatic coast to about 400km inland during winter precipitation.

2.2.1.5 Interannual variation

Interannual variation in isotopic rainfall characteristics describes changes in the isotopic composition of rainfall from year to year. Interannual variation of $\delta^{18}O$ varies from area to area. In regions with temperate climates, the value of $\delta^{18}O$ rarely fluctuates by more than 1‰, and changes in the average yearly temperature drive a major percentage of the fluctuation (Cluett *et al.*, 2021). In semi-arid climate regions with less than regular rain, distribution experiences larger variations of $\delta^{18}O$.

Interannual fluctuation is mainly driven by climatic oscillations like the El Niño-Southern Oscillation (ENSO) and monsoons, which impact the moisture sources and transport pathway of precipitation in various seasons. A study by Ichiyanagi *et al.* (2002) at the Antarctic Peninsula showed a relation between Interannual variation of the isotopic composition of precipitation and ENSO signal. It further discovered that variation of the moisture flux and transport of the Southway moisture flow in low latitude regions control the interannual variation of stable isotope in the Antarctic precipitation.

2.2.2 Meteoric water line

The meteoric water line is a commonly used tool in environmental geochemistry, hydrology, meteorology, and hydrogeology to describe the relationship between stable isotopes of oxygen and hydrogen in natural meteoric waters, such as precipitation. Various factors such as amount effect,

altitude effect, continentality, seasonality, temperature and humidity contribute to the isotopic composition of rainfall. The above-mentioned factors ultimately determine a region's meteoric water line's position and slope. Various studies (Ferronsky *et al.*, 2012; McIntosh and Ferguson, 2021; Adachi and Yamanaka, 2024) have shown that there is a global meteoric water line constructed by Craig (1961). The GMWL is the global average relationship between $\delta^{18}O$ and $\delta^{2}H$ ratios in natural meteoric waters. Therefore, the GMWL serves as a baseline for understanding how these ratios vary in natural water on a global scale. However, because local environmental conditions such as temperature, evaporation, and humidity can influence the isotopic composition of precipitation, each geographic location can have its own Meteoric water line (Jouzel *et al.*, 2000).

By comparing the LMWL to the GMWL, researchers can determine if the local meteoric waters have undergone processes such as condensation, evaporation, or mixing of water bodies that have altered their isotopic composition from the global average. The position and slope of the LMWL in relation to the GMWL can provide insight into the water's source, transport history, and climatic conditions in the region (Dar *et al.*, 2024). This allows the origin and history of the local meteoric waters to be better understood. For example, groundwater that plots below the GMWL has likely undergone evaporation, while water that plots above the line could have been affected by kinetic fractionation processes (**Figure 2.3**). Therefore, any shift or deviation in the meteoric water line, whether globally or locally, is regarded as a result of hydrological processes and environmental conditions affecting the isotopic composition of precipitation (Terzer-Wassmuth *et al.*, 2023).

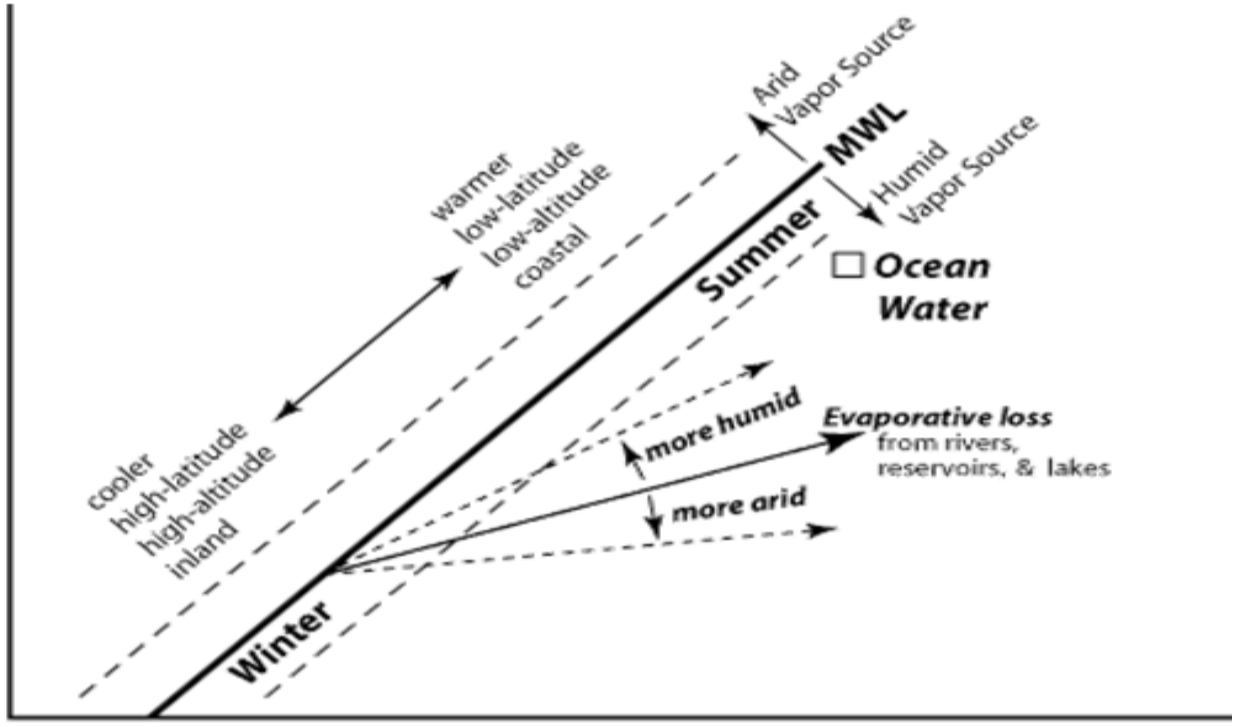

Figure 2.3: Meteoric water Line (Zega et al., 2020)

2.2.3 Deuterium excess

The deuterium excess (d-excess) is a second-order isotope parameter that provides information about the conditions during the evaporation of water from the ocean surface, i.e. the moisture source conditions. The d-excess is defined as:

$$d = \delta^2 H - 8 \times \delta^{18} O \qquad 2\text{-}2$$

The d-excess is correlated with environmental conditions such as humidity, air temperature, and sea surface temperature in the oceanic source area of the precipitation. Furthermore, the d-excess is primarily controlled by the conditions under which the water evaporated, particularly the relative humidity and temperature, rather than the initial isotopic composition of the water (Zhang *et al.*, 2021). During evaporation, the d-excess of the water vapour increases as relative humidity decreases and the temperature rises (Benetti *et al.*, 2014). Conversely, the d-excess decreases as relative humidity increases and temperature falls. Specifically, higher evaporation degrees lead to

larger d values, while stronger re-evaporative fractionation under the cloud results in smaller d values after raindrop condensation (Tang *et al.*, 2024). For example, a study by Leketa and Abiye (2020) highlighted the correlation between the d-excess and evaporation; the study stated that heavy rainfall (≥20 mm) has a higher d-excess than lighter rainfall (<20 mm). The low d-excess in light rainfall suggests the occurrence of post-condensation sub-cloud re-evaporation, a process that is more prevalent in light rainfall events. Furthermore, the study elucidated that the high d-excess of incoming moisture signifies primary evaporation under warm sea surface temperatures and low relative humidity, contributing to an increase in d-excess.

2.2.4 Isotopic composition of surface water

The isotopic composition of surface water refers to the relative abundance of different isotopes of elements, such as oxygen and hydrogen, present in water bodies like lakes, rivers, and oceans. The isotopic composition of surface water varies depending on factors such as precipitation, evaporation, and water sources. Studies have shown that different water bodies have distinct isotopic compositions (Xie *et al.*, 2023; Bhagwat *et al.*, 2024). For example, pond water tends to be enriched with heavy isotopes like δ^2H and $\delta^{18}O$ due to evaporation, and surface water bodies such as lakes and rivers exhibit higher evaporation levels compared to reservoirs and are therefore characterised by greater enrichment of heavy isotopes (Kim and Lee, 2011). However, if the basin consists mainly of mountains with abundant rainfall, river water would be depleted in heavy isotopes due to the altitude effect. As a result, the isotopic composition of river water reflects the isotopic signature of precipitation over the basin. According to Xiao *et al.* (2023), heavy rainfall following a relatively dry period can cause distinct shifts in river water isotopic composition, typically resulting in depleted δ^2H and $\delta^{18}O$ values due to the influx of isotopically lighter rainfall. This also demonstrates the amount effect. For instance, the study demonstrated that during a heavy precipitation event in June 2017 that brought 487.1 mm of precipitation, the river water δ^2H decreased by -27.5‰.

2.2.5 Isotopic composition of groundwater

The isotopic composition of groundwater can provide valuable insights into the sources, origin, and chemical composition of groundwater (Gat, 1971; Ahmed *et al.*, 2022). Groundwater can be categorised based on its origin: meteoric water, paleo-waters, saline groundwater and geothermal.

The isotopic composition of groundwater often resembles meteoric waters, which originate as precipitation or snow, indicating that groundwater in that area is recharged by precipitation. Moreover, the isotopic composition of shallow and locally derived groundwater closely mirrors that of the local average meteoric water. This is because shallow groundwater is replenished by recent precipitation and has not experienced substantial isotopic fractionation (Gonfiantini *et al.*, 1998). The isotopic composition of aquifers varies from region to region, especially in regions with different environments. For instance, the isotopic composition of groundwater in arid and semi-arid regions, such as the Karoo, Kalahari, and Northwest regions in South Africa, demonstrates a more enriched $\delta^{2}H$ and $\delta^{18}O$ signature compared to humid regions (Ahmed *et al.*, 2022). This enrichment of heavy isotopes is because of limited precipitation and high evaporation rates found in arid environments.

2.2.2 Case studies: Stable isotope use in South Africa

Case study 1: A study by Leketa *et al.* (2019) in Johannesburg, South Africa, stable isotopes ($\delta^{2}H$ and $\delta^{18}O$) were used to assess recharge and subsequent groundwater flow path dynamics of the Upper Crocodile River Basin. To achieve this, daily rainfall events were sampled for 3 years at two selected stations. The results from the rainfall sampling constructed the Johannesburg Local Meteoric Water Line (JLMWL) to better understand the source and mechanism of recharge of the study area. The JLMWL of $\delta^{2}H = 6.78\delta^{18}O +10‰$ indicated that the recharge of the aquifer was obtained from rainfall events of different moisture and condensation conditions (temperature and humidity), which can be due to seasonality and amount effect.

Case study 2: A study by Durowoju *et al.* (2019b) investigated the isotopic composition of rainwater in Thohoyandou, South Africa. The study generated the Thohoyandou Local Meteoric Water Line (TLMWL) and investigated the climatic factors controlling the isotopic composition of the rain in Thohoyandou. The TLMWL was useful in assessing the origin and recharge mechanism of groundwater in the locality. To develop the TLMWL, 12 monthly samples were collected over a year. The stable isotopes ($\delta^{2}H$ and $\delta^{18}O$) analysis from the study demonstrated that there was an effect of seasonality observed. Furthermore, the amount effect was evident as the rainfall with lower volume was more depleted in stable isotopes. Additionally, the TLMWL of $\delta^{2}H = 7.568\delta^{18}O +10.64‰$, n=12 had a similar slope to the GMWL (equation 2.1) but a slightly higher

intercept, indicating that the rain in Thohoyandou occurs under equilibrium conditions with minor evaporation during rain.

Case study 3: A Stable isotope study was done by Harris *et al.* (2010) in the Western Cape at the University of Cape Town (UCT). The study's objective was to examine the stable isotopes of δ^2H and $\delta^{18}O$ in rainfall to better understand their association with climate, storm events, and groundwater recharge. Subsequently, an LMWL was constructed to understand the relationship between these factors. The Cape Town Local Meteoric Water Line (CLMWL) was constructed using monthly rainfall data collected over 12 years (1996 to 2008) at UCT. The equation of the CLMWL was found to be $\delta^2H = 6.41\delta^{18}O + 8.66‰$, $n = 163$. Moreover, it was observed that the δ^2H and $\delta^{18}O$ monthly data from UCT showed seasonal variation, with higher values in summer and lower values in winter.

Case study 4: A study conducted by Braun *et al.* (2017) explored the rainfall variability intersection between summer and winter rainfall regimes on the Coast of South Africa, specifically in Mossel Bay, Western Cape Province. The study was focused on characterising variation patterns of δ^2H and $\delta^{18}O$ and evaluating the relationship between isotopic composition, temperature and rainfall amount. One hundred and forty (140) daily rain samples were collected from January 2009 and December 2012 and analysed for δ^2H and $\delta^{18}O$. The results of the isotopic composition of rainfall from Mossel Bay indicated seasonal variation, with the highest values in summer and the lowest in winter. Furthermore, it was evident that isotopic composition was influenced by tropical, subtropical and temperate pressure. Additionally, a LMWL for Mossel Bay was constructed from the weighted monthly rainfall data. Furthermore, the Mossel Bay LMWL ($\delta^2H = 7.70\delta^{18}O + 12.10‰$, $n=140$) was found to be similar to the GMWL (Equation. 2.1) and to the LMWL of Cape Town ($\delta^2H = 6.41\delta^{18}O + 8.66‰$) and Pretoria ($\delta^2H = 6.78\delta^{18}O + 7.2‰$), this indicated that there was a low influence of evaporation and recycled moisture on the isotopic composition of rainfall.

Table 2.1: Summary of case studies on stable isotopes in South Africa

Author	Study site	LMWL equation	Sampling period
Leketa *et al.* (2019)	Upper Crocodile River Basin, Johannesburg	$\delta^2H = 6.78\delta^{18}O + 10‰$	3 years, daily sampling
Durowoju *et al.* (2019b)	Thohoyandou, Limpopo Province	$\delta^2H = 7.568\delta^{18}O + 10.64‰$	1-year, monthly sampling, (n=12)
Harris *et al.* (2010)	University of Cape Town, Western Cape Province	$\delta^2H = 6.41\delta^{18}O + 8.66‰$	12 years, monthly sampling, (n=163)
Braun *et al.* (2017)	Mossel Bay, Western Cape Province	$\delta^2H = 7.70\delta^{18}O + 12.10‰$	4 years, daily sampling, (n=140)

2.3. Factors affecting the connection of GW-SW interactions.

The following are geological and environmental conditions that are widely believed to control the rate of GW-SW exchange, such as geology (lithology, dykes, and lineaments), topography and land use/land cover.

2.3.1 Geology

2.3.1.1 Lithology

Lithology plays a vital role in GW-SW interactions. Hydrogeologists have identified that recharge and discharge of both GW and SW are determined or highly dependent on the soil and rock type. The lithology of an area plays a crucial role in determining the type and characteristics of the existing aquifer. The lithology also determines how much water can be stored deep underground in the aquifer, how it can be accessed and the movement of water through the subsurface (Kasenow, 2001). Aquifers commonly occur in geological formations such as sandstone and limestone (which are sedimentary rocks), as well as in unconsolidated sediments. These sedimentary rocks have a high porosity and permeability, as demonstrated by several studies (Stueck *et al.*, 2013; Olivarius *et al.*, 2015; Singh *et al.*, 2023), which allows surface water to seep into the ground and replenish the underlying aquifer. Furthermore, the high permeability of these sediments allows groundwater to discharge to the surface through springs, seeps or other natural outlets. Nonetheless, some geological formations, such as aquitard, which is made up of silts and clays in the underlying geology, typically obstruct the recharge and discharge of GW and SW because of their low porosity and permeability (Margat and Van der Gun, 2013).

A study by Kresic (2006) showed that an area with porous rocks or highly permeable rocks, such as sandstone or limestone, has higher rates of groundwater recharge and discharge, while areas that have low-permeability rocks, such as granite and shale, have lower recharge and discharge. Wirth *et al.* (2020) demonstrated that geology does have a significant impact on groundwater flow. Furthermore, the study stated that the geology and permeability of bedrock and the alluvial aquifers along a river valley play a vital role in groundwater discharge to surface water during low-flow conditions.

2.3.1.2 Lineaments

Lineaments are natural linear surface elements such as faults, joints, foliations, or bedding planes that are interpreted directly from satellite imagery (Al-Nahmi *et al.*, 2016). Lineaments are vital in groundwater dynamics as they act as barriers or conduits for groundwater flow depending on their characteristics such as orientation, density, connectivity, and permeability (Acocella *et al.*, 2003; Mihret and Wuletaw, 2025). A study by Prabu and Rajagopalan (2013) stated that the presence of lineaments favours the presence or occurrence of groundwater in crystalline terrains because they control groundwater recharge, transmission, and discharge. However, a study by Travaglia (1984) discovered that not every lineament is related to groundwater occurrence. Additionally, Caponera (1989) later discovered that the features supporting the occurrence of groundwater are tensional features, which are directly related to the main direction of tectonic stress.

2.3.1.3 Dykes

Dykes are rock structures that act as conduits or barriers for groundwater flow, depending on the intensity of the dyke structure. Whether dykes act as barriers or a conductor of groundwater flow depends on their location, orientation, and structure (Singh and Jamal, 2002; Nilsen *et al.*, 2003; Babiker and Gudmundsson, 2004). The orientation of dykes relative to the hydraulic gradient is critical in controlling groundwater flow. Dykes aligned perpendicular to the gradient can act as flow barriers, while those parallel may allow or channel flow, depending on their hydraulic properties (Mathew and Samant, 2012). The orientation of dykes with respect to hydraulic gradient is an important factor that impacts groundwater flow.

A study by Babiker and Gudmundsson (2004) discovered that intersections between dykes and faults affect groundwater flow. When fault trends are parallel or subparallel to the hydraulic gradient and the dykes are perpendicular to the hydraulic gradient, it affects the groundwater flow in two ways. Firstly, is when a lot of groundwater is carried down through high-permeability faults, where it partially rises to the surface as springs when it meets low-permeability, transverse dykes. Secondly, many of the dykes are substantial and extend over considerable miles. Groundwater is transported toward the dykes not only through high-permeability fault zones but also through regional groundwater flow, as the dykes are oriented transverse to the main hydraulic gradient. This positioning allows them to intercept and potentially concentrate groundwater flow. As a result,

long, thick dykes with low permeability may draw groundwater from a wide region. This indicates that groundwater is pushed to concentrate at low permeability dykes and flows along their boundaries. In general, the water that is gathered in this way at the low-permeability dykes tends to flow along the west edges of the dykes towards the direction of the surrounding fault zones.

2.3.2 Topography

The recharge and discharge of GW and SW can be highly determined by the topography landscape. Groundwater discharge to surface water is mainly influenced by the hydraulic gradient. The hydraulic gradient is the change in hydraulic head per unit distance in the flow direction. Thus, topography plays a crucial role in controlling the gradient of water flow, the position of the water table, and the direction of water movement across both the surface and subsurface (Li *et al.*, 2023). This influence affects how water seeps into the ground, flows, and the rate at which it is transmitted through the hydrogeological system (Condon and Maxwell, 2015). Essentially, variations in elevation and surface features impact water flow dynamics, including how water infiltrates the ground and moves within the hydrogeological system. This ultimately shapes the dynamics of GW-SW interactions (Bresciani *et al.*, 2016). The groundwater table's topography mirrors the land surface's topography: high beneath hills and low under valleys. However, the topography of the groundwater table is more subdued than that of the land surface, primarily due to the depth of the water table, which tends to be deeper beneath hills and shallower beneath valleys. Rivers, lakes, and springs typically occur where the groundwater table intersects the land surface, allowing groundwater discharge to surface water bodies; however, this is primarily true for gaining systems and may not apply to disconnected or losing streams (Winter, 1999). A study by Hokanson *et al.* (2019) in the subhumid lowlands of the Boreal Plains region showed that topography primarily controls the water table position and groundwater flow scale, closely following surface topography. Furthermore, it was observed in this study that sites with higher elevation have higher water table fluctuation and have more discharge than sites of lower elevation with more stable water table.

2.3.3 Land use

Variations in Land use/Land cover (LULC) that humans cause have impacted the whole hydrological system; it has affected recharge and runoff (Yadav, 2023). Land use changes such as

urbanisation, deforestation and afforestation alter groundwater recharge; it affects the amount of water that seeps into the ground and replenishes the underlying aquifer (Salem *et al.*, 2023). A study by Scanlon *et al.* (2007), reported groundwater recharge rates and processes are significantly impacted when land is utilised for agriculture, whether irrigation or rainfed. Various studies have shown that vegetation, as a key component of LULC, can significantly influence groundwater recharge by enhancing infiltration, reducing surface runoff, and minimising soil erosion (Owuor *et al.*, 2016; Mensah *et al.*, 2022; Siddik *et al.*, 2022). A study conducted by Booth *et al.* (2016) discovered that the removal of native vegetation and replacement with crops with shallower root systems increases groundwater recharge.

A study by Warku *et al.* (2022) assessed the impact of LULC on groundwater recharge in the upper Gibe watershed of Ethiopia, demonstrating that groundwater recharge varies with changes in LULC. The study further stated that the increase in agricultural and built-up areas, while reducing forests, grassland and shrubs, was the major factor for the decline in groundwater recharge; this change in land use reduces percolation and increases surface runoff.

2.4 Groundwater recharge, discharge and lateral groundwater flow

2.4.1 Groundwater recharge

Groundwater recharge refers to the process by which water infiltrates the soil and percolates down to replenish aquifers (Freeze, 1969; Seiler and Gat, 2007). There are two methods of groundwater recharge: diffuse recharge, from rainfall infiltration, and focused recharge, from temporary rivers and lakes (Shanafield and Cook, 2014). Diffuse groundwater recharge is the process by which water seeps into the soil and replenishes aquifers across vast areas, and it is dominant in humid regions (Healy, 2010). Both diffused and focused recharge are influenced by various factors such as topography, geology, climate and LULC.

Topographic features, including slope, elevation, flow paths, and aquifer thickness, determine how and when water replenishes the land. Substantially, flat or gently sloping areas with thick aquifers generally experience shallow groundwater levels and higher groundwater discharge due to enhanced focused recharge, while steep slopes with thin aquifers tend to have deep groundwater levels and lower groundwater discharge associated with diffuse recharge (Benjmel *et al.*, 2020).

The type of geology also influences the amount of groundwater recharge that occurs. The geological structure, permeability, and porosity of rocks and soils, as well as the presence of karst features and fractures, all play a role in determining the relative importance of diffuse and focused recharge processes (Stevanović, 2015).

Climate also plays a significant role in groundwater recharge. For instance, climate variability influences changes in precipitation and evapotranspiration rates, affecting diffused recharge. However, in focused recharge, extreme climate events like heavy rainfall can significantly impact the process, leading to substantial recharge in semi-arid regions beneath temporary surface water bodies (Geris *et al.*, 2022). The influence of LULC on groundwater recharge is complex and multifaceted. Highly vegetated areas can decrease groundwater recharge because precipitation is intercepted by plants and lost through evapotranspiration. Conversely, urbanisation can decrease groundwater recharge by inhibiting water infiltration into the soil. However, various studies have also demonstrated that reduced evapotranspiration and increased urban sources, such as excessive irrigation and water main leaks, can increase groundwater recharge in some urban areas (Garcia-Fresca and Sharp, 2005; Han *et al.*, 2017; Wakode *et al.*, 2018) .

2.4.2 Groundwater discharge

Groundwater discharge refers to the release of groundwater from the underlying aquifer into the surrounding environment. This discharge happens in parts of the drainage basin where the net saturated flow of groundwater is directed upward towards the water table (Schwartz and Zhang, 2024). In these areas, the groundwater level is at or near the surface. Groundwater discharge is essential for sustaining baseflow in streams, ensuring they do not run dry despite periods without rain. This continuous flow is sustained by groundwater that originated from distant recharge areas and has moved slowly through the subsurface over time, eventually discharging into the stream.. Furthermore, a study by Kendall and McDonnell (2012) highlighted, based on a synthesis of multiple isotope and hydrograph separation studies across various climatic and geological settings, that a significant portion of streamflow—often around 50%—can be attributed to groundwater discharge. However, this is not a universal figure and varies by region. Their work reflects general patterns observed in temperate catchments rather than a specific river system. It's important to note that in semi-arid regions such as southern Africa, diffuse groundwater recharge is typically much

lower—ranging from 5% to 15%—and therefore contributes proportionally less to baseflow, especially during dry periods.

2.4.3 Lateral groundwater flow

The term "lateral groundwater flow" describes the multiple flow patterns, such as shallow, intermediate, and deep-water flow patterns that link discharge areas (streams) with recharge zones (mountains). The various flow patterns enter the unsaturated zones from high-elevation regions where precipitation flows downward (**Figure 2.4**). Research has indicated that comprehending the lateral geothermal flow between mountains and valleys is essential for managing water resources, forecasting groundwater depletion in the context of a global climate, and measuring regional groundwater and geochemical cycles (Somers and McKenzie, 2020). The water table, climate, geology, and topographic gradient all have an impact on the lateral groundwater flow. Research has shown that the above-mentioned effect helps groundwater flow patterns return to stream networks (Fan *et al.*, 2007; Zeng *et al.*, 2018). However, only the shallow and intermediate flows return to the nearby stream networks. The deep flows, also known as mountain block recharge, are hidden from direct observation. Nonetheless, 60% of the recharge into the valley aquifers originates from the adjacent mountain block (Markovich *et al.*, 2019).

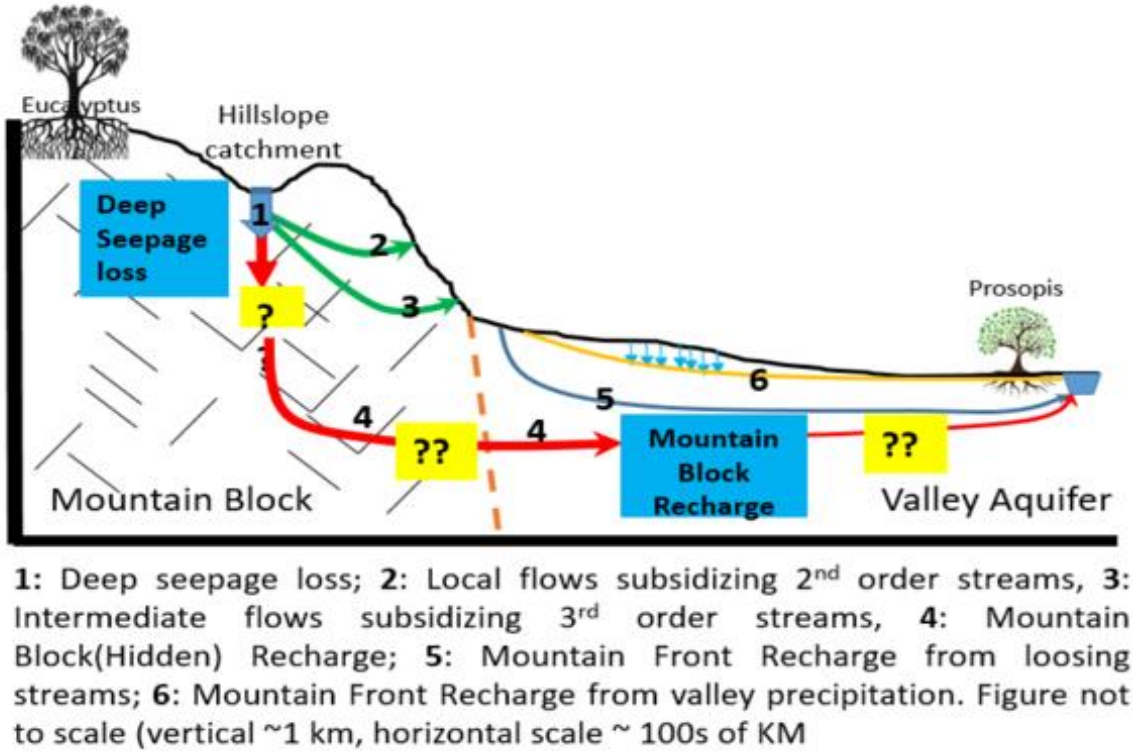

Figure 2.4: Lateral groundwater flow (Kebede, 2023)

2.5 Contributions of extreme rainfall patterns in groundwater recharge

Various studies have proven that climate change can alter the time and magnitude of potential groundwater recharge, resulting in the risk of water availability, droughts, and floods (Herrera-Pantoja and Hiscock, 2008; Hashemi *et al.*, 2015; Al Atawneh *et al.*, 2021). Various global phenomena, such as the El Niño–Southern Oscillation (ENSO) and tropical storms, are natural climatic events whose intensity, frequency, or impacts can be significantly influenced by climate variability and change. These phenomena have a direct impact on rainfall and temperature. However, it is important to note that climate change/variability affects the frequency and severity of tropical storms but does not alter the storms themselves. These phenomena are part of the broader climate system and are subject to changes in the climate, such as increasing temperatures, altered rainfall patterns, and changes in atmospheric conditions (Trenberth, 2011). Studies have shown that these global phenomena that influence climate contribute significantly to groundwater storage, groundwater recharge and precipitation, thus affecting all water resources (Simmers, 2003; Earman and Dettinger, 2011).

2.5.1 El Nino Southern Oscillation

The El Niño–Southern Oscillation (ENSO) is a naturally occurring climate phenomenon characterised by periodic fluctuations in sea surface temperatures and atmospheric pressure in the equatorial Pacific Ocean. It has two main phases—El Niño and La Niña—which influence weather patterns globally, including shifts in precipitation and temperature. These shifts in precipitation patterns associated with ENSO can, in turn, affect hydrological processes such as groundwater recharge and surface water flow in many regions. A study in a river basin of Central India by Rishma and Katpatal (2019) revealed that the groundwater level is deeper, and discharge is higher during El Niño years; during La Niña years, the groundwater levels were shallower, and recharge was higher during La Niña.

Various studies have shown that ENSO may impact groundwater recharge and discharge (Anderson Jr and Emanuel, 2010; Mitra *et al.*, 2014; Batista *et al.*, 2018). It's important to note that El Niño and La Niña have varying impacts on different regions of the world. Some regions may experience above-average precipitation, while others may experience below-average precipitation. El Niño and La Niña in Southern Africa can significantly affect groundwater recharge due to their influence on precipitation patterns. Typically, El Niño events are associated with below-average precipitation in Southern Africa, which can lead to reduced groundwater recharge or even depletion. For example, Kolusu *et al.* (2019) discovered that the El Niño event in 2015-2016 led to reduced GW recharge in East and Southern Africa, worsening the region's existing water scarcity issues. Another study by Hund *et al.* (2021), through a model-based analysis of groundwater recharge processes across various tropical regions, found that extreme El Niño events can lead to a reduction in groundwater recharge by up to 60%. This reduction was attributed to prolonged dry conditions and suppressed rainfall during strong El Niño phases, particularly in areas that are heavily reliant on seasonal precipitation for recharge.

2.5.2 Tropical storms

Tropical storms are powerful circular storms with low air pressure, strong winds, and heavy rain that form over warm tropical waters. Tropical storms generate extremely strong winds, heavy rain, large waves, and, occasionally, extremely damaging storm surges and coastal floods.

Tropical storms have a complex relationship with groundwater; through heavy rainfall, they can contribute to aquifer recharge, but they can also lead to increased surface runoff and reduced infiltration, depending on land cover and storm intensity (Jasechko and Taylor, 2015). Tropical storms can bring heavy rain, which can cause groundwater discharge. Rainfall is a dominant driver of stream discharge, as supported by Ouyang *et al.* (2022) who found a direct correlation between daily precipitation and streamflow response. However, the relationship between rainfall and recharge is not always straightforward. For instance, Breña-Naranjo *et al.* (2015) demonstrated that in Mexico, tropical storms—characterized by intense, short-duration rainfall—can significantly enhance groundwater recharge, particularly in fractured or karst systems. These findings highlight the importance of storm characteristics (intensity, duration, and antecedent soil moisture) in determining whether rainfall contributes more to surface runoff or infiltrates to recharge groundwater.

2.6 Subsurface path flows

The subsurface flow paths within hillslope catchments significantly influence groundwater recharge and, in turn, the contribution of baseflow to streams. Hillslope catchments are land areas with slopes or inclines that collect and distribute water (Calver *et al.*, 2019). In a typical hillslope catchment, water movement is primarily facilitated through three key flow pathways: overland flow, subsurface lateral flow, and bedrock flow. Flow pathways in hillslope catchments play a critical role in influencing groundwater recharge, baseflow contributions to streamflow, and overall hydrological processes (Tetzlaff *et al.*, 2014). Hillslope water movement is controlled by various factors such as topography, soil characteristics, climate conditions, geological features, and vegetation cover.

2.6.1 Overland flow

According to Kirkby (2019), overland flow occurs when the intensity of rainfall surpasses the soil's infiltration capacity in a given area. This phenomenon can occur as either saturation excess or infiltration excess. Infiltration excess depends on the characteristics of the soil, such as thicker soils having less infiltration excess compared to thinner soils. In thicker soils, a higher level of infiltration is anticipated because a larger volume of water is required to saturate the entire soil

profile. Additionally, thicker soils support more vegetation, thus decreasing overland flow as it enhances water infiltration and retention (Wang *et al.*, 2013a).

In hillslope catchments, soils are often thicker at the break of slope (the transition between the steeper upper slope and the gentler lower slope) due to sediment deposition and the effects of erosion processes (van Beek *et al.*, 2008). This increased soil thickness enhances infiltration capacity. Additionally, the change in gradient at the slope break reduces the velocity and volume of overland flow, allowing more water to infiltrate the thicker soil. Runoff slows down on the gentle lower slope due to the reduced gradient. The quantity of overland flow is significantly influenced by soil texture, particularly the proportions of clay and sand present in the soil (Li *et al.*, 2014). Generally, clay soils are less permeable and have lower infiltration rates because their small, compact particles restrict water movement. As a result, clay soils tend to produce higher overland flow compared to sandy soils, which have larger particle sizes and greater porosity, allowing water to infiltrate more easily.

2.6.2 Subsurface lateral flow

According to Chen *et al.* (2009), this is the lateral movement of water through the soil and rock layers beneath the land surface, typically in saturated conditions. Subsurface lateral flow occurs through two primary pathways: soil matrix flow and macropore flow (Hardie *et al.*, 2012). In the soil matrix flow, water moves through small pores and voids in the soil matrix. Flow paths in soil matrix occur due to unpredicted pathways created by plant roots, biological activity and cracks. Soil matrix flow is influenced by the soil texture, structure and soil moisture content. It dominates in conditions where the soil is saturated, especially when a less permeable layer is present beneath the surface layer, leading to the buildup of water that can then move laterally. The macropore flow openings and voids are larger than the soil matrix flow. The macropore flow is mainly associated with large openings in the soil, such as root channels, earthworm burrows and structural cracks (Nimmo, 2016). Water can move rapidly through macropores, largely bypassing the soil matrix. The macropore flow is primarily determined by accessibility, size of macropores and the continuity of the pores.

2.6.3 Bedrock flow

According to Hencher (2010), this is the movement of water that occurs through fractures, joints and solution cavities in the underlying bedrock. In hillslope catchments, soils in the steeper upper slope are vital for water intake that supplies the bedrock flow path. The movement of this flow path is vertical. However, depending on the geometry of the bedrock, including its curvature and the presence of fractures, can dictate how water is stored and released. This can lead to varying recession characteristics and affect how quickly water moves from the hillslope to the stream network. In various studies, researchers found that the structure of the bedrock influenced how quickly water could move laterally to streams (Whipple, 2004; Rempe and Dietrich, 2014; Naganna *et al.*, 2017). The highly fractured nature of bedrock allowed for rapid lateral flow, connecting saturated areas with stream zones. However, the water was mainly sourced from surface infiltration rather than deeper groundwater levels.

2.7 Case studies of GW-SW interaction at a global scale

Case study 1: A study by Unland *et al.* (2013) investigated GW-SW interaction along the Tambo and Nicholson rivers in southeast Australia using ^{222}Rn, Chloride, EC, different surface water flow gauging, temperature profiles and head gradients. The techniques mentioned above were used to assess groundwater fluxes. The findings from these diverse methods indicated elevated groundwater fluxes to the Tambo River in regions with significant topographic diversity, suggesting substantial GW-SW interactions. Additionally, the study revealed that groundwater discharge peaked following intense rainfall periods. The study suggested that extensive groundwater sampling is required to characterise groundwater accurately.

Case study 2: A study by Martinez *et al.* (2015) conducted a spatial analysis of hydrochemical data of GW-SW to identify GW-SW interaction in the headwaters of the Condamine River catchment, southeast Queensland, Australia. The study utilised long-term hydrochemical and water level data complemented by stable and radioactive isotopes (^{222}Rn) and baseflow. Results from the water level data and stable and radioactive isotopes demonstrated that the majority of the tributaries in the river are connected to alluvial and basalt aquifers. Additionally, the results revealed that the local geomorphology is the major driver of groundwater discharge into the streams in the upper

reaches of the tributaries. The study suggested that one-off sampling for stable and radioactive isotopes may not be enough to show the variability of GW-SW interaction.

Case study 3: A study by Bhat and Jeelani (2018) investigated the interactions between GW-SW in the Bringi watershed in the Kashmir Himalayas, India. The researchers used environmental isotopes ($\delta^{18}O$,$\delta^{2}H$ and $\delta^{3}H$) to quantify the GW-SW interactions in this karst terrain. Through the results of isotopic signatures of precipitation, streams, and springs, the researchers found that winter precipitation significantly impacts stream and spring water in the late spring season, indicating snowmelt as the primary recharge source. Additionally, the isotopic signatures of spring waters in September showed enrichment from summer rainfall. Additionally, the findings from Chloride and isotopic mass balance studies have indicated that surface water plays a crucial role in recharging groundwater. On average, it contributes around 75% of groundwater recharge during high flow periods, while the contribution is around 18.6% during low flow periods. The study recommended that using environmental isotopes alongside conventional hydro-geochemistry is valuable for studying and monitoring GW-SW interactions in karst terrains. This method can aid in protecting and conserving water resources in such fragile environments.

Case study 4: A study by Kebede *et al.* (2021) aimed at investigating the relationship between GW-SW at a regional scale in the River Awash Basin of Ethiopia. The researchers employed various methods of environmental tracers ($\delta^{18}O$, $\delta^{2}H$ and ^{222}Rn), hydrochemistry and piezometric analysis. The study findings suggest that groundwater inflow can be detected in tributary networks in humid upland areas. However, in the arid middle and lower reaches of the basin, most of the regional groundwater flow does not return to stream networks. Thermal springs found in these areas are believed to originate from regional groundwater flow systems that are several hundred kilometres away from where they eventually discharge.

Case study 5: A study by Tadesse *et al.* (2023) characterising GW-SW interaction by using geological and environmental tracers (^{222}Rn, EC, $\delta^{18}O$ and $\delta^{2}H$) also baseflow index method in the upper Awash and the adjacent Blue Nile in Ethiopia. The research discovered that ^{222}Rn, EC and Baseflow index varied along the streams depending on the geology, faults, lineaments, and groundwater contribution. The isotope signatures were used to identify the origin and flow of GW-SW. The isotopes in the study demonstrated that most surface water is from the shallow and deep

sources in the plateau, and summer rains of the Addis Ababa recharged some parts of the upper Awash; this indicated hydraulic connectivity of aquifers through faults. The study concluded that ^{222}Rn, EC, $\delta^{2}H$ and $\delta^{18}O$are vital techniques for locating interaction zones for GW-SW.

Table 2.2: Case studies of GW-SW interaction at a global scale

Source	**Study area**	**Techniques or methods**	**Findings**	**Limitation**
Unland *et al.* (2013)	Tambo and Nicholson rivers in southeast Australia	• Chloride • ^{222}Rn • EC	• Groundwater discharge peaked after intense rainfall periods	• Extensive groundwater sampling required to characterise groundwater accurately
Martinez *et al.* (2015)	Condamine River catchment, southeast Queensland, Australia	• Hydrochemistry • Stable water isotopes ($\delta^{2}H$ and $\delta^{18}O$). • Radioactive isotopes • Baseflow index • Water level	• Local geomorphology is the main driver of groundwater discharge into streams	• One sampling is not enough
Bhat and Jeelani (2018)	Bringi watershed in the Kashmir Himalayas, India.	• Environmental isotopes ($\delta^{18}O$,$\delta^{2}H$ and ^{3}H)	• Snowmelt is the primary recharge source • Surface water contributes 75% of	• Not included

			groundwater recharge during high-flow periods	
Kebede *et al.* (2021)	River Awash Basin of Ethiopia	• Environmental isotopes ($\delta^{18}O$, $\delta^{2}H$ and ^{222}Rn) • Hydrochemistry • Piezometric analysis	• Regional groundwater flow does return to stream networks. • Thermal springs are believed to originate from regional groundwater	• Not included
Tadesse *et al.* (2023)	Upper Awash and the adjacent Blue Nile in Ethiopia	• Environmental tracers (^{222}Rn, $\delta^{18}O$, $\delta^{2}H$ and EC) • Baseflow Index	• Surface water recharge from shallow and deep sources in the plateau • Summer rains of the Addis Ababa recharge parts of the upper Awash	• Limited number of sampling points and did not cover the entire basin.

2.8 Case studies of GW-SW interaction in South Africa

Case study 1: A study by Roets *et al.* (2008) investigated whether coastal wetlands in lowland settings could be dependent on groundwater from the deep circulation confined Table Mountain

Group (TMG) aquifer in the Western Cape, South Africa. The researchers measured groundwater and surface water quality parameters, such as electrical conductivity (EC), sodium (Na+), iron (Fe^{2+}), and chloride (Cl-), as well as groundwater levels at selected sites in the wetlands. The results showed that there is direct groundwater discharge from the TMG aquifers to one of the selected wetland sites. This indicates that the coastal wetland in this location is dependent on groundwater from the deep, confined TMG aquifer system rather than solely on surface water inputs.

Case Study 2: A study by Weitz and Demlie (2014) investigated GW-SW interactions in the Lake Sibaya Catchment, KwaZulu-Natal, South Africa, using major ion chemistry, stable isotopes ($\delta^{18}O$ and $\delta^{2}H$), and chloride mass balance. The study supported the development of a conceptual model of groundwater flow and recharge processes in the catchment. Results from the study indicate a hydraulic connection between groundwater and Lake Sibiya, confirmed through local geology, environmental isotopes, hydrochemistry, lake level, and groundwater head distribution. The stable isotopes ($\delta^{2}H$ and $\delta^{18}O$) readings also showed that the lake water travels beneath the coastal dune barrier before flowing into the Indian Ocean. In the eastern region, the stable data revealed that the lake recharges the aquifers.

Case Study 3: A study by Mahlangu *et al.* (2020) focused on GW-SW interactions using tritium and stable water isotopes in Middleburg, Mpumalanga, South Africa. The study utilised environmental isotopes ($\delta^{2}H$ and $\delta^{18}O$) along with available geology, water chemistry, and hydrogeology information from various sources. The study's main findings show that analysis of ^{3}H indicates direct rainfall recharge into surface water and groundwater. Additionally, stable isotope results from surface water indicate a contribution from nearby surface water sources during dry periods in the rainy seasons and from groundwater sources in the middle of the dry season. Additionally, the groundwater depth decreases as you move closer to the streams, indicating that this is a gaining stream. A key limitation of this study was the limited number of rainfall samples, which weakens the temporal and spatial reliability of the finding.

Case Study 4: A study by Abiye *et al.* (2015) investigated the interaction between GW-SW in the upper Crocodile River basin in Johannesburg, South Africa, using environmental isotopes ($\delta^{2}H$, $\delta^{18}O$ and $\delta^{14}C$) and stream discharge measurements. The study area is known for its fractured crystalline rock and dolomitic aquifers. The findings revealed that mine water extensively

interacted with shallow groundwater and streams. Moreover, the dolomitic aquifers contained uncontaminated, old groundwater with low tritium levels, suggesting a long residence time of water and depleted ^{18}O and ^{2}H, indicating recharge prior to evaporation and a long circulation time. Furthermore, it was found that the streams lose water into the dolomitic aquifer through sinkholes and fractures, pointing to an intimate connection between surface water and groundwater in the area.

Case Study 5: A study by Welgus and Abiye (2022) investigated GW-SW interactions in the Vredefort Dome, South Africa. The study employed stable isotopes ($\delta^{2}H$ and $\delta^{18}O$), hydrochemistry and multivariate statistics (principal component analysis and hierarchical cluster analysis). The combination of the various data analyses offered a unique, multifaceted strategy to strengthen and justify the interpretation of the hydrological activity in the study area. The stable isotope ratios confirmed mixing between depleted groundwater and enriched surface water, producing a composition that reflected an integration of the isotopic variations. Furthermore, the multi-method approach revealed how GW-SW interactions occurred in the study area. Firstly, it is a losing stream system in the northern and south-western reaches, meaning that there is a recharge zone to the underlying aquifer, and secondly, in the southeastern reach, it is a gaining system, providing baseflow to groundwater discharge. This study had the limitation of focusing on connectivity during the dry season, and it is necessary to investigate the seasonal effect of GW-SW interactions.

Case study 6: A study by Lorentz *et al.* (2007) investigated the quantification of hydrological processes in the Weatherley Hillslope Catchment in the Eastern Cape. It employed a combination of tensiometers, electrical resistivity surveys, and isotope analysis (specifically $\delta^{2}H$ and $\delta^{18}O$) to map subsurface conditions. This approach aimed to understand how geological factors influence runoff, streamflow generation, lag times, and water storage. The study highlighted that 60-70% of total stream discharge originates from hillslope water, primarily from subsurface water accumulated at the soil/bedrock interface during the wet season. This emphasises the significant role of subsurface hydrology in contributing to streamflow in this catchment area.

Table 2.3: Case studies of GW-SW interaction in South Africa

Source	Study area	Techniques or methods	Findings	Limitation
Roets *et al.* (2008)	Table Mountain Group (TMG) aquifer in the Western Cape, South Africa	• GW-SW quality parameters (EC, Na+, Fe^{2+} and Cl^{-})	• Groundwater discharge from TMG aquifer to wetlands	• Not included
Weitz and Demlie (2014)	Lake Sibiya Catchment, KwaZulu-Natal, South Africa.	• Environmental isotopes ($\delta^{18}O$ and $\delta^{2}H$) • Geological data • Groundwater level	• Groundwater and lake Sibiya are hydraulically connected. • $\delta^{2}H$ and $\delta^{18}O$revealed that lake water travels beneath the coastal dune barriers before flowing into the Indian Ocean.	• Limited data
Mahlangu *et al.* (2020)	Middleburg, Mpumalanga, South Africa	• Environmental isotopes ($\delta^{18}O$ and $\delta^{2}H$) • Water chemistry	• Depth of groundwater decreases as you move closer to the stream,	• Limitation of rainfall samples collected

		• Hydrogeology and geology	indicating that it is a gaining stream.	
Abiye *et al.* (2015)	Upper Crocodile River Basin in Johannesburg, South Africa	• Environmental isotopes ($\delta^{18}O$, $\delta^{2}H$, and $\delta^{14}C$) • Stream discharge measurements	• Mine water extensively interacted with shallow groundwater and streams	• Not included
Welgus and Abiye (2022)	Vredefort Dome, South Africa	• Stable isotopes ($\delta^{2}H$ and $\delta^{18}O$) • Hydrochemistry • multivariate statistics	• In the northern and southern reaches the groundwater is recharging the underlying aquifer. • In the southeastern reach, groundwater discharge to the groundwater.	• One season data

Lorentz *et al.* (2007)	Weatherley Hillslope Catchment, Eastern Cape, South Africa	• Tensiometers, • Electrical resistivity surveys • Isotope analysis (δ^2H and $\delta^{18}O$)	• that 60-70% of total stream discharge originates subsurface water in the bedrock.	• Not included

2.9 Synthesis of literature

The existing literature on rainfall characteristics, the connection between GW-SW interactions, groundwater recharge, discharge and flow, and groundwater recharge mechanisms was synthesised. The literature presented various studies that align with the objectives of this study, spanning different scales from global to local. Case studies that have characterised rainfall isotopes in South Africa were reviewed, and the gaps were identified. On a global scale, the literature was reviewed to identify the different methodologies used and their limitations. Local-scale studies on GW-SW interactions using different methodologies were discussed.

The literature on rainfall characteristics demonstrated various studies that showed evidence of variation in the isotopic composition of rainfall because of amount, altitude, seasonality, continentality and interannual. Most of the studies did not demonstrate the mechanism that controls these effects of isotopic composition variation, so there is limited knowledge of this mechanism, particularly what controls the isotope composition of daily rainfalls. For example, Durowoju *et al.* (2019b) found that the depletion of heavy isotopes is due to the amount of effect. However, no insight into the mechanism was given. Furthermore, there was a contradiction of the altitude effect in other studies; for instance, Clark and Fritz (2013) demonstrated that the isotopic composition of rainfall depletes with an increase in the altitudinal effect. However, Jing *et al.* (2022) demonstrated that there was an isotopic enrichment with an increase in altitude.

A review of South African case studies on rainfall isotopes indicates that most previous research utilised data from single rainfall sampling points, with some datasets based on monthly collections. While these studies were not designed to assess the altitudinal effects on isotopic composition, the limited spatial and temporal resolution of their datasets makes such analysis difficult. To contribute toward filling this knowledge gap, the current research employed multiple rainfall samplers positioned at different elevations and collected daily rainfall samples. This methodological enhancement allows for a more detailed examination of isotopic variability across altitudinal gradients. Future studies are encouraged to build on this approach by expanding sampling networks and increasing the frequency of data collection to better understand altitude–isotope relationships in rainfall.

The mechanism that controls recharge and discharge of GW and SW was discussed, and how they affect GW-SW interactions. The effects of geology, lineaments, dykes, topography, and land use were discussed based on global and local studies. The various studies demonstrated how and which geology mostly contributes to the recharge and discharge of water and how lineaments and dyke contribute to the discharge of groundwater. The studies also illustrated the relationship between topography and hydraulic gradient and how they contribute to the discharge and recharge of GW-SW. A study by Yadav (2023) illustrated that variation in land use has affected groundwater recharge and groundwater runoff.

Contributions of extreme rainfall patterns in groundwater recharge were discussed along with ENSO and tropical cyclones. ENSO occurs in two phases: El Nino and La Nina. Hund *et al.* (2021) reported that extreme El Niño events can reduce groundwater recharge. In contrast, studies on tropical cyclones, such as by Ouyang *et al.* (2022) indicate that heavy rainfall from cyclones can increase groundwater discharge due to a rising water table. Similarly, Breña-Naranjo *et al.* (2015) found that tropical cyclones enhance groundwater recharge.

The reviewed literature on GW-SW interactions highlights several limitations in both global and local case studies. At the global scale, there is a scarcity of sampling points, resulting in limited data availability. Conversely, local studies often focus on a single season, which restricts the understanding of seasonal effects on GW-SW interactions. Furthermore, many studies lack integrated methods for analysing these interactions. This study aims to address these limitations

by conducting comprehensive sampling across multiple sites and over two different seasons. This approach will facilitate a more robust comparison of data and seasonal effects. Additionally, the study integrates various methods for analysing GW-SW interactions, such as $\delta^{18}O$, $\delta^{2}H$, ^{222}Rn, Hydrochemistry, baseflow separation, and piezometric analysis.

The literature reviewed in this chapter is aligned with the study's objective. The first objective is to investigate the characteristics of rainfall isotopes; the study investigates the rainfall characteristics of the specific study areas and how they align with the previous studies that have been done. The second objective of the study is to investigate factors of GW and SW interactions, such as geology, topography, lineaments, dykes and land use. Literature on the discussion of these factors was discussed and in this study, they were investigated on how they affect the connection of GW-SW interactions. Furthermore, the mechanism of groundwater recharge is the last objective, and in this study, literature on contributions of extreme rainfall patterns in groundwater recharge, such as ENSO and tropical cyclones, was discussed.

This study aims to investigate GW-SW interactions within the uThukela Catchment by developing a conceptual model that elucidates the dynamics governing water movement in the area. By understanding these interactions, the study assessed the vulnerability of the stream network, which will lead to improved water resource management strategies tailored to the catchment's specific conditions. The conceptual model is expected to serve as a foundation for future hydrological modelling efforts, ultimately enhancing the knowledge of the factors driving water behaviour in the uThukela Catchment and supporting sustainable water management practices.

CHAPTER THREE: DESCRIPTION OF THE STUDY AREA

3.1 Introduction

This chapter describes the location, geology, lineaments, topography, rainfall, climate and land use for the study area, which are important for understanding GW-SW interactions. The study area is in KwaZulu-Natal, South Africa, as shown in **Figure 3.1**. The main areas of interest for the research study are Cathedral Peak, Winterton and uThukela River. The interest of the areas is to investigate the different roles of groundwater at multiple spatial scales.

3.2 Location of study area

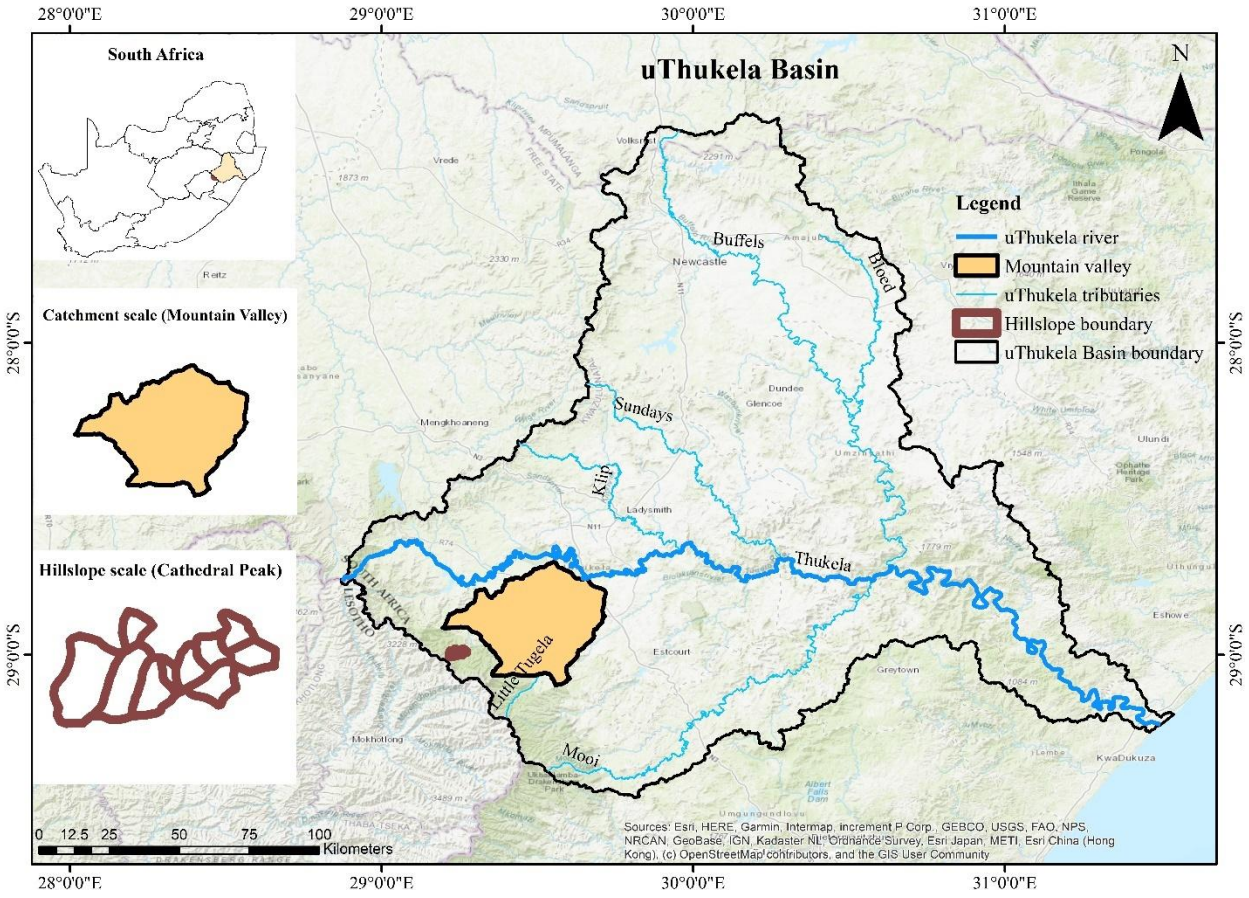

Figure 3.1: Location of study area

The study area encompasses three distinct spatial scales for investigation: hillslope scale (Cathedral Peak), catchment scale (Winterton), and regional scale (uThukela Catchment). The

uThukela Catchment is located in the KwaZulu-Natal province of South Africa, covering an area of approximately 29,100 square km (**Figure 3.1**). The river originates as a stream on the 3050-metre-high Mont-aux of the Drakensberg Mountains and flows for a distance of 405 km through the KwaZulu-Natal midlands (Ingrid Dennis and Rainer Dennis, 2009), making it the province's largest river. Along its course, it is joined by several other tributaries (**Figure 3.1**). Eventually, the uThukela River empties into the Indian Ocean, approximately 84 km north of Durban.

Winterton is a small town situated on the banks of the Little Tugela River in the foothills of the Drakensberg Mountains. Cathedral Peak is a mountain catchment located within the Drakensberg Mountains, serving as the uThukela River's headwater. The Cathedral Peak catchments comprise ten instrument catchments, including rain gauges and streamflow monitoring stations, that provide valuable hydrological data for research. This area is considered the most significant mountain catchment in South Africa due to its high-quality water and yield.

3.3 Geology

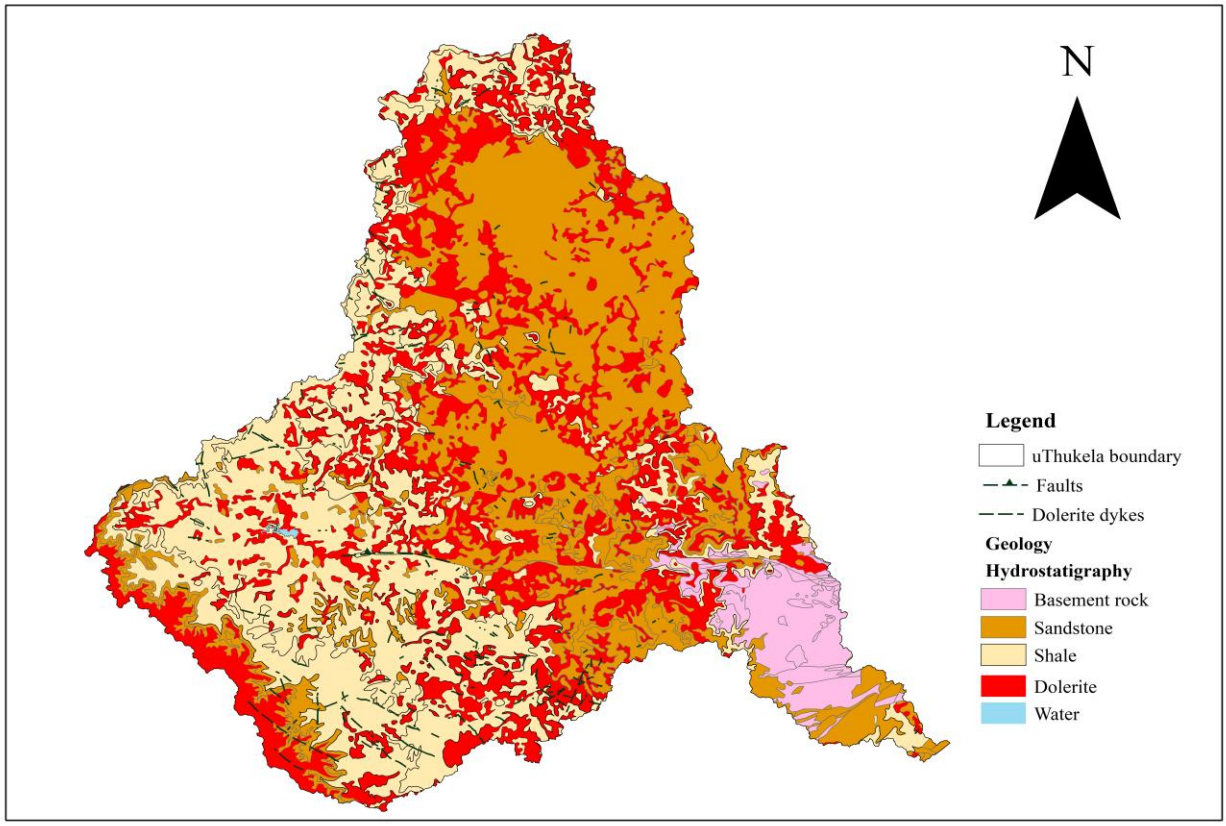

Figure 3.2: Geological map of the uThukela Catchment (source: Council for Geoscience)

Figure 3.2 demonstrates the geology of the uThukela River. According to the Council for Geoscience, the uThukela Catchment is dominated by the Karoo dolerite suite, which consists of dolerite and ultrabasic rocks. The Karoo dolerite suite is a group collection of dolerite intrusions that serve as a shallow feeder system for the Drakensberg flood basalt eruption in South Africa. Dolerite intrusion in the form of dykes and sills is common in the area (**Figure 3.2**). The dykes and sills can act either as a conduit or barrier of groundwater flow, having a significant effect on GW-SW interactions (Babiker and Gudmundsson, 2004).

The geology of the upper sections (Cathedral Peak) of the uThukela Catchment is the Drakensberg group, which is composed of basalts with minor sandstones, tuff, and agglomerate. Volkrust formation makes up the mid-reach of the uThukela, whereas Vryheid formation, which corresponds to fine-to-coarse grained sandstone, shale, and coal seams, makes up the lower reaches of the uThukela. The soil type of the catchment is closely associated with the area's underlying geology.

3.4 Lineaments

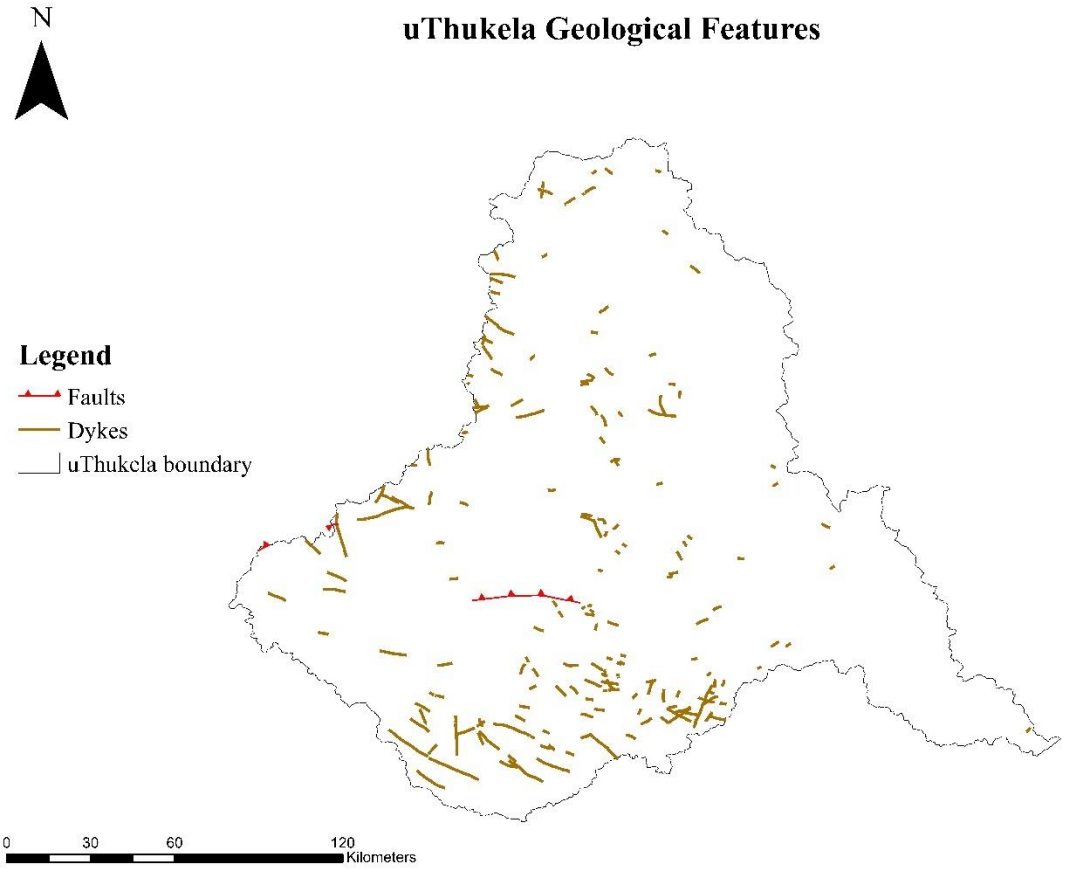

Figure 3.3: Lineaments of uThukela Catchment (source: Council for Geoscience)

The uThukela Catchment is characterised by an array of faults and fractures. According to **Figure 3.2**, the faults and fractures are mostly present within the Karoo dolerite suite, Volkrust formation (shale, siltstone and minor sandstone) and the Balfour formation (mudstone, siltstone). The faults and fractures zone are preferred groundwater storage and circulation zones in secondary aquifers, making them common for groundwater exploration targets. VonVeh and Andersen (1990) grouped the major lineaments of the uThukela based on their age and characteristics. Group I was tarche early and accurate faults consisting of the Mhlatuzi Fault in the Ngoye horst, Gingindlovu Fault, Amatikulu Fault in Darnall and the Ihloko Fault at the mouth of the uThukela. Group II included the coastal parallel faults, including the Darnall Fault at the mouth of the uThukela and the Umvoti Fault at passing through the Umvoti River Valley.

3.5 Topography

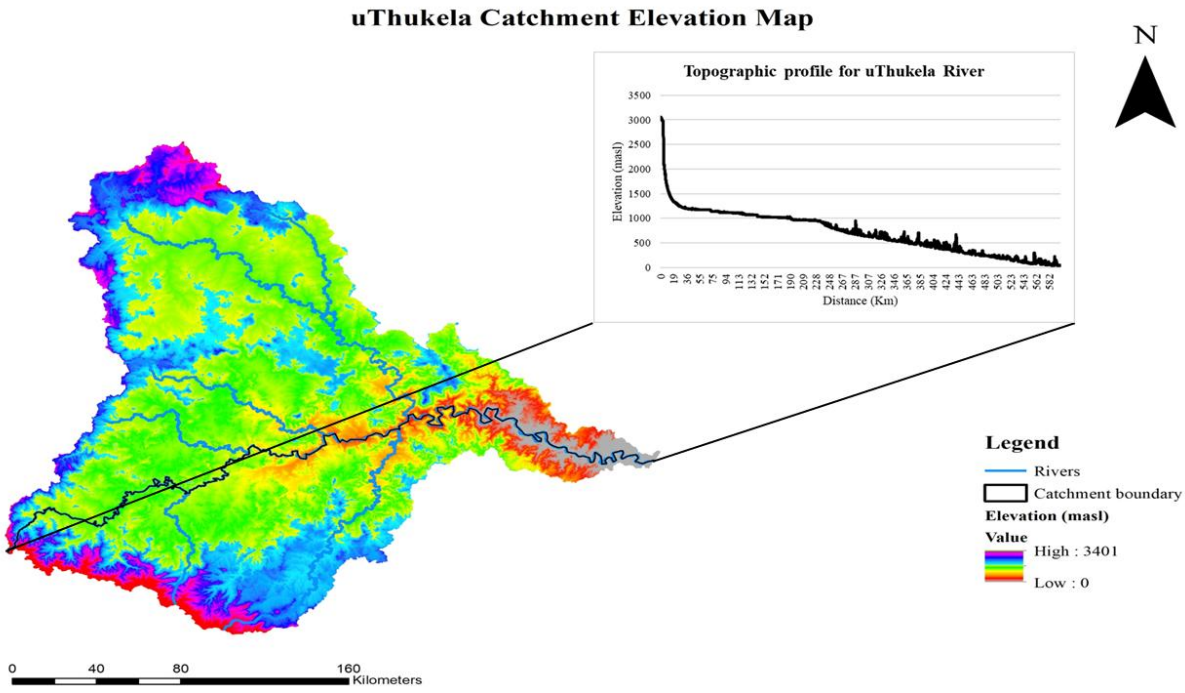

Figure 3.4: Topography of uThukela Catchment (source: Shuttle Radar Tropical Mission (STRM) 90m)

The uThukela Catchment spans an elevation range from 3,401 meters above sea level (masl) in the Drakensberg Mountains to just 0 masl in the low-lying coastal regions (**Figure 3.4**). This significant topographical variation contributes to the climate variability observed within the catchment. The high-elevated areas receive a mean annual precipitation (MAP) over 1300 mm, while the low-lying regions experience much drier conditions with only 600 mm of yearly rainfall (Mathinya *et al.* (2022). The uThukela River flows from the high Drakensberg peaks at 3,001 masl to the low-lying areas at just 0 masl.

3.6 Rainfall

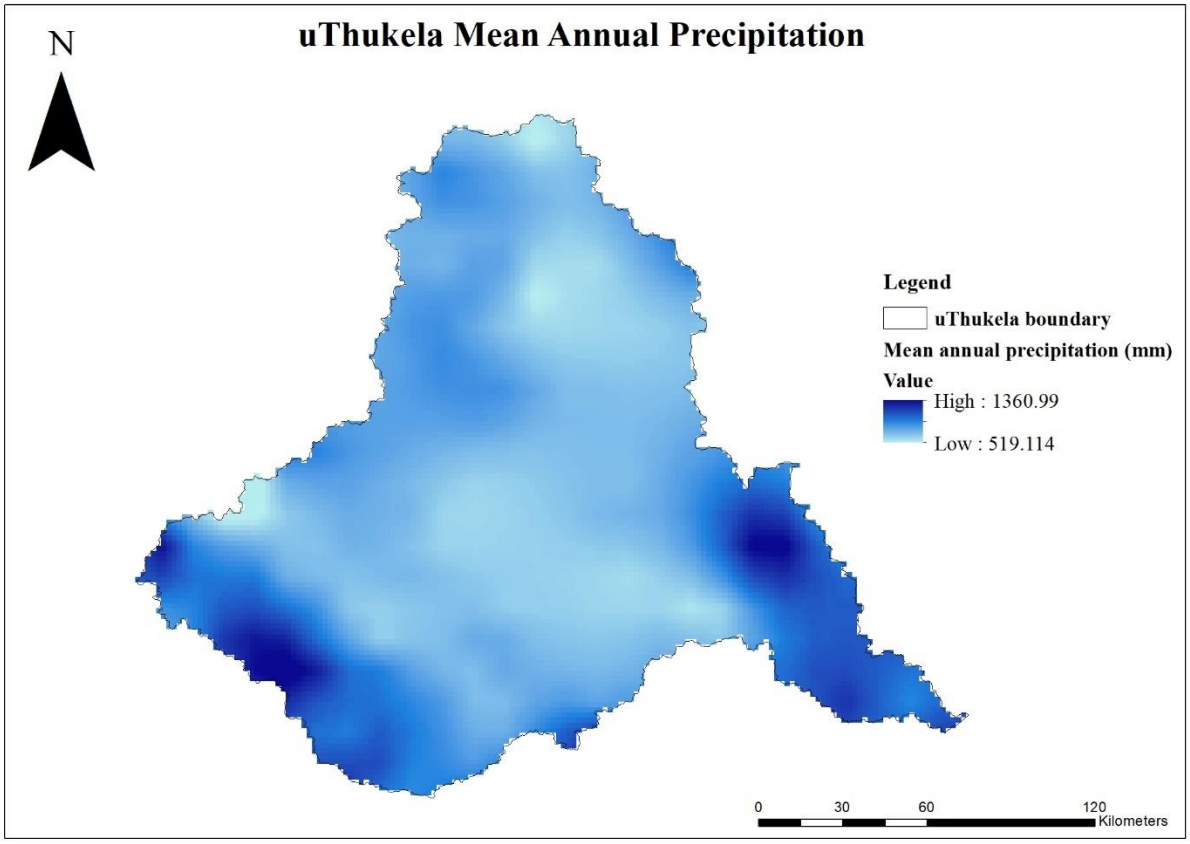

Figure 3.5: Mean Annual Precipitation for uThukela Catchment (source: Pegram DVD Backup. (2024). Retrieved from \pmb-cloud10\data\TRANSFER\Richard\Pegram_DVD)

Rainfall within the catchment exhibits significant variability and strongly correlates with relief. The rainfall is vividly seasonal, with over 80% occurring as thunderstorms during the periods between October and March. Inland areas experience peak rainfall from December to February, while coastal areas experience peak rainfall from November to March primarily because this period corresponds to the summer rainfall season in the region, which is influenced by warm, moist air masses from the Indian Ocean. MAP in the uThukela Catchment varies significantly across different regions. In the headwater areas of the catchment (Northern Drakensberg), MAP ranges over 1300 mm (**Figure 3.5**). In contrast, the western side of the catchment receives less than 600 mm of precipitation annually. Meanwhile, the coastal regions experience MAP of over 1000 mm.

3.7 Climate

The uThukela Catchment falls under the Mediterranean Maritime climate, characterised by moderately hot summers and mild to chilly winters (Ingrid Dennis and Rainer Dennis, 2009). Within the uThukela catchment, there is a wide range of climatic gradients and variability, spanning from the cool, wet conditions of the high-altitude Drakensberg to the hot, dry conditions of the lower-lying Thukela Valley and coastal regions. During summer season, the temperatures often exceed 35°C. In contrast, winter months are typically cold, particularly on the western and northern sides of the catchments, where temperatures frequently drop below freezing and frost is a regular occurrence.

3.8 Land use

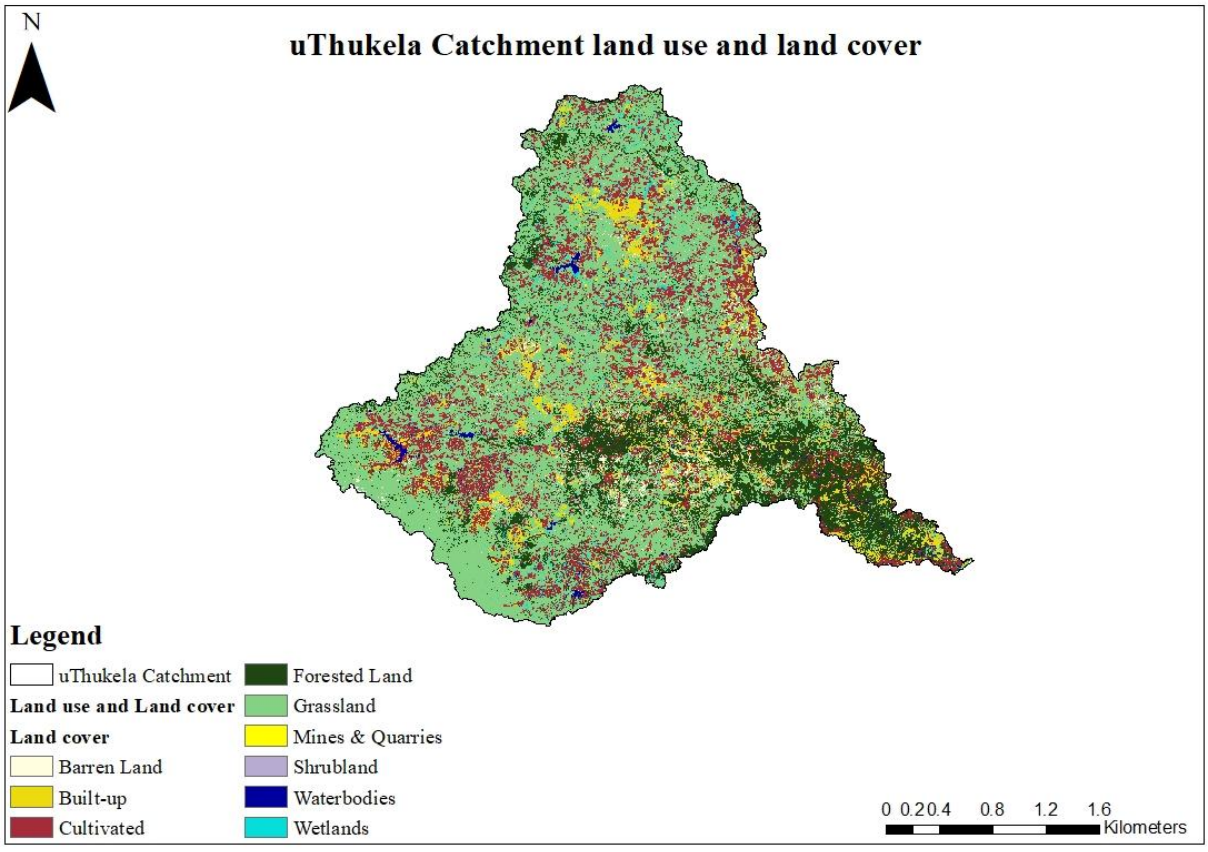

Figure 3.6: LULC in uThukela Catchment (source: South African National Land Cover (SANLC) 2018)

Figure 3.6 demonstrates the uThukela Catchment's various LULCs, such as built-up areas, forested land, waterbodies, barren land, mines, and quarries. A significant part of the Thukela Catchment is dedicated to agricultural activities, which primarily include subsistence farming, seasonal commercial dryland farming, temporary commercial irrigation, and commercial forestry (Ingrid Dennis and Rainer Dennis, 2009). LULC vary across the catchment with large areas of grassland; 15% of the catchment is utilised for agriculture, 8% is barren terrains, and around 1% is used for urban purposes (Moodley *et al.*, 2023). It is critical to study LULC change during GW-SW interaction because varied land use, for example, forested land, can increase groundwater recharging and control flow, while barren regions can inhibit infiltration (Rahman, 2008).

CHAPTER FOUR: MATERIALS AND METHODS

4.1 Introduction

This chapter outlines the methodologies and materials utilised in this research study focused on GW-SW interactions. A field programme was piloted from June 2023 to December 2024, during which data was collected monthly and seasonally to gather site-specific information within the study area. The field program encompasses a variety of data collection sites, including boreholes, streams, wetlands, springs, lakes, and rainfall stations. Different methods and materials were utilised to investigate GW-SW interactions, including stable isotopes, radon, hydrochemistry, baseflow separation, and piezometric analysis. Data analysis and interpretation of the data from these methods assisted in achieving the study's objectives.

4.2 Sampling procedure and analysis

4.2.1 Field sampling

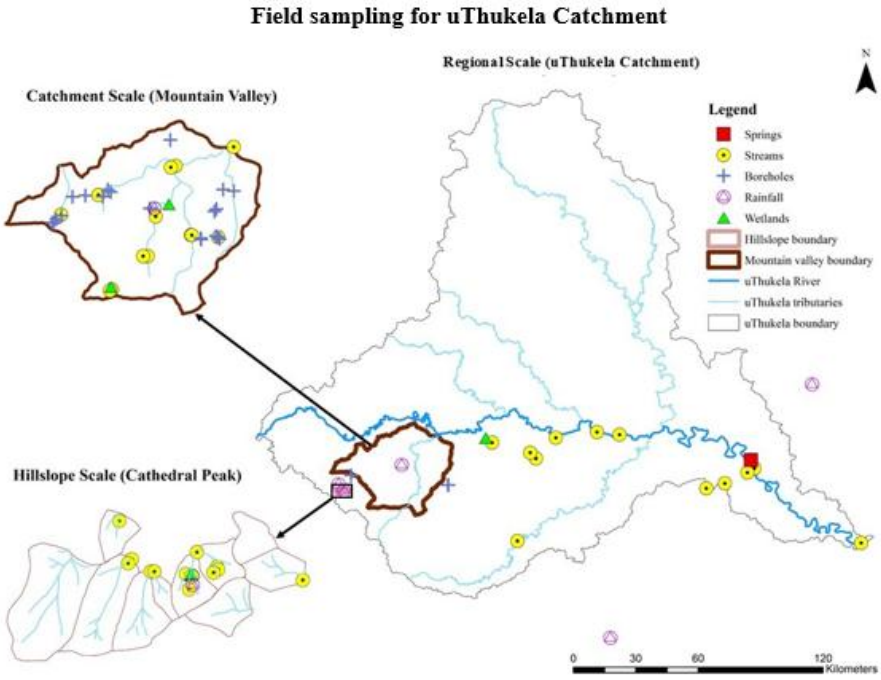

Figure 4.1: Field sampling map

The field sampling for this study was organised into three spatial scales: the hillslope scale, the catchment scale, and the regional scale. The hillslope scale sampling was conducted at Cathedral

Peak monthly (July 2023 to December 2024). This approach aimed to investigate the role of local groundwater recharge in the area. The catchment scale sampling occurred at Winterton (the mountain valleys), where samples were collected during the dry and wet seasons (July 2023 to December 2024). This sampling was designed to explore the influence of intermediate groundwater, specifically groundwater that originates from the surrounding mountains and discharges to the valley. Finally, the regional scale samples were obtained from the main uThukela River during the wet season (March 2024 to April 2024). The objective here was to examine the role of deep regional groundwater discharge. Sampling sites were selected based on accessibility, ensuring that each location was practical for data collection.

During the sampling process, careful procedures were implemented to ensure proper sampling techniques. The geographical coordinates (longitude and latitude) and elevation were recorded for each sampling site. For measuring all water samples (groundwater, surface water, and rainfall), a 500 mL beaker was used to collect the samples for in-situ measurements (Temperature, EC, pH). To ensure accurate measurements and prevent contamination from previous samples, the beaker was rinsed three times with the water sample before collecting the final sample.

For surface water sampling, shallow stream samples were taken from the centre of the flow. In the case of wide, deep streams, a bailer was used to collect samples from the centre of the stream to ensure that the water was well-mixed. For sampling groundwater from boreholes, the following procedure was followed:

1. The borehole was pumped or purged for five minutes to flush out any residual water in the borehole.
2. After flushing, the beaker was rinsed thrice with the flowing water from the borehole.
3. Finally, the sample for in-situ measurements was collected using the rinsed beaker.

Wet season data collection was conducted from December 1, 2023, to May 31, 2024, while dry season sampling took place from July 1 to September 30, 2024. This seasonal sampling aimed to capture significant variations in the isotopic composition of natural water sources, including precipitation, surface water, and groundwater. A total of 95 sites were sampled throughout the study, which included 5 rainfall samplers, 55 streams, 27 boreholes, and 4 springs

4.2.2 Rainwater collection

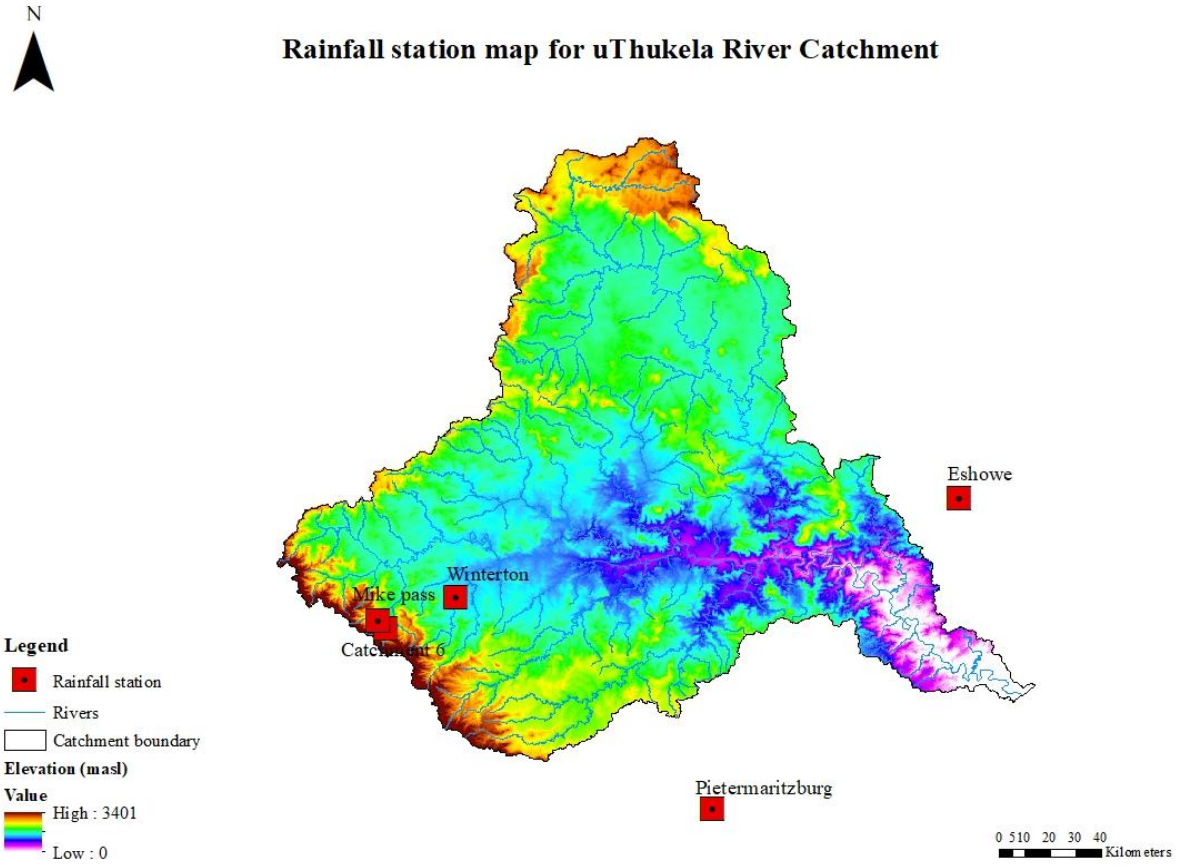

Figure 4.2: Installed rainfall stations at uThukela Catchment (source: STRM 90m)

Rainfall collectors were installed at five different locations that vary in elevation to investigate the effects of altitude on rainfall characteristics, amount, seasonality, interannual variability, and continentality. Two collectors were installed at Cathedral Peak, Drakensberg, the headwater of the uThukela Catchment, at Catchment 6 (Lat: -28.993°S, Long: 29.251854°E, Elevation: 1921 masl) and Mike Pass (Lat: -28.975°S, Long: 29.235°E, Elevation: 1620.9 masl). Another collector was installed at the foot of Cathedral Peak at Winterton (Lat: -28.882°S, Long: 29.501°E, Elevation: 1102.7 masl). The remaining two collectors were located outside the uThukela Catchment in Pietermaritzburg (Lat: -29.628°S, Long: 30.403°E, Elevation: 627 masl) and Eshowe (Lat: -28.886°S, Long: 31.461°E, Elevation: 522.42 masl) due to accessibility and permission considerations.

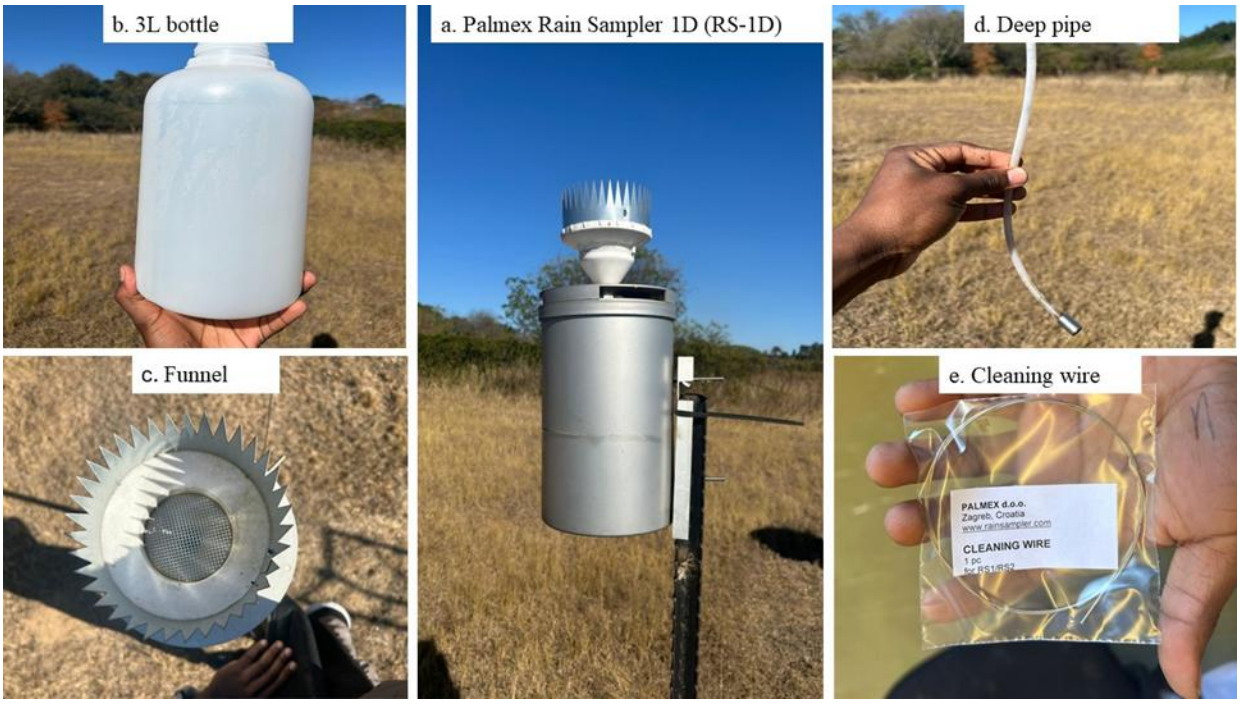

Figure 4.3: Palmex Rain Sampler (RS-1D)

The rainwater was collected using a Palmex Rain Sampler RS-1D, specifically designed to store precipitation without evaporation or fractionation for extended periods, making it ideal for collecting rainwater isotope samples over long durations. The rainwater enters the plastic bottle (**Figure 4.3b**) through the funnel (**Figure 4.3c**) and the deep pipe (**Figure 4.3d**). The funnel has sharp edges at the top to protect against birds and insects and a stainless-steel mesh inside to prevent dirt from entering the bottle. After collecting the rainwater sample using a 15 mL sampling bottle, the deep pipe is cleaned using a cleaning wire (**Figure 4.3e**) to remove any dirt or green algae growth.

Monthly rainwater samples were collected at four locations (Catchment 6, Mike Pass, Winterton, and Eshowe) during the dry and wet seasons. Daily samples were collected at the Pietermaritzburg rain sampler, installed on the University of KwaZulu-Natal campus for easy collection. The sampling occurred daily at 8:00 AM. The rainfall samples were stored in 15 mL centrifuge tubes and taken to the hydrology isotope laboratory at the University of KwaZulu-Natal, where they were refrigerated at 5°C until stable isotope analysis.

4.2.3 Event-based sampling

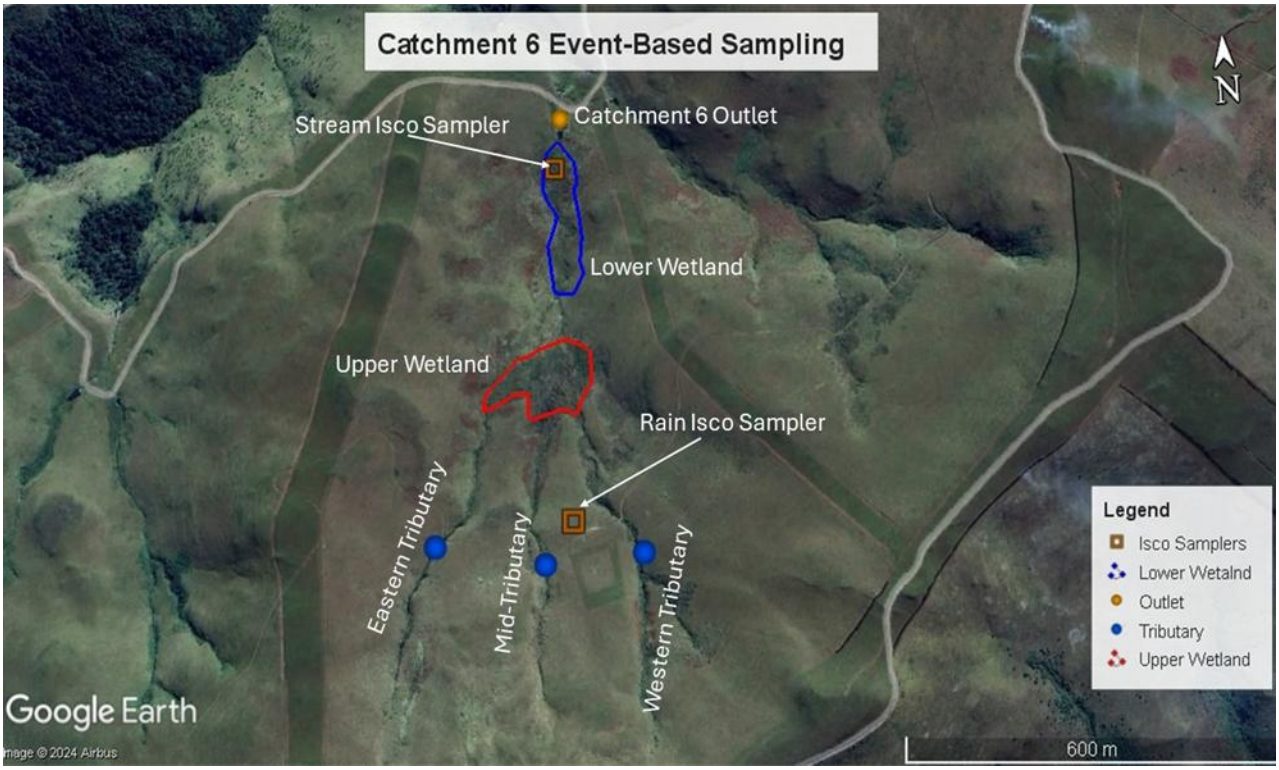

Figure 4.4: Event-based sampling points

Event-based sampling was conducted for 48 hours at Catchment 6 on Cathedral Peak to study the GW-SW interaction on a hillslope scale during a rainfall event. An automatic ISCO 2900 sampler was installed at the headwater for rainfall collection and at the outlet of Catchment 6 for streamflow sampling, to enable high-frequency event-based sampling during rainfall events. At the head of Catchment 6, a Rain Isco Sampler was installed to collect rainfall near the three tributaries. This sampler consisted of 24 rotating bottles that were programmed to collect samples within an hour. A funnel attached to a metal rod, pegged to the ground, directed rainwater into the sampler. After the initial 24 hours of sampling, the cycle was repeated for another 24 hours to complete the 48-hour sampling period. 48 rainwater samples were collected for stable isotope analysis, and in-situ measurements of hydrochemistry were also taken. The volume of water in each bottle was recorded along with the time of collection for each sample.

The Stream Isco Sampler, installed at the outlet of catchment 6, was used to sample water from the stream originating from the three tributaries at the top. A pipe installed in the Stream Isco

Sampler was placed into the stream, and water samples were collected for 48 hours into the 24 sampling bottles in the automatic sampler. After the 24-hour sampling was completed, the sampling cycle was repeated to finish the 48-hour sampling. This was done to trace GW-SW interactions in the catchment using stable isotopes and EC. The event-based sampling aimed to investigate how the groundwater-fed tributaries in the catchment contribute to the catchment outlet during the rainfall period.

Figure 4.5: Isco Sampler

4.1.2 Stable isotopes

Stable isotope samples were collected in the dry and wet seasons from typical surface water (wetlands, springs, and streams), groundwater (boreholes and monitoring wells) and rainfall samples from the five installed rainfall collectors on the catchment (**Figure 4.2**). The rainfall samples were collected monthly from all five rainfall collectors, and the Pietermaritzburg samples were collected daily for stable isotopes. In Cathedral Peak, monthly stable isotope samples were taken from the nine different catchments. The stable isotopes from Cathedral Peak were used to

quantify the contribution of groundwater to streamflow generation at a hillslope scale, with a particular focus on baseflow.

During the stable isotope sampling, elevation, longitude and latitude coordinates were recorded. The samples were collected using 15 mL centrifuge tubes; the bottles were sealed tightly and stored in a cooler box to avoid evaporation and fractionation. The samples were then taken to the isotope hydrology laboratory at the University of KwaZulu-Natal, where they were stored in a refrigerator at 5°C until stable isotope analysis.

4.1.3 Stable isotope data analysis

Before the analysis, the isotope samples were taken from the 15 mL centrifuge tubes that had collected the water samples using a 10 mL syringe and filtered through a 0.45 µm syringe filter to remove contaminants from the samples before the analysis. The filtered samples were transferred into 2 mL vials sealed with a silicon septum to avoid evaporation during analysis and stacked into an autosampler tray with specific positions according to the Laboratory Information Management System (LIMS) for Stable Hydrogen and Oxygen Isotopes in Water. The analysis was conducted in the Isotope Hydrology Laboratory at the University of KwaZulu-Natal using the LGR-ICOS GLA431 Series Analyser. With the help of a fully automatic sampler, the analyser automatically measured the isotope samples according to a computer program. Each vial underwent nine injections, with the initial three measurements discarded to mitigate the memory effect, which refers to the impact of the previously injected sample on the isotopic content. The final reportable value was determined by averaging the results of the last six injections.

Three reference standard samples from the Vienna Standard Mean Ocean Water (VSMOW) were measured at intervals of three water samples to diagnose whether an abnormality occurred during the measurements. The standards help to determine whether the sample is isotopically enriched or depleted. The VSMOW is used as a reference point for comparing the water samples' isotope ratios ($^{2}H/^{1}H$ and $^{18}O/^{16}O$) to a known and stable baseline. The Isotope Laboratory at the University of KwaZulu-Natal used its own standards (Evian water, Midmar water and a mixture of both Evian and Midmar) calibrated against the primary VSMOW standard. The isotope results were reported

as a notation δ (delta) and expressed as ‰ (per mille). The general equations for calculating δ for ^{18}O and ^{2}H are:

$$\delta^{18}O = \frac{\left(\frac{^{18}O}{^{16}O}\right) sample - \left(\frac{^{18}O}{^{16}O}\right) standard}{\left(\frac{^{18}O}{^{16}O}\right) standard} \times 1000 \quad (4\text{-}3)$$

$$\delta^{2}H = \frac{\left(\frac{^{2}H}{^{1}H}\right) sample - \left(\frac{^{2}H}{^{1}H}\right) standard}{\left(\frac{^{2}H}{^{1}H}\right) standard} \times 1000 \quad (4\text{-}4)$$

The raw isotope data measurements were taken from the LGR-ICOS GLA431 Series Analyser and imported to LIMS for Lasers 2015 (v10.092) for quality control. The isotope raw data measurements were checked, and any bad samples were discarded and repeated. All samples in this study underwent strict quality control check measures, and the isotopic measurement results were successful.

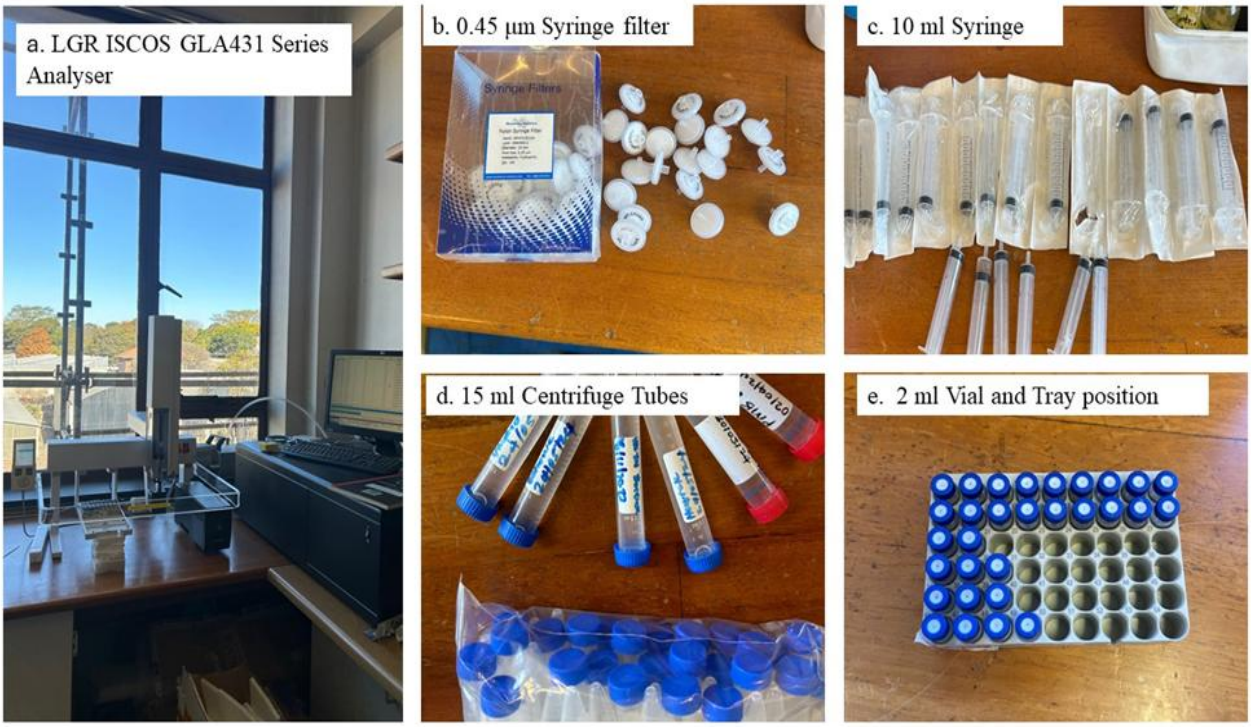

Figure 4.6: Isotope analysing equipment

4.1.4 Radon

Twenty-one radon measurements were taken from the main uThukela River during the wet season to identify the locations and amounts of groundwater entering streams. This approach has been utilised in several previous studies (Ellins *et al.*, 1990; Cook *et al.*, 2003; Baskaran *et al.*, 2009) that have highlighted the usefulness of radon in this regard. ^{222}Rn concentration measurement of water samples was carried out using a portable radon instrumentation RAD-7 (Durridge, USA). The radon measurement was performed in situ using the big bottle system (2.5L); an accessory to the RAD-7 radon monitor was used.

Before taking measurements, it was essential to ensure that the RAD7 was dry and free of radon. To achieve this, the device was purged for an extended period using a large laboratory drying unit. The duration of the purging process was contingent upon the relative humidity of the RAD7; purging continued until the relative humidity approached 10%. The 2.5L big bottle was used to collect water from the surface. The sample was taken carefully and cautiously. The bottle was submerged in the open surface water, and the water was allowed to fill it. The bottle was quickly

sealed with a cap to avoid contact with air. A few mL was decanted to leave a few air spaces to enable aeration of the water and to prevent the bottle from breaking during the expansion of water. During the sample collection, the temperature was also taken using the Hanna Hl-98129, which was taken to interpret the radon data later. The RAD7 pump was set to on, which aerated the water sample. One sample took one hour with intervals of a 15-minute cycle, so four cycles were done per sample. However, after 45 minutes from the start, the aeration was complete, the pump was turned to auto mode, and the clip was opened. This is because the radon in the air loops is close to equilibrium with the radon remaining in the water.

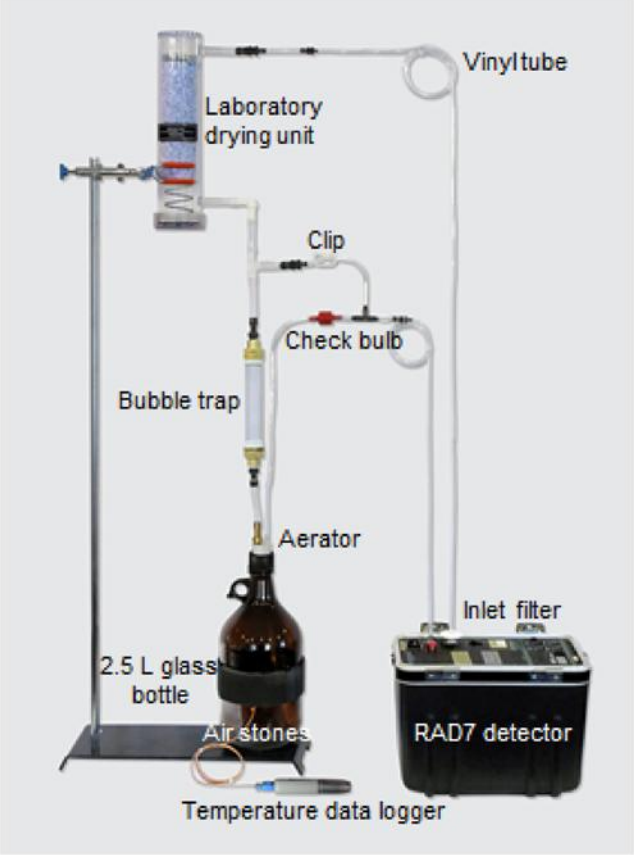

Figure 4.7: Big bottle system set up (Durridge Company Inc, 2022)

4.1.5 Radon analysis

The radon data was downloaded from the RAD-7 to the computer using Capture software version 6.2.7 (Rad7 (radonlab.com)), which facilitates effective data management and analysis. The radon measurement method was set to the Big Bottle System to automate the calculation of radon in

water based on the RAD7's reported radon in air. The temperature data collected during the radon sampling was stored in the Capture software for each radon run. After storing the temperature data, Capture converted the RAD-7's radon in air measurements to radon in the water sample, taking into account the equilibrium ratio influenced by the temperature at the air/water interface. Additionally, it is noted that out of the four radon cycles performed, the first cycle was discarded to eliminate potential outlier data. The average of the remaining cycles was then calculated to determine the mean radon concentration for that specific site.

4.1.4 Hydrochemistry

In situ (temperature, pH, and EC) measurements were conducted using a Hanna (Hl-98129 and Hl-98130) Waterproof Portable Meter. The Hanna Waterproof Portable Meters were calibrated before each field sampling to ensure accurate measurements. The hydrochemistry of rainfall, groundwater and surface water was measured in situ using a 200 mL beaker; the beaker was rinsed 3 times with the sample water and distilled water to ensure accurate readings. Hydrochemistry, especially EC, is used in various hydrogeological studies as a tracer of groundwater recharge and discharge (Kebede *et al.*, 2005; Liu and Yamanaka, 2012; Wang *et al.*, 2013b). Therefore, hydrochemistry (EC) helped determine the sources of groundwater recharge, groundwater discharge to streams, and the role of groundwater in streamflow generation.

4.1.5 Baseflow separation

Baseflow separation is used to separate and interpret baseflow from streamflow in hydrographs. This technique is important for understanding the dynamics of groundwater discharge into streams (Rumsey *et al.*, 2015). Baseflow is the sustained flow of a stream that originates primarily from groundwater discharge, representing the release from groundwater storage, and may also include delayed subsurface flow through unsaturated zones (Singh, 1968; Winter, 2007). This study used baseflow separation to determine the contribution of groundwater to the stream networks along the uThukela Catchment. To do so, streamflow data for the uThukela Catchment was downloaded from the Department of Water and Sanitation's website (https://www.dws.gov.za/). Streamflow data was downloaded from 23 selected drainage stations **(Figure 4.8**) based on the long duration of data availability. The long dataset assists in accurate baseflow estimation across the years.

The streamflow data was then imported into the BFI+ 3.0 software (BFI+ 3.0 Download (Free) - BFI+ 3.0.exe (informer.com)). In BFI+ 3.0, the local minimum method was chosen among the other baseflow separation techniques. This approach is advantageous in identifying baseflow recession patterns, which are essential for understanding GW-SW interactions and managing water resources effectively. From the streamflow data, BFI+3.0 computes baseflow and the Baseflow Index (BFI), which measures the proportion of baseflow to total streamflow. The data was then exported to Microsoft Excel 2022, and the average BFI index was calculated for each of the 23 drainage stations. Finally, a spatial variation analysis was conducted in ArcMap 10.8 to determine how baseflow varies within the uThukela Catchment.

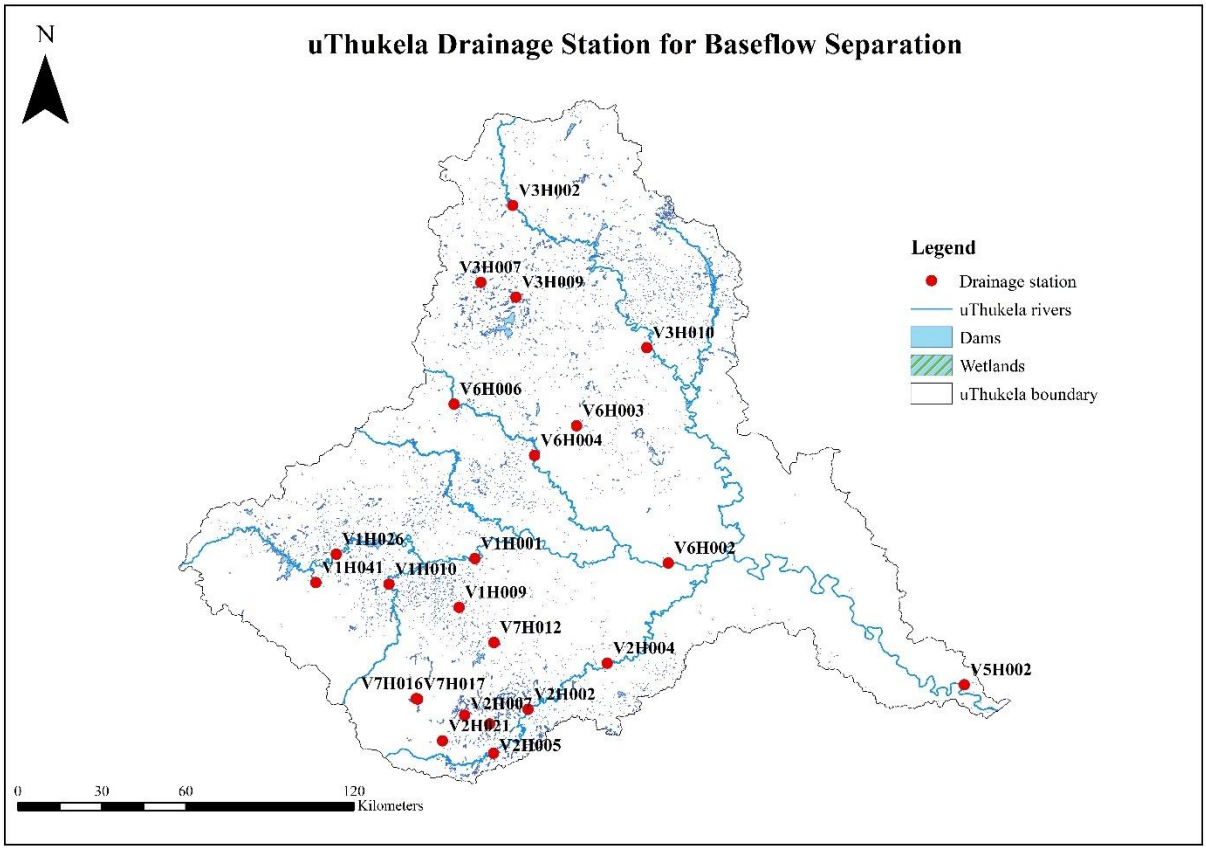

Figure 4.8: Drainage station for baseflow separation

4.1.6 Piezoemtric analysis

The piezometric analysis is a method used to monitor fluctuations in groundwater levels in aquifers and their correlation to rainfall. This analysis assists in determining the behaviour and

characteristics of the aquifer in that area. The rainfall and groundwater level time series data used in this study were obtained from the Department of Water and Sanitation (https://www.dws.gov.za/Hydrology/Verified/HyStations.aspx?Region=V&StationType=rbRiver) and the National Groundwater Archive website: https://www.dws.gov.za/NGANet/Security/WebloginForm. Six boreholes (BHs) within the uThukela Catchment were selected based on data quality and the duration of monitoring records. Corresponding rainfall stations near each borehole were also selected. The groundwater level and rainfall data were processed and plotted in Microsoft Excel 2022. Time series graphs were generated to visually assess trends, while cross-correlation analysis was used to quantify the relationship between rainfall events and subsequent changes in groundwater levels.

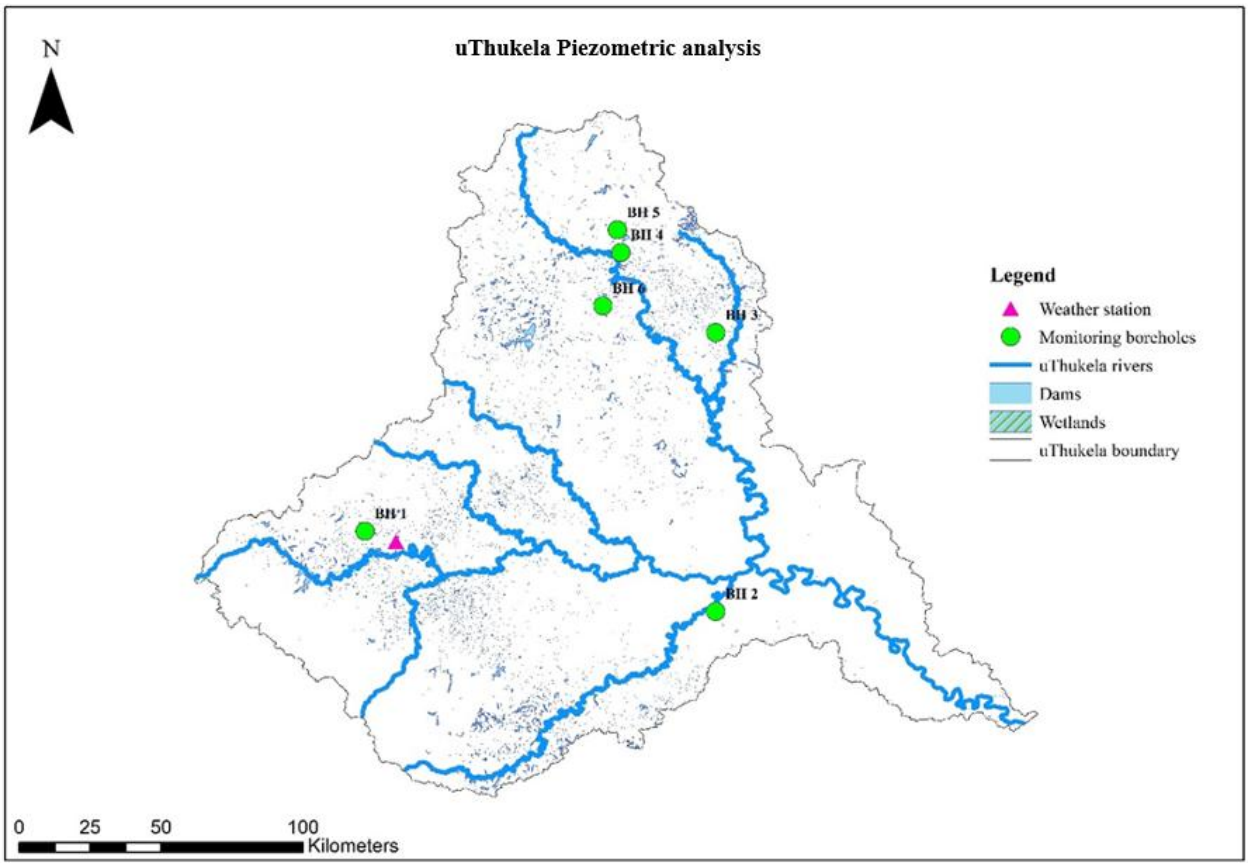

Figure 4.9: Monitoring boreholes and weather stations used for piezometric analysis

CHAPTER 5: RESULTS

5.1 Introduction

This chapter presents the findings obtained through various methodologies applied during this research. The initial results focus on the rainfall isotope characteristics, illustrating the isotope effects. The following sections include interactions between GW and SW at three different scales: regional, catchment, and hillslope. At the regional scale, ^{222}Rn, baseflow separation, hydrochemistry, and piezometric analysis are presented. On the catchment scale, stable isotope and hydrochemical data are presented. Similarly, at the hillslope scale, hydrochemical and isotope data are also presented.

5.2 Rainfall isotopic composition

A total of 250 rainfall samples were analysed for stable isotope composition (δ^2H and $\delta^{18}O$) to characterise rainfall isotopes across varying altitudes. Specifically, 198 samples were collected from Pietermaritzburg, 10 from Eshowe, 16 from Winterton, 19 from Mike Pass, and 7 from Catchment 6. The Pietermaritzburg samples were collected daily from March 2022 to July 2024, while the monthly rainfall samples for Eshowe, Winterton, Mike Pass, and Catchment 6 were based on the cumulative rainfall recorded between the dates of the previous and subsequent sample collections.

Table 5.1: Summary of rainfall isotope data from five sampling stations

Stations	**Sampling Period**	**Rainfall Range (mm)**	**δ^2H Range (‰)**	**$\delta^{18}O$ Range (‰)**	**Amount-Weighted Mean δ^2H (‰)**	**Amount-Weighted Mean $\delta^{18}O$ (‰)**
Eshowe	Jun 2023 – Jul 2024	5.2 – 598.8	-12.92 to 1.5	-3.69 to -0.69	-8.53	-2.94

Winterton	Mar 2023 – Jun 2024	1.8 – 246.8	-15.3 to 20.8	-4.31 to 0.68	2.15	-1.27
Mike Pass	Dec 2022 – Jun 2024	13.46 – 411.22	-26.4 to 11.1	-6.63 to -1.29	-9.6	-3.73
Catchment 6	Dec 2023 – Jun 2024	8.13 – 336.8	-23.4 to -3.2	-6.97 to -2.56	-10.69	-3.79
Pietermaritzburg	Mar 2022 – Jul 2024	0.26 – 107.4	-90.9 to 36.7	-13.11 to 4.36	-9.12	-3.21

5.2.1 D-excess

The d-excess provides useful information about evaporation processes, moisture sources (inland and oceanic moisture), and seasonal variations. It is influenced by the meteorological conditions in the regions where the water vapour originates. A high d-excess value (>10‰) indicates the presence of an additional moisture source, such as moisture recycling, among other possibilities (Wirmvem *et al.*, 2014; Durowoju *et al.*, 2019b). Equation 2.1 was used to calculated the d-excess for all rainwater samples (*n*-250) collected from the five stations.

In Pietermaritzburg, the d-excess values exhibited a wide range, fluctuating between -5.38‰ and 27.7‰, with a mean d-excess value of 15.75‰. In Eshowe, the d-excess values ranged from 7.02‰ to 22.14‰, resulting in a mean d-excess of 15.87‰. For Winterton, the d-excess value varied from 4.02‰ to 19.18‰ and had a mean d-excess of 12.19‰. For Mike Pass, d-excess ranged from 11.7‰ to 26.64‰, with a mean d-excess value of 20.07‰. Lastly, Catchment 6 displayed d-excess values of 15.28‰ to 32.36‰, with a mean d-excess value of 21.61‰.

Table 5.2: Minimum, maximum and mean values for d-excess for five different stations in the uThukela Catchment

Stations	**Min (‰)**	**Max (‰)**	**D-excess (‰)**

Pietermaritzburg	-5.38	27.7	15.75
Eshowe	7.02	22.14	15.87
Winterton	4.02	19.18	12.19
Mike Pass	11.7	26.64	20.07
Catchment 6	15.28	32.36	21.61

The results from **Table 5.2** demonstrated a variation in d-excess at the five stations in the uThukela Catchment, which could indicate variations in humidity and evaporation processes at the different locations. However, Mike Pass and Catchment 6 station located at the Drakensberg had the highest d-excess, which is correlated to temperature variations directly influencing moisture recycling, retention and distribution at the Drakensberg (Grab, 2013).

5.2.2 Local Meteoric Water Line (LMWL)

The LMWL represents a linear relationship between the isotopic compositions of δ^2H and $\delta^{18}O$ in local precipitation. Extensive datasets were utilised to construct the LMWL. Daily samples were used to develop the Pietermaritzburg LMWL, while monthly datasets were employed for the Eshowe, Winterton, Mike Pass, and Catchment 6 LMWLs. **Figure 5.1** illustrates the five different LMWLs created from rainfall isotope compositions (δ^2H and $\delta^{18}O$). The LMWLs for the various locations were established as follows: Pietermaritzburg; $\delta^2H = 7.36 * \delta^{18}O + 14.32$, Eshowe; $\delta^2H = 5.54*\delta^{18}O + 10.46$, Winterton; $\delta^2H= 6.5*\delta^{18}O + 11.76$, Mike Pass; $\delta^2H= 6.43*\delta^{18}O + 14.66$ and Catchment 6; $\delta^2H= 5*\delta^{18}O + 8.81$. These LMWLs constructed were compared to the GMWL ($\delta^2H = 8. * \delta^{18}O + 10.8$).

All the constructed LMWLs are placed above the GMWL. Three LMWLs exhibited slightly higher d-intercept values than the GMWL. Specifically, the d-intercept values are as follows: Pietermaritzburg (14.32), Winterton (11.76), and Mike Pass (14.66), while the GMWL has a d-intercept of 10.8; this implies that the processes of rain formation in these areas occur under near-

equilibrium conditions, with minimal evaporation effects during rainfall. The slightly elevated d-intercept values may also indicate that the rainwater originates from water vapour that has evaporated close to the land surface, which could result from either the re-condensation of previously evaporated rainfall or the evaporation of surface waters (Durowoju *et al.*, 2019b). However, Eshowe (10.46) and Catchment 6 (8.81) had a d-intercept lower than the GMWL; this could be attributed to changing atmospheric conditions, moisture and local climatic effects such as re-evaporation (Gonfiantini *et al.*, 1998; Durowoju *et al.*, 2019b).

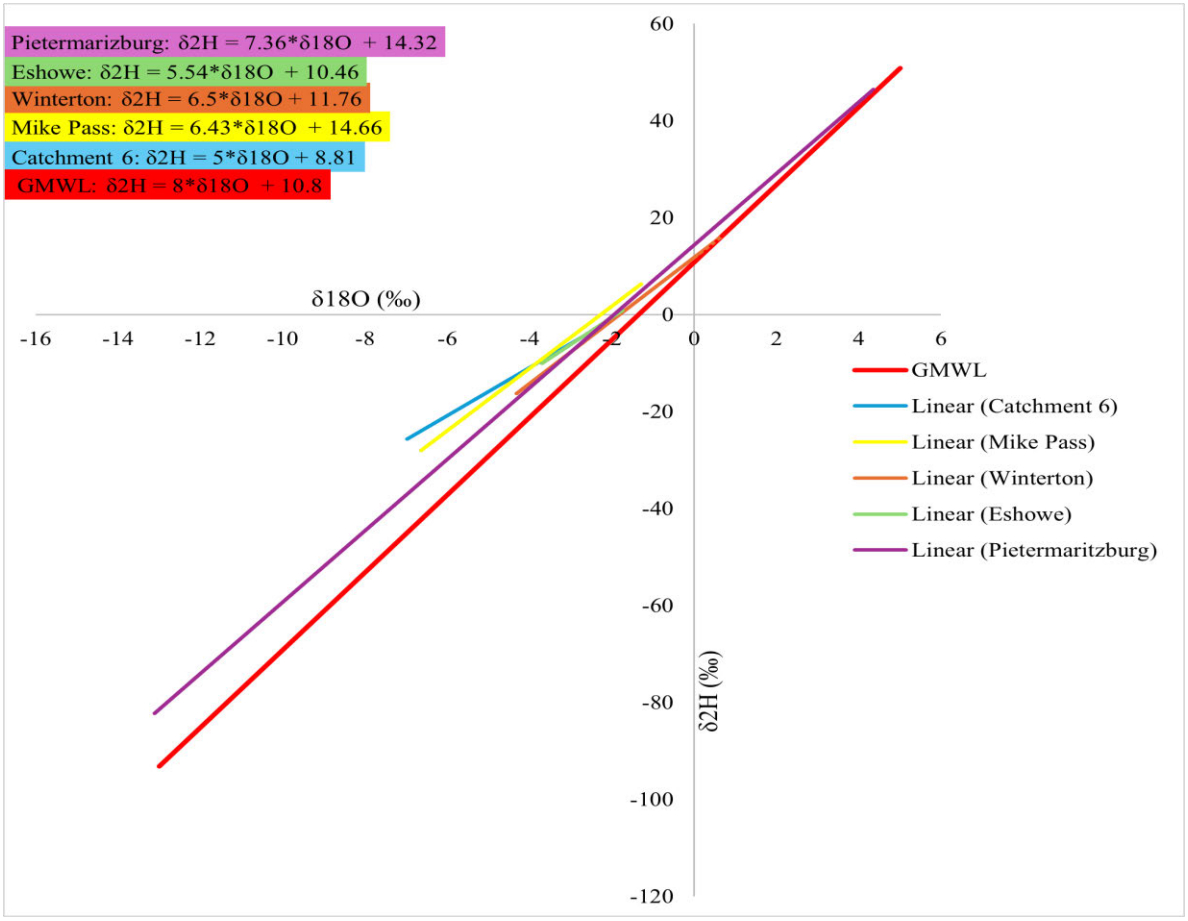

Figure 5.1: LMWL for all 5 stations and the GMWL

5.2.3 Rainfall Isotope Effects

5.2.3.1 Amount effect

The amount effect is primarily driven by differences in the evaporation and condensation processes of water. Consequently, during periods of high rainfall, the heavier isotopes are preferentially removed from the vapour phase and precipitate out as rain, leading to lower $\delta^{18}O$ values in the

remaining vapour. **Figure 5.2** shows the amount effect of all five stations of precipitation; this was assessed by plotting rainfall amount (mm) with $\delta^{18}O$. Most rainfall occurred during the wet season (October to April). In this study, the amount effect varies from location to location. **Figure 5.2** shows trends of the most light rainfalls having high $\delta^{18}O$ and high rainfall showing depletion of $\delta^{18}O$ (**Figure 5.2a,b**). However, Mike Pass and Catchment 6 show high rainfall having enriched values of $\delta^{18}O$ (**Figure 5.2c,d**). This data demonstrates that depleted values of $\delta^{18}O$ are not always affiliated with high rainfall. This may be due to the warm temperatures that facilitate evaporation and the use of monthly data sets. However, similar findings were demonstrated by Abiye *et al*. (2013), who showed that low $\delta^{18}O$ values are not always associated with high rainfall.

Clear evidence of the rainfall amount effect was observed from the Pietermaritzburg station (**Figure 5.2e**); on the 5th of April 2022, there was an intense storm in Pietermaritzburg, and on this day, a high rainfall amount was received (71.12 mm), and the lowest $\delta^{18}O$ value of -13.11‰ was recorded. The data provided a clear indication of $\delta^{18}O$ depletion during periods of high rainfall. However, in contrast, on the 17th of April 2022, a rainfall amount of 107.4 mm was observed in the Pietermarzitburg station, and an $\delta^{18}O$ value of -4.22‰ was observed. The variation in $\delta^{18}O$ value in these high rainfall events could be attributed to the intensity and duration of the rainfall period. Similarly, a study by You *et al.* (2021) indicated typhoon rainfall tends to have higher $\delta^{18}O$ values compared to plum rains due to shorter durations and less isotopic fractionations. Furthermore, the $\delta^{18}O$ data in **Figure 5.2** could be due to moisture recycling .

a. Winterton

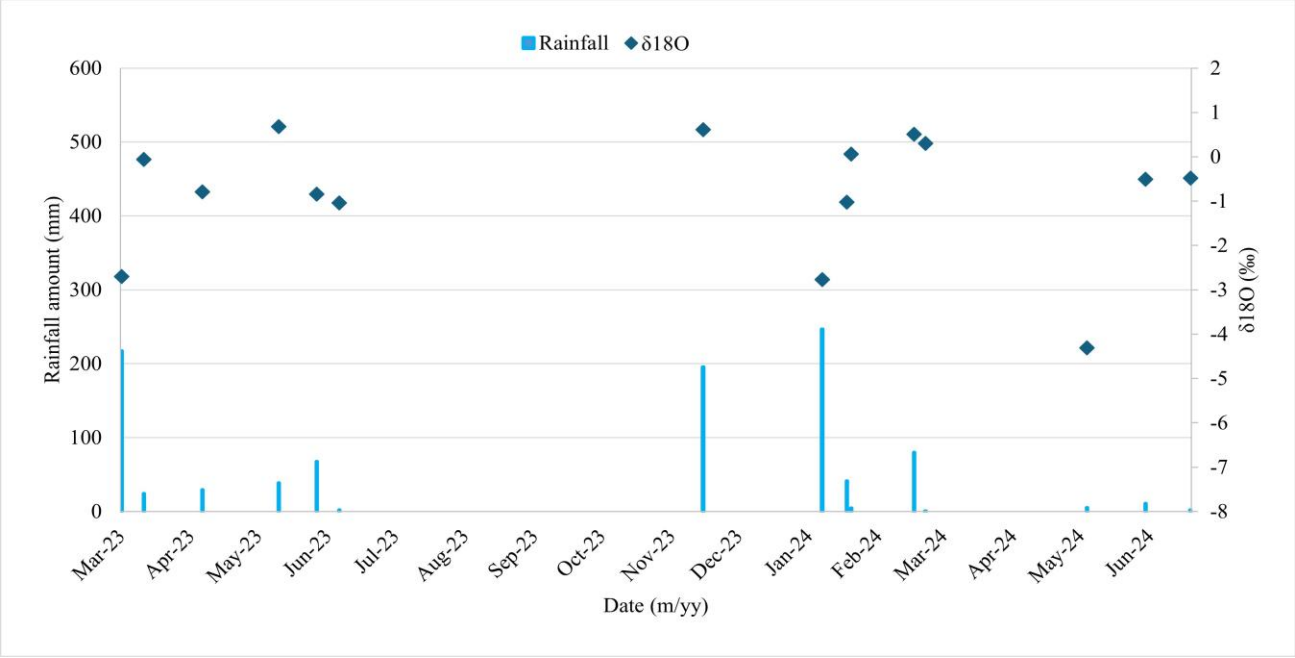

b. Eshowe

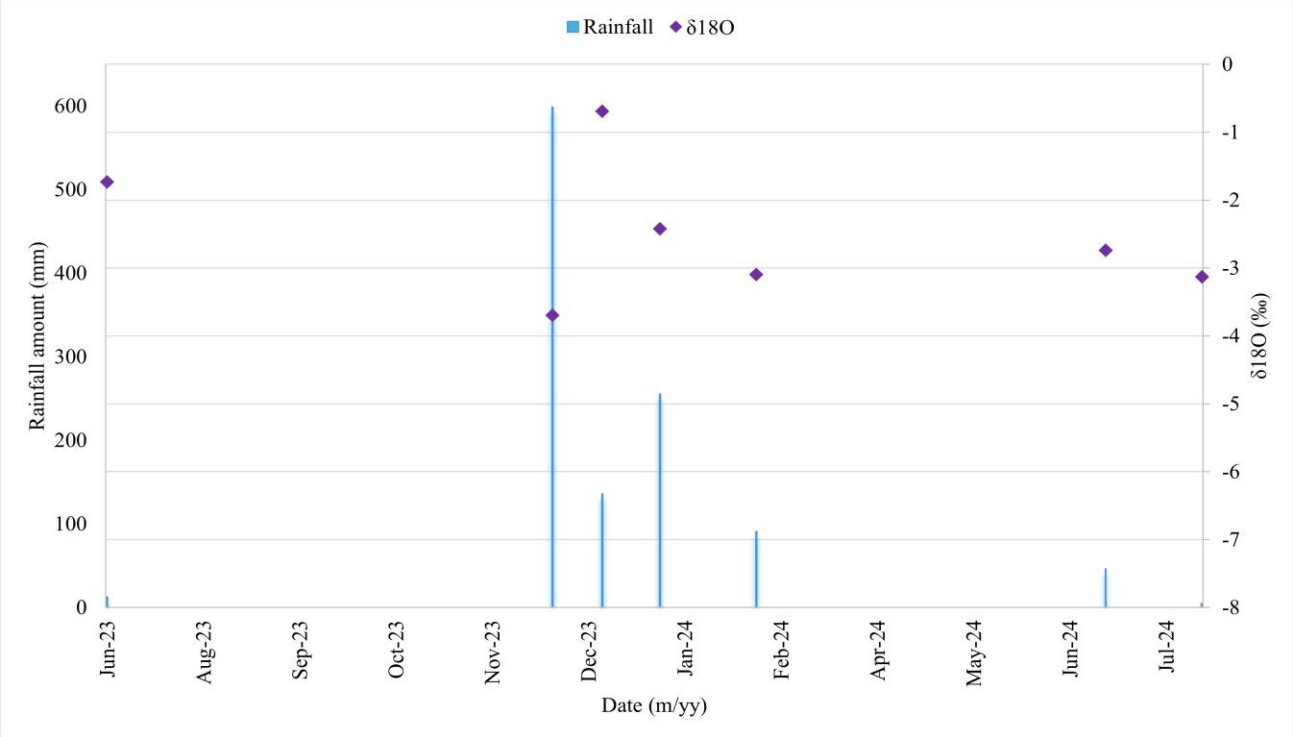

c. Mike Pass

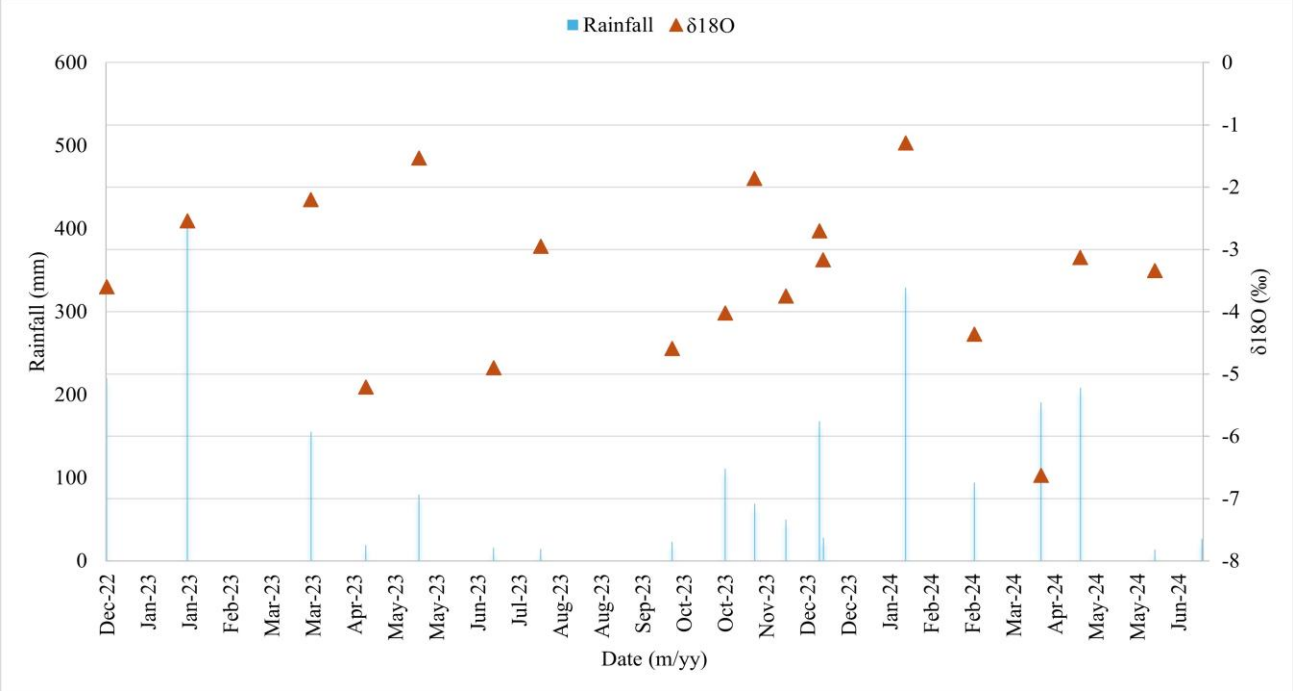

d. Catchment 6

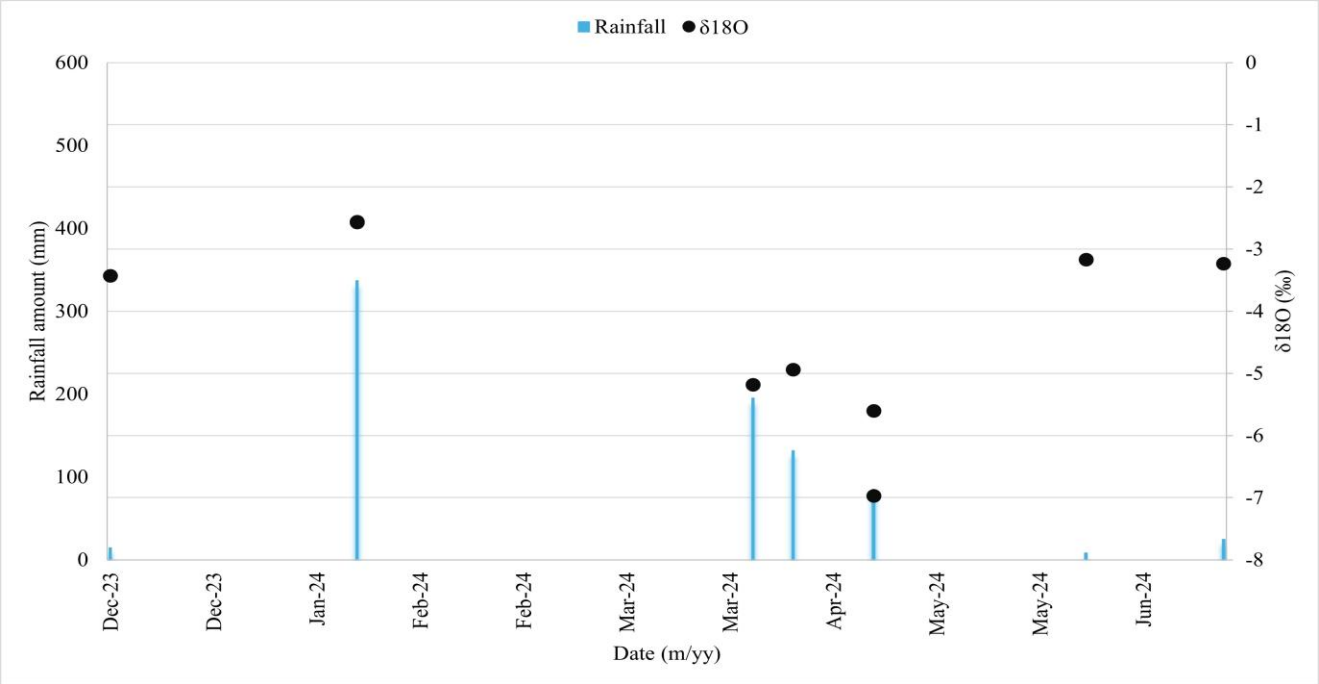

e. Pietermaritzburg

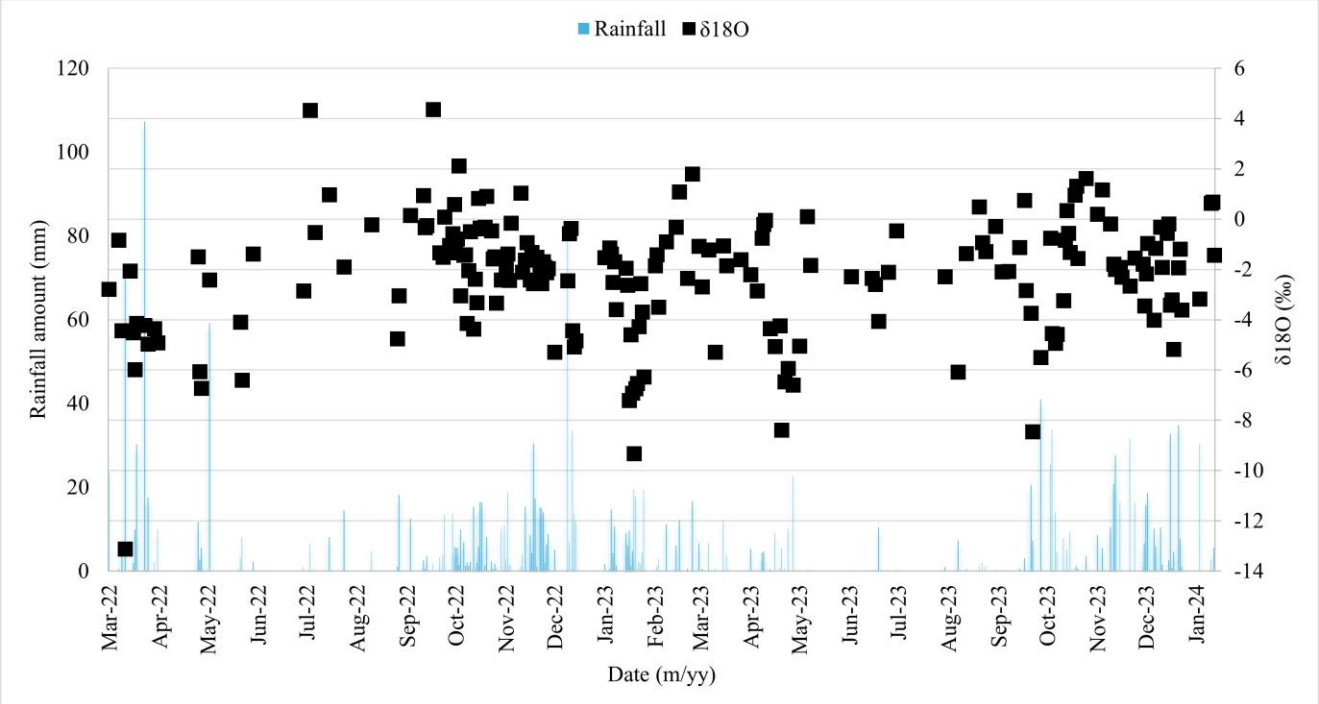

Figure 5.2: Amount effect for all five stations: (a) Winterton, (b) Eshowe, (c) Mike Pass, (d) Catchment 6, (e) Pietermaritzburg

5.2.3.2 Altitude effect

The altitude effect occurs as air masses are lifted orographically, leading to adiabatic cooling and heavy isotope depletion due to increased altitude. **Figure 5.3** shows the altitude effect for the uThukela Catchment. There is a significant difference between $\delta^{18}O$ values from the highlands (Catchment 6; -3.79‰, Mike Pass; -3,73‰, Winterton; -1.27‰) and the lowlands (Pietermaritzburg; -3.21‰, Eshowe; -2.94‰). The isotopic altitude lapse rate for the uThukela Catchment is -0.06‰ for $\delta^{18}O$ per 100m, which is significantly lower than the isotopic lapse rates observed in other regions of the world, where the typical rate is -0.28‰/100m (Poage and Chamberlain, 2001). The weak isotopic lapse rate observed in the uThukela Catchment may be due to non-uniform atmospheric moisture movement across the rainfall stations in the Catchment because if stations don't fall under the same atmospheric moisture trajectory, this could lead to high variation in $\delta^{18}O$ (Treble *et al.*, 2005). Another reason for the weak isotopic lapse rate may be the absence of a strong temperature lapse rate. When the temperature lapse is not pronounced, the anticipated depletion in $\delta^{18}O$ with altitude is less evident. Moreover, Grab (2013) reported that the High Drakensberg Escarpment exhibits a lack of strong temperature lapse rates, demonstrating that the lapse rate varies with altitude. However, it remains generally lower than what is typically expected in mountainous regions.

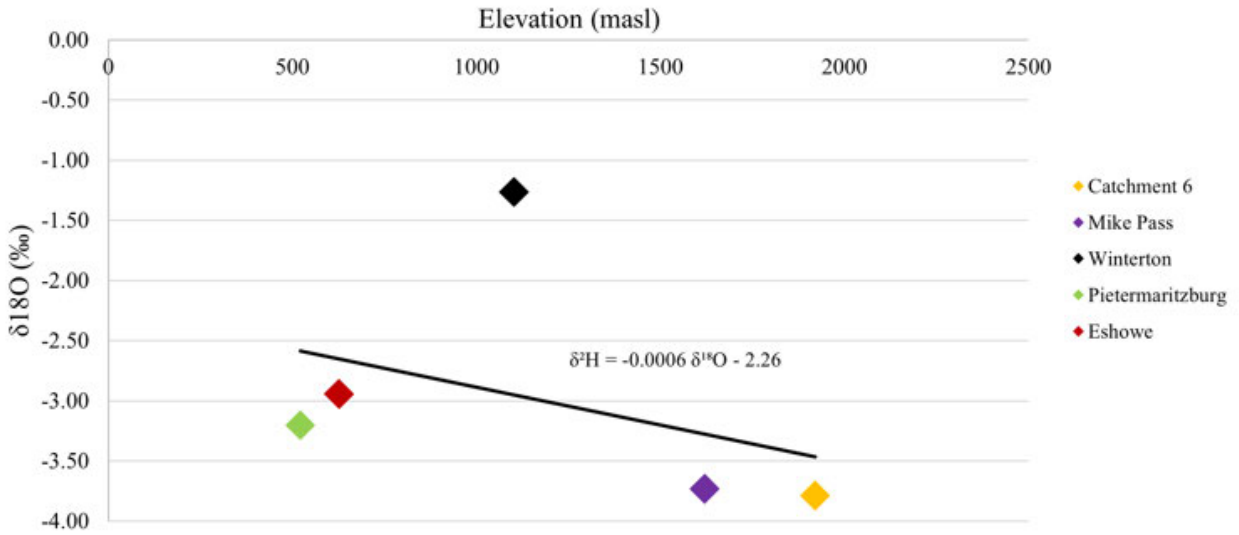

Figure 5.3: Change in $\delta^{18}O$ with elevation

5.2.3.3 Continentality effect

The continentality effect occurs as precipitation moves from the ocean and air loses moisture as it travels overland. **Figure 5.4** shows the rainfall amount-weighted mean of $\delta^{18}O$ for each site, based on samples collected between March 2022 and July 2024, and illustrates how $\delta^{18}O$ values change with increasing distance from the coast. The values represent the overall weighted mean across the full sampling period for each site. Studies in Central and East Africa found an almost negligible continentality effect, described as "no discernible depletion" in $\delta^{18}O$ with distance from the coast. (Joseph *et al.*, 1992; Kebede and Travi, 2012; Muhammad and Sadiq, 2014; Wirmvem *et al.*, 2017). This is illustrated in **Figure 5.4**, which shows a relatively small isotopic gradient of -0.04‰ for $\delta^{18}O$ per 100km, indicating a gradual decrease in the continentality effect with increasing distance from the coast.

Similar results have been linked to the role of recycled moisture from inland sources in contributing to precipitation (Taupin *et al.*, 2000; Wirmvem *et al.*, 2017). Furthermore, Salati *et al.* (1979) explained that a high d-excess (greater than 10) suggests a contribution of recycled inland moisture. Data from Catchment 6 and Mike Pass further support this notion, as the weighted mean values of $\delta^{18}O$ and the high d-excess (**Table 5.2**) suggest that much of the moisture contributing to precipitation in these regions does not solely originate from oceanic sources. Instead, it is significantly influenced by moisture that has been recycled within the catchment itself.

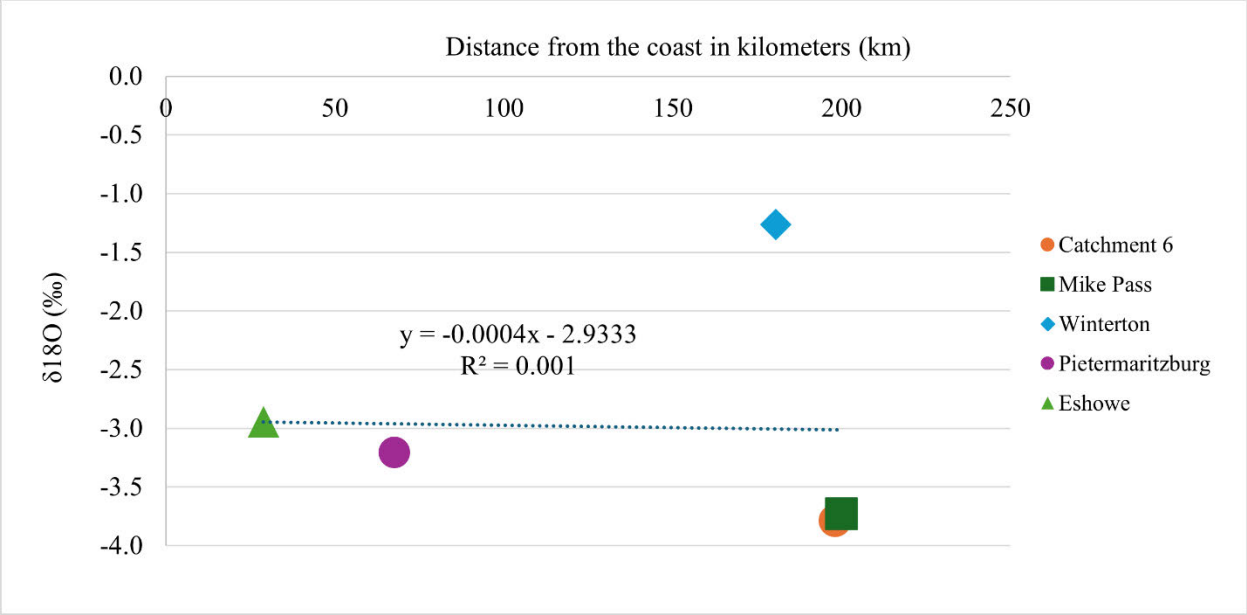

Figure 5.4: $\delta^{18}O$ vs Distance from the coast

5.2.3.4 Seasonality effect

The data presented in **Figure 5.5** illustrates the relationship between daily rainfall and δ^2H values for Pietermaritzburg over a three-year period from March 2022 to January 2024. Both rainfall amounts and δ^2H exhibited seasonal variations throughout the months. Notably, the two lowest δ^2H values, recorded at -90.2‰ (5th April 2022) and -65.3‰ (13th February 2022), occurred during the wet season. In contrast, the highest δ^2H value of 36.7‰ (28th July 2022) and 29.5‰ (12th October 2022) during the dry season. These findings demonstrate a strong seasonality effect in Pietermaritzburg. Similarly, other studies in South Africa have observed a seasonality effect, such as Thohoyandou (Durowoju *et al.*, 2019b), Mossel Bay (Braun *et al.*, 2017) and Cape Town (Harris, 2023).

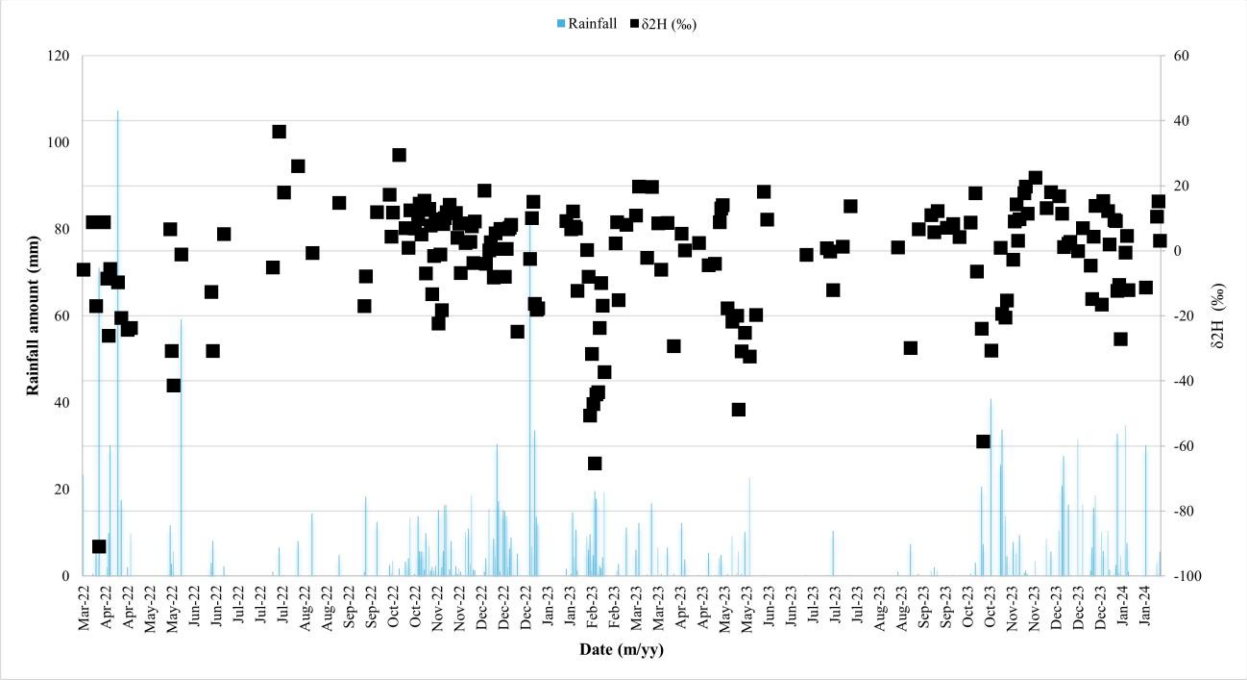

Figure 5.5: Seasonal variation of d-excess of Pietermaritzburg for three years (March 2022 to January 2024)

5.3 GW-SW interaction at multiple scales

5.3.1 Regional scale

5.3.1.1 Radon

Twenty-one radon samples were collected at the uThukela Catchment along the main uThukela River during the wet season. The ^{222}Rn (Bq/m³) measurements were taken to investigate GW discharge in streams along the Main uThukela River. **Figure 5.6** displays ^{222}Rn in the uThukela Catchment. The ^{222}Rn concentration varies upstream and downstream of the catchment, with the highest values upstream of the Catchment (151 - 617 Bq/m³) and the lowest downstream of the catchment (1.7 – 150 Bq/m³). The elevated ^{222}Rn concentration observed upstream in the uThukela Catchment may be linked to the presence of thick dolerite dykes within the dolerite formations (**Figure 3.2**). These dykes likely enhance groundwater discharge into streams by acting as conduits for subsurface flow. In contrast, downstream areas exhibit lower ^{222}Rn concentrations, likely due to the absence of dolerite intrusions. The downstream region, where river ^{222}Rn samples were collected, is primarily underlain by basement rocks such as granite-gneiss, schists, and amphibolites. These basement rocks exhibit very low permeability, which may further reduce groundwater discharge into streams in this zone.

When comparing the concentration of ^{222}Rn in the uThukela River to that in other global river studies, it is evident that the uThukela has a significantly lower radon concentration. Studies conducted globally have reported ^{222}Rn ranging from 3000 to 20000 Bq/m³ (Hall *et al.*, 1985; Ellins *et al.*, 1990; Wu *et al.*, 2004; Schubert *et al.*, 2008). Furthermore, when examining the ^{222}Rn concentrations in South African rivers, the uThukela still demonstrates significantly lower levels. For instance, a recent study done in the Western Cape by Strydom *et al.* (2021) in the Gevandon and Molennars Rivers found significantly high radon concentrations ranging from 1000 Bq/m³ to 118800 Bq/m³. Another study by Masevhe *et al.* (2017) in the Gauteng Province's rivers, South Africa revealed high ^{222}Rn concentrations ranging from 130 to 2870 Bq/m³. Thus, while other regions exhibit high ^{222}Rn concentration, the uThukela River notably shows low ^{222}Rn concentration.

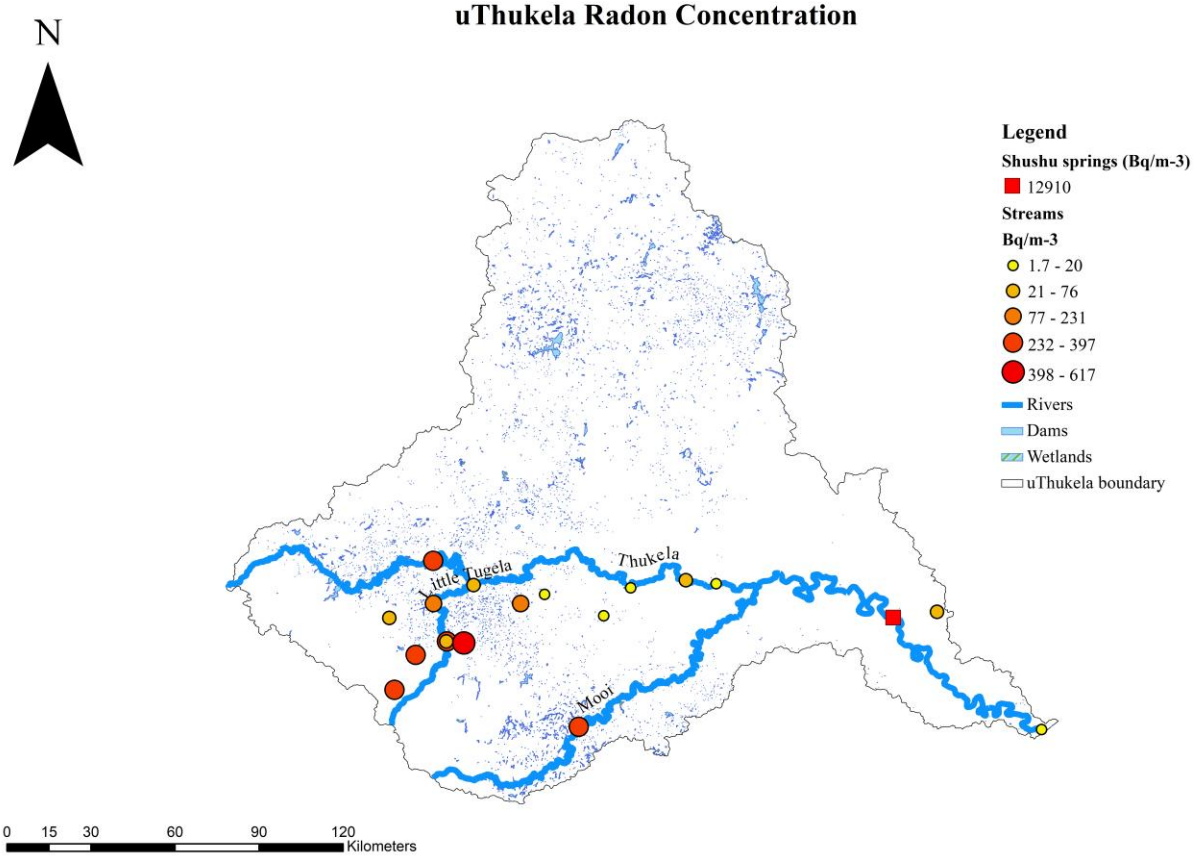

Figure 5.6: uThukela ^{222}Rn Concentration in Bq/m^3

5.3.1.2 Baseflow separation

The BFI data displayed variation along the catchment, but the upstream of the uThukela Catchment (**Figure *5.7***) showed the most groundwater contribution (high BFI), similar to the ^{222}Rn concentration obtained. In the upstream region, high BFI values (ranging from 0.610 to 0.951) and elevated ^{222}Rn concentrations indicated substantial groundwater contributions to streamflow. This is attributed to the presence of dolerite dykes and geological fractures, which enhance groundwater discharge, aligning with findings Le Maitre and Colvin (2008) that highlight the role of geological features like dykes in directing groundwater flow.

In contrast, the downstream areas presented a contradiction: high BFI values were observed, but ^{222}Rn levels were low, suggesting minimal natural groundwater input. This discrepancy is likely due to artificial baseflow contributions from dam releases, as noted by Adams *et al.* (2023) the presence of impermeable basement rocks that limit natural groundwater recharge.

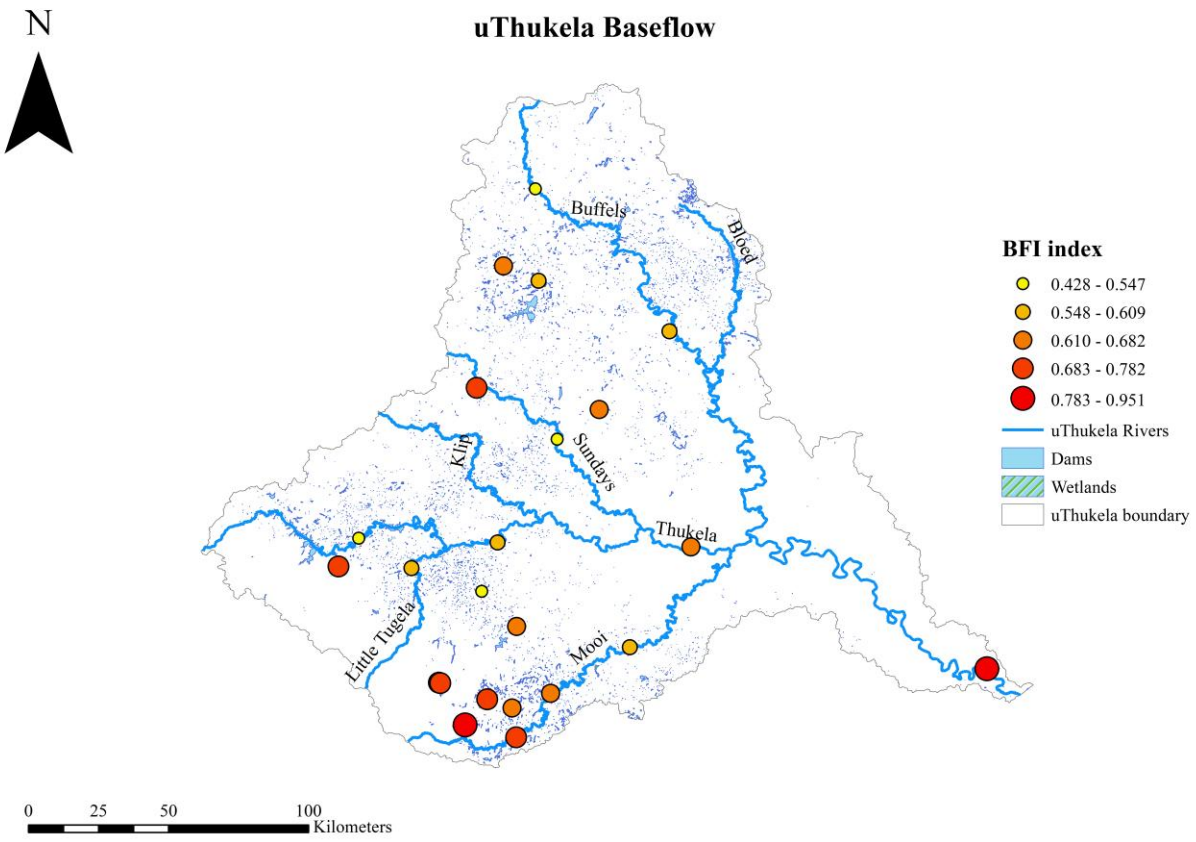

Figure 5.7: BFI index for uThukela

5.1.3.3 Piezometric analysis

The piezometric analysis determined the relationship between groundwater level variability and rainfall. Additionally, the results depicted in **Figure 5.8** illustrate analyses of groundwater level variability over a span of 21 years (from 2002 to 2023), alongside daily rainfall data collected from a single meteorological station within the uThukela Catchment during the same period. This time series data reveals a discernible trend of increasing and decreasing groundwater levels, as shown in **Figure 5.8**. Furthermore, all groundwater monitoring boreholes in the uThukela are drilled into fractured and weathered secondary aquifer systems, which are composed of Ecca Group rocks and dolerite sills, exhibiting varying yield capacities (Ndlovu and Demlie, 2018). Consequently, the time series in **Figure 5.8** reflects this increasing and decreasing trend.

The highest water level was observed at BH 5, located near Utrecht. In contrast, BH 1, situated around Bergville, exhibited a notable rise in water level beginning in 2017 and this is increase is mainly due to rainfall. To this end, BH 3, located near Tugela Ferry north of Greytown,

demonstrated an overall decline in water level. Moreover, BH 6 experienced a significant decline in groundwater levels, particularly from the years 2009, 2012, and 2015; this decline may be attributed to below-average rainfall experienced area. These findings coincide with a study done by Ndlovu and Demlie (2018).

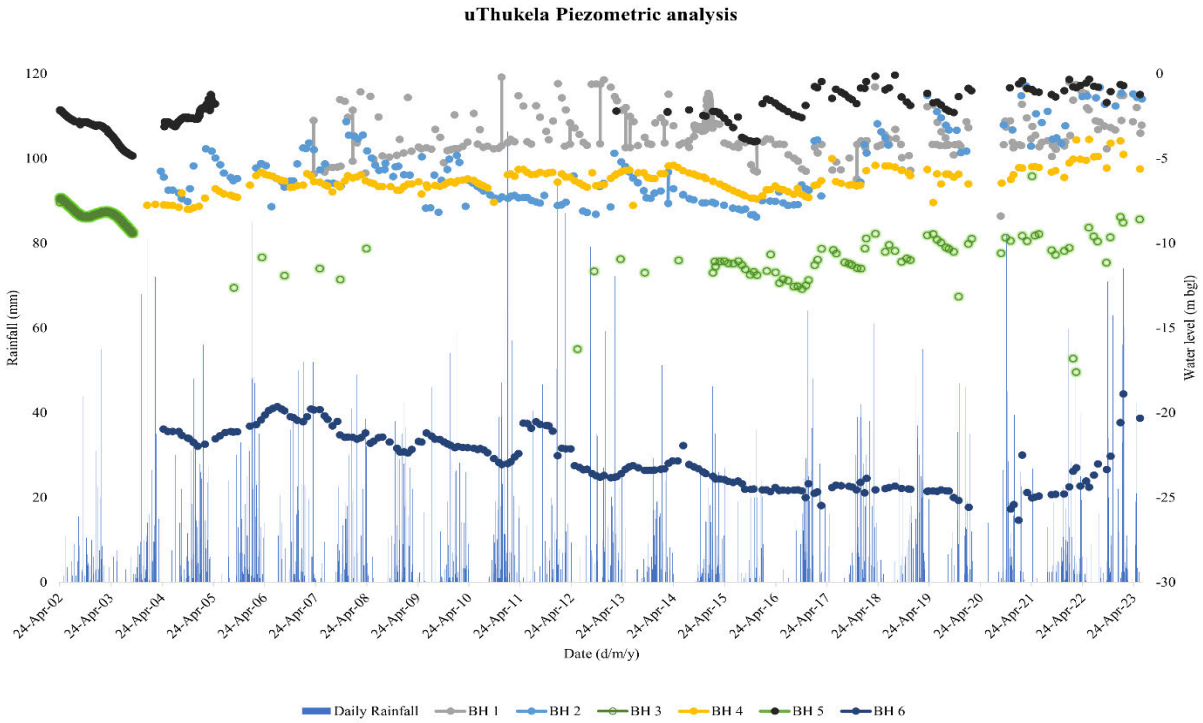

Figure 5.8: Monthly time series of groundwater level vs daily rainfall for selected boreholes

5.1.3.4 Isotope composition (δ^2H and $\delta^{18}O$) for regional-scale groundwater and surface water

The investigation of regional GW-SW interaction in the uThukela Catchment utilised δ^2H and $\delta^{18}O$ isotopes to assess evidence of recharge from higher altitudes. The Mike Pass LMWL served as a reference for investigating deep regional groundwater recharge originating from the highlands of the uThukela. Specifically, the Shu Shu thermal springs were analysed to explore this recharge from higher altitudes.

The isotopic composition of the Shu Shu thermal springs exhibited $\delta^{18}O$ values ranging from -3.97‰ to -3.13‰ and δ^2H values from -18‰ to -13.5‰. Similarly, the surface water in the uThukela Catchment displayed $\delta^{18}O$ values that varied from -3.97‰ to 2.15‰ and δ^2H values ranging from -18.5‰ to 12.4‰. Notably, both the surface water and Shu Shu thermal springs'

isotopic signals were plotted along and below the evaporation line, indicating evidence of evaporation (**Figure 5.9**). In **Figure 5.9**, the Shu Shu thermal springs show a similar isotope composition to the local surface water, suggesting that they might not be recharged from the higher altitude but recharged locally. The Shu Shu thermal springs are positioned away from the Mike Pass LMWL. However, these findings contradict Gravelet-Blondin (2013), who demonstrated that the Shu Shu thermal springs are recharged from higher altitudes.

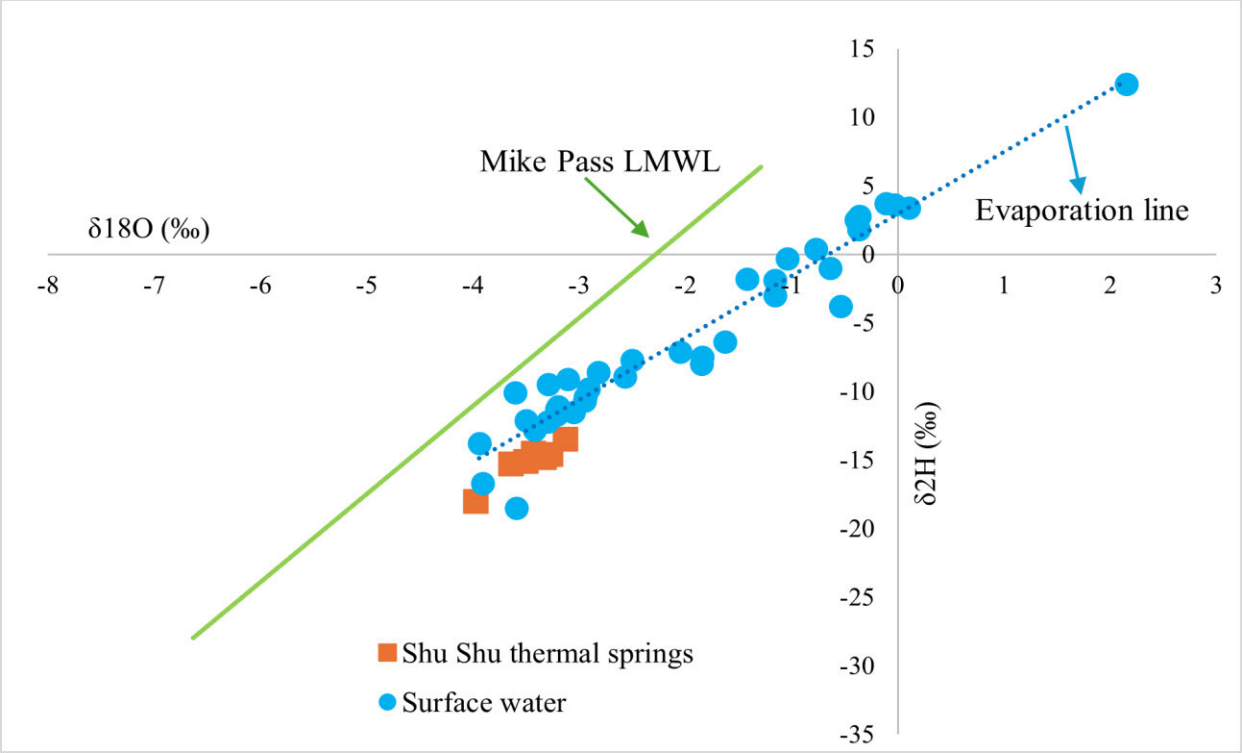

Figure 5.9: δ^2H and $\delta^{18}O$ for Mike Pass LMWL, Shu Shu thermal springs and uThukela surface water

5.3.2 Catchment scale

5.3.2.1 Isotope composition of δ^2H and $\delta^{18}O$ for Winterton rainfall and mountain valley boreholes and streams.

This investigation of intermediate groundwater was done at the catchment scale (mountain valley) using δ^2H and $\delta^{18}O$ to investigate the recharge mechanism of the groundwaters. 39 groundwater samples from both the dry and wet seasons were used; the isotope signals for the groundwater ranged from -4.2‰ to -2.6‰ of $\delta^{18}O$, and δ^2H ranged from -20.3‰ to-10.1‰, and the streams

had isotope signals that ranged from -3.5‰ to 2.15‰ for $\delta^{18}O$ and $\delta^{2}H$ ranged from -12.2‰ to 12.4‰. The Mike Pass LMWL was plotted in **Figure 5.10** to determine whether the boreholes in the mountain valleys are recharged from higher altitudes, and the Winterton LMWL was used as a reference to determine if the recharge of the boreholes was recharged locally. **Figure 5.10** shows that the borehole waters are closer to the Winterton LMWL, highlighting that this recharge might be local instead of from the highlands. However, the boreholes fall below the Winterton LMWL indicating that they might have undergone evaporation before recharge.

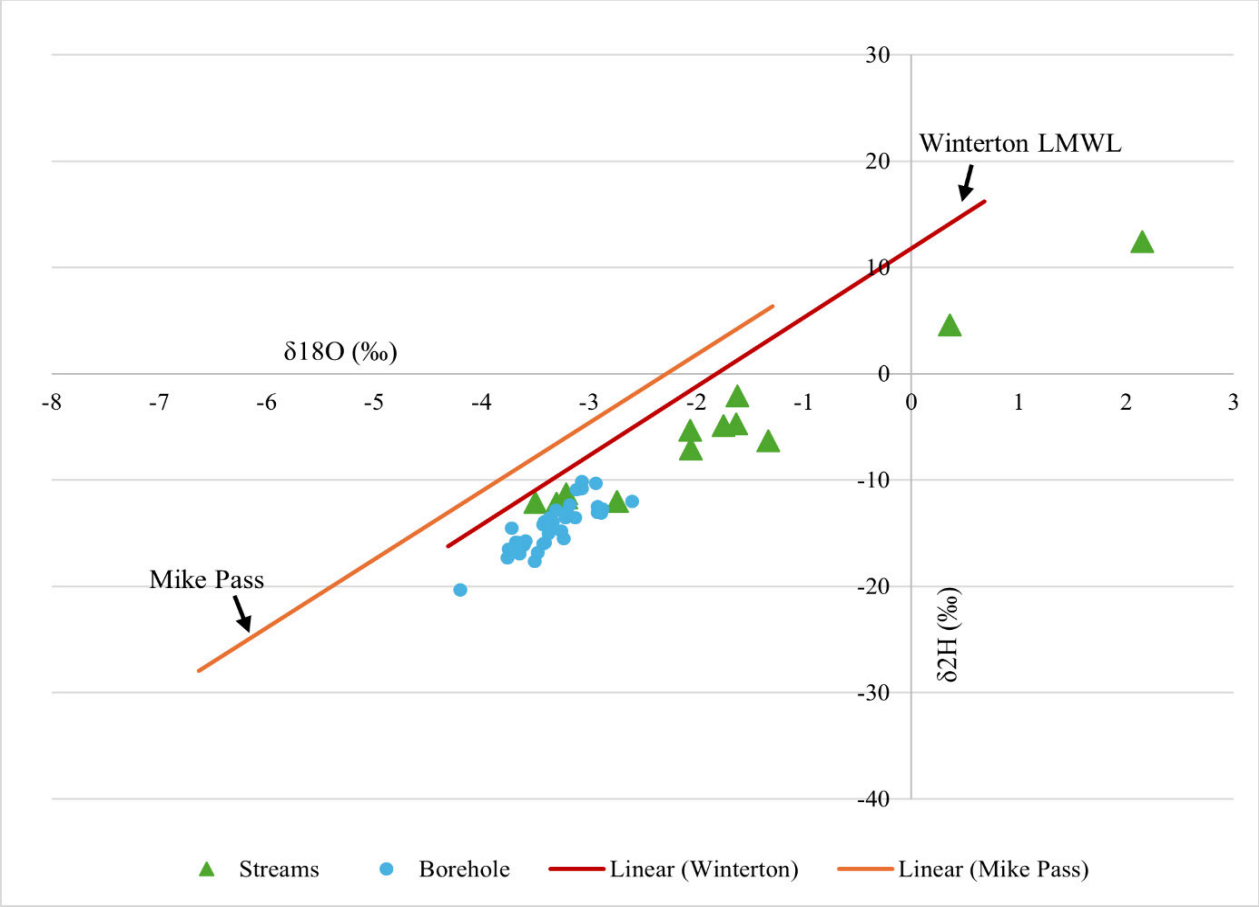

Figure 5.10: Winterton LMWL, Mike Pass LMWL, and $\delta^{2}H$ and $\delta^{18}O$ for boreholes and streams at the Mountain valley

5.3.2.2 Electrical conductivity of boreholes and rivers in the Mountain valley

Figure 5.11 illustrates the EC of boreholes and streams throughout different seasons in the Mountain valley. This analysis was conducted to investigate the role of intermediate groundwater.

By measuring the EC of rivers and groundwater at various locations, we can detect changes that suggest the influx of groundwater. An observable increase in the EC of a river at a certain point may indicate groundwater discharging into that river (Cartwright *et al.*, 2008; Unland *et al.*, 2013).

To conduct this investigation, 25 boreholes and 10 surface water points were measured for EC during the dry season. The EC values from the boreholes ranged from 59 to 965 µS/cm, while the surface water EC ranged from 57 to 262 µS/cm. In the wet season, 14 boreholes and 6 surface water points were assessed for EC. The EC values for the boreholes varied from 103 to 1,057 µS/cm, whereas the surface water values ranged from 63 to 295 µS/cm. During the wet season, a marked rise in EC was observed in the boreholes, accompanied by a slight increase in stream EC. The upper section of Mountain valley exhibited notably low EC levels for both boreholes and streams. In contrast, the lower section revealed an increase in EC for both boreholes and streams, suggesting a potential influx of groundwater. Furthermore, this indicates local groundwater circulation rather than intermediate groundwater from the mountains.

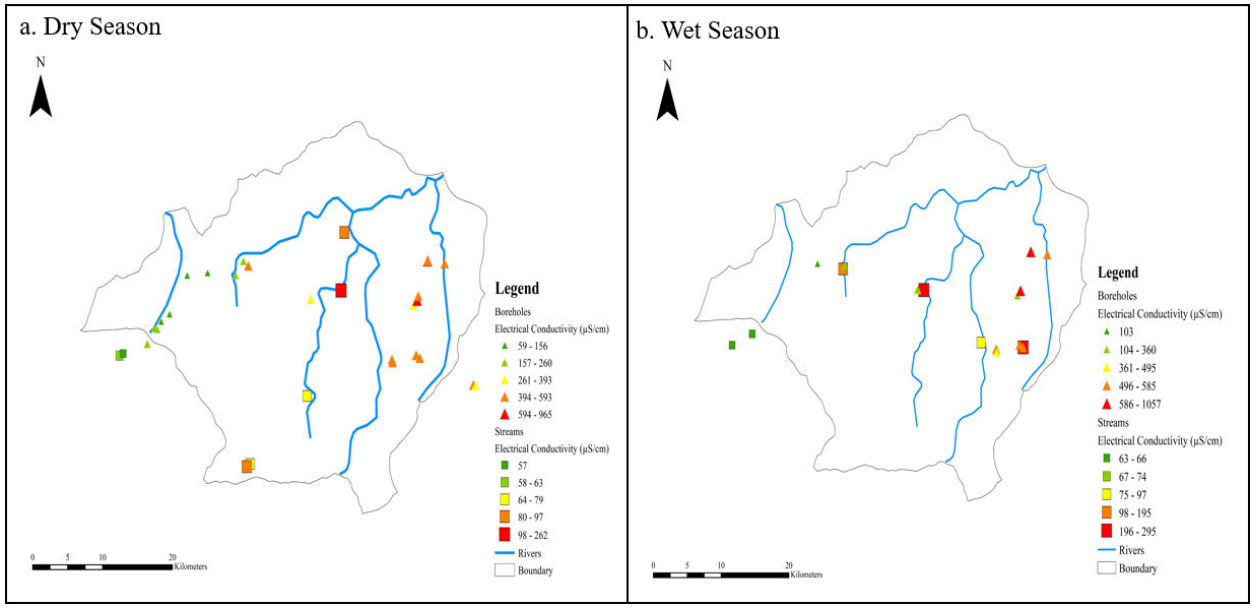

Figure 5.11: Illustrates EC measurements of boreholes and streams in the Mountain Valley during dry and wet season

5.3.3 Hillslope scale

5.3.3.1 EC comparison for seven catchments at Cathedral Peak

EC concentrations were measured from the headwaters and outlets of catchments 2, 3, 6, 7, and 9 to assess how groundwater contributions vary across these catchments. In contrast, the EC concentrations from catchments 4 and 5 were only collected downstream at the weir. The data collection spanned from February 2023 to July 2024.

Catchment 2 exhibited EC values ranging from 58 to 101 µS/cm, while Catchment 3 varied from 44 to 91 µS/cm. Catchment 4 showed values between 80 and 103 µS/cm, and Catchment 5 fluctuated from 87 to 109 µS/cm. Additionally, catchment 6 ranged from 75 to 122 µS/cm, catchment 7 varied from 76 to 112 µS/cm, and catchment 9 ranged from 65 to 93 µS/cm. Moreover, **Figure 5.12e** illustrates that catchment 6 exhibits the highest EC among all the catchments at Cathedral Peak. Furthermore, catchment 7 (**Figure 5.12f**), which is in close proximity to catchment 6, also displays a high EC level.

The comparison of EC between the upstream and downstream sections of the catchments is illustrated in **Figure 5.12**. Catchments 2 and 3 had a higher EC upstream of the catchment than downstream, which might be due to factors of groundwater ridging diluting the EC downstream. In contrast, catchments 4 and 5, located close to each other, did not show a decline in EC throughout the data collection period. Catchment 6 features three groundwater tributaries and two wetlands that feed its outlet, and the EC is always higher at the three groundwater tributaries (**Figure 5.12e**), indicating significant groundwater contributions, which typically have higher EC values. During the dry season, the EC at the outlet closely resembles that of the three groundwater tributaries; however, in the wet season, it aligns more closely with the EC levels of the lower and upper wetlands. Furthermore, catchment 7 has two groundwater tributaries, the EC at the upstream at the two groundwater tributaries has a higher EC compared to the downstream. In catchment 9, the trend reverses, as the EC is generally higher downstream than upstream.

a. Catchment 2

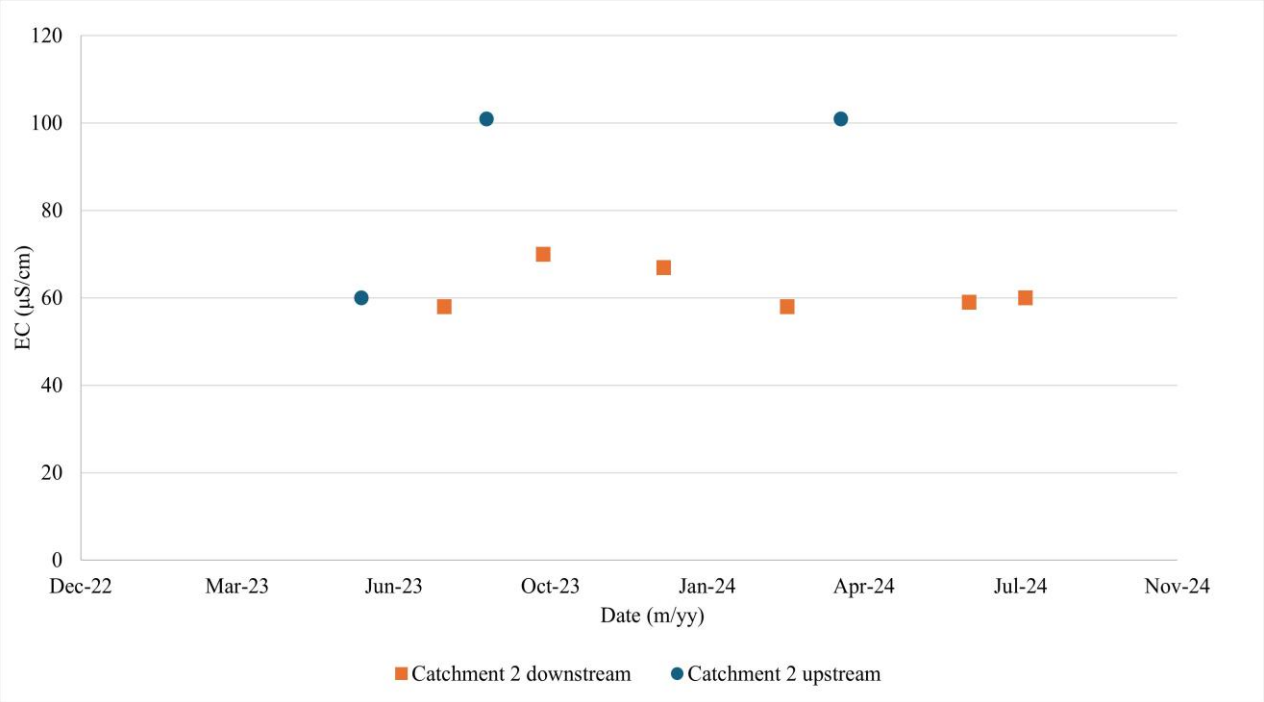

b. Catchment 3

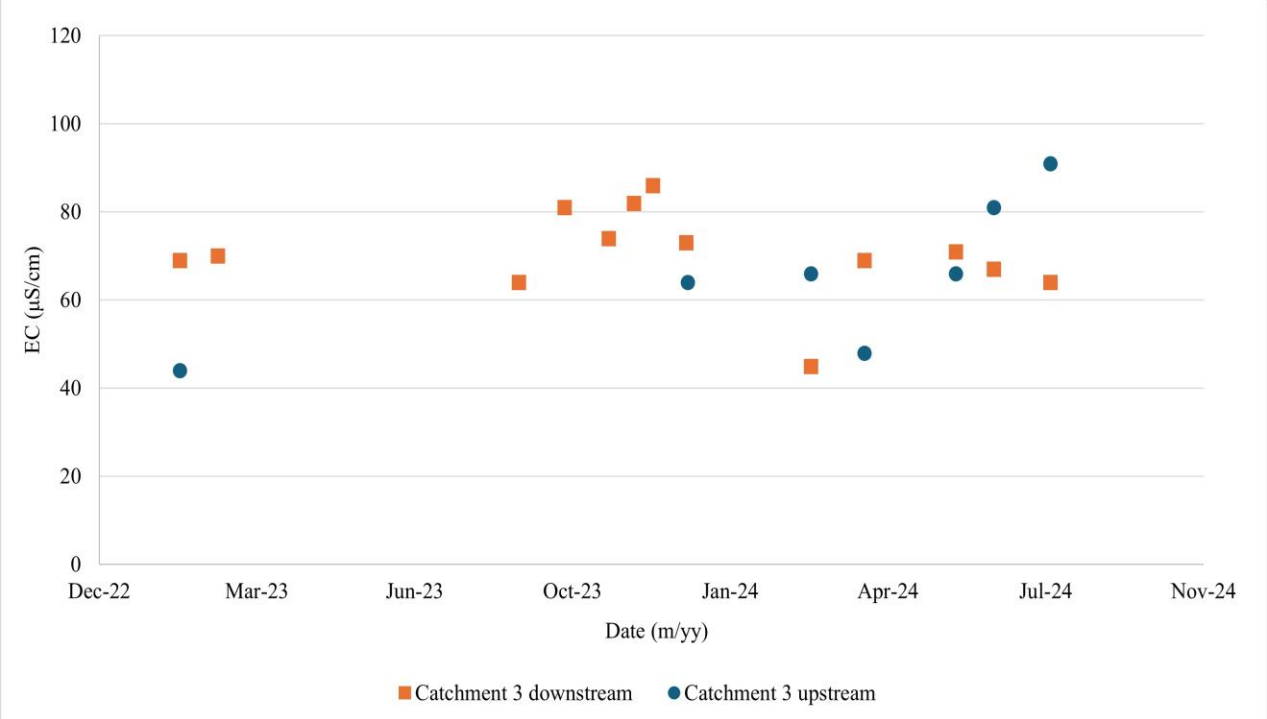

c. Catchment 4

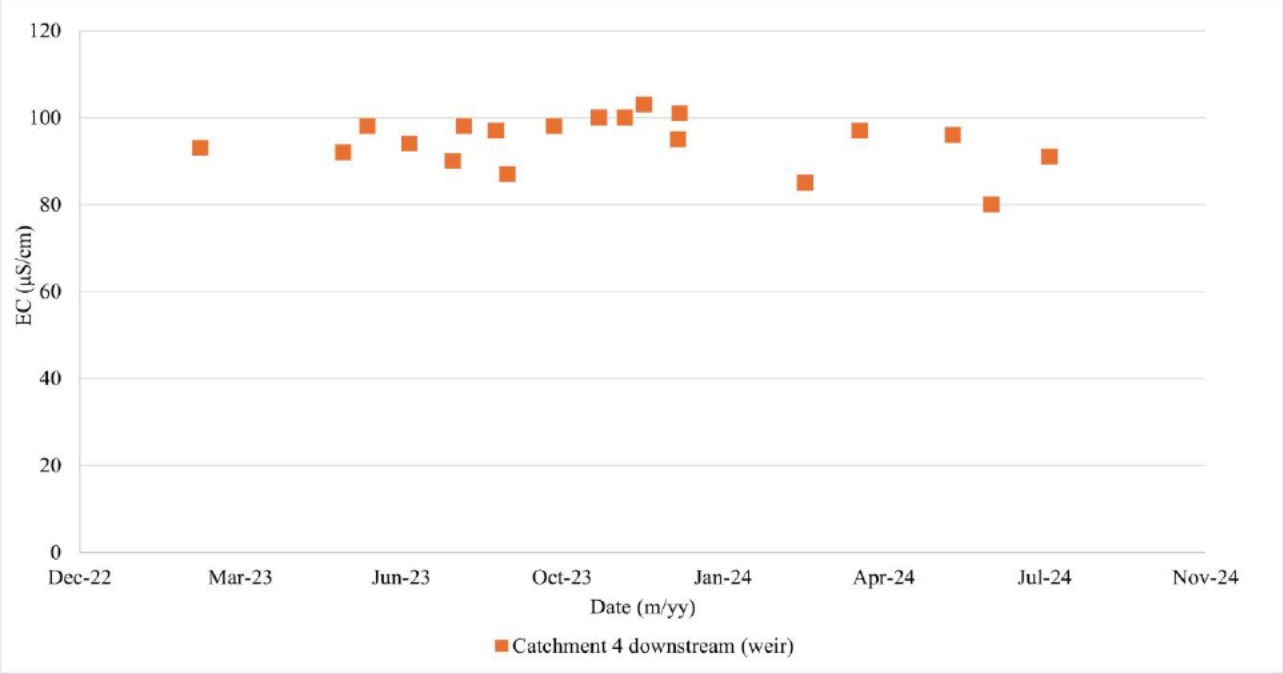

d. Catchment 5

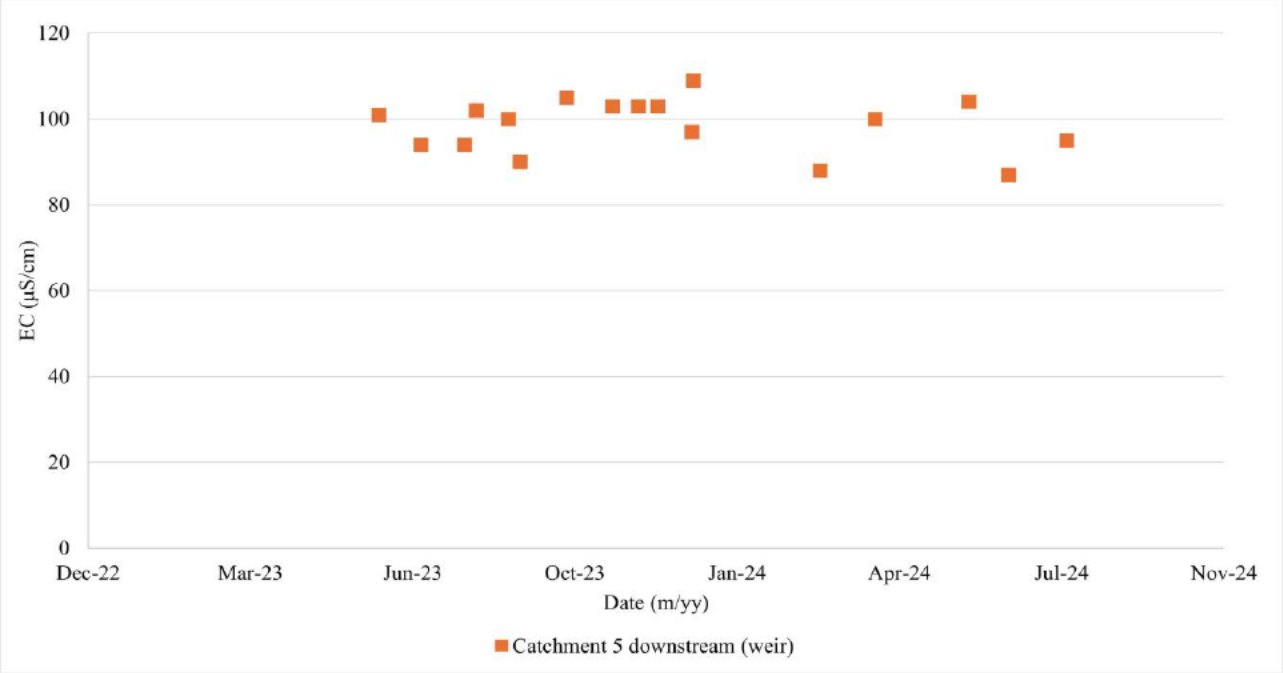

e. Catchment 6

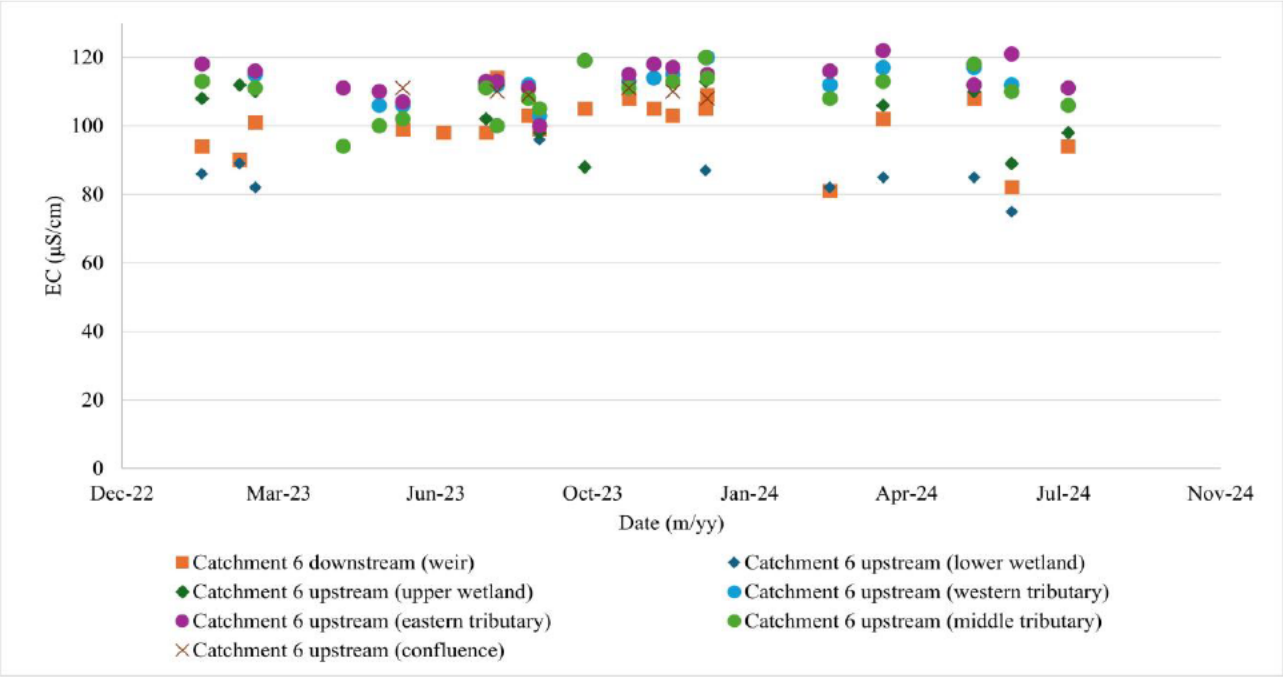

f. Catchment 7

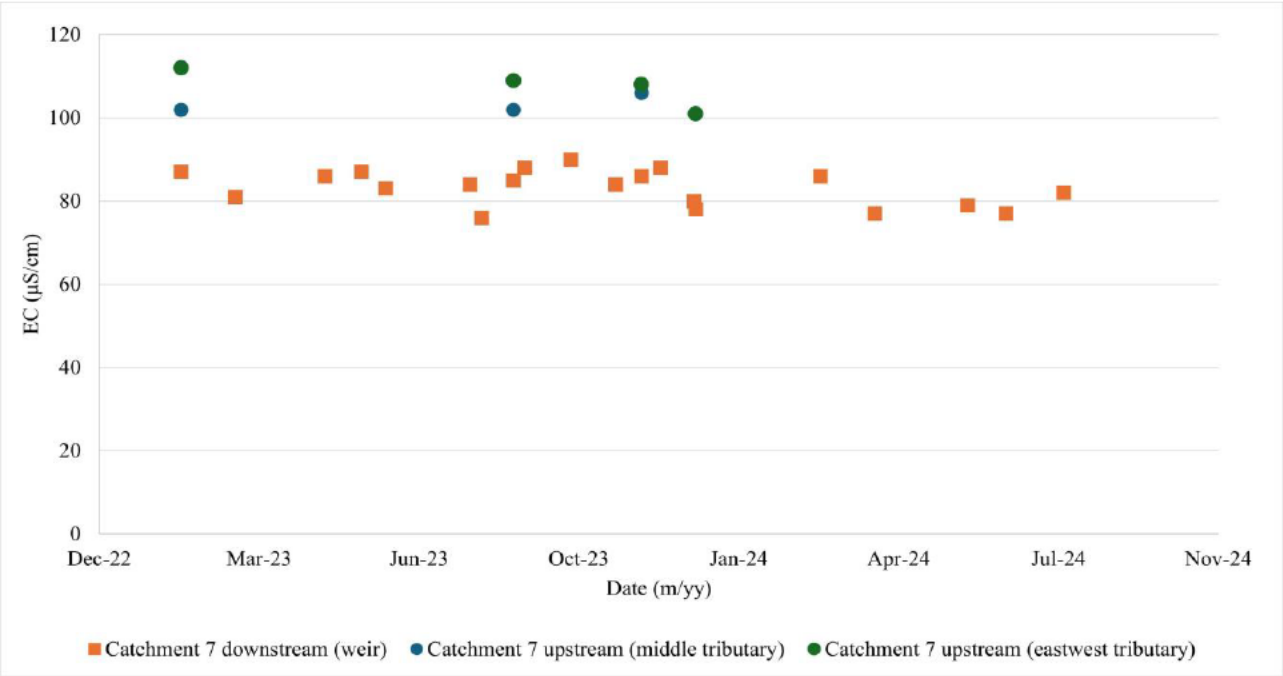

g. Catchment 9

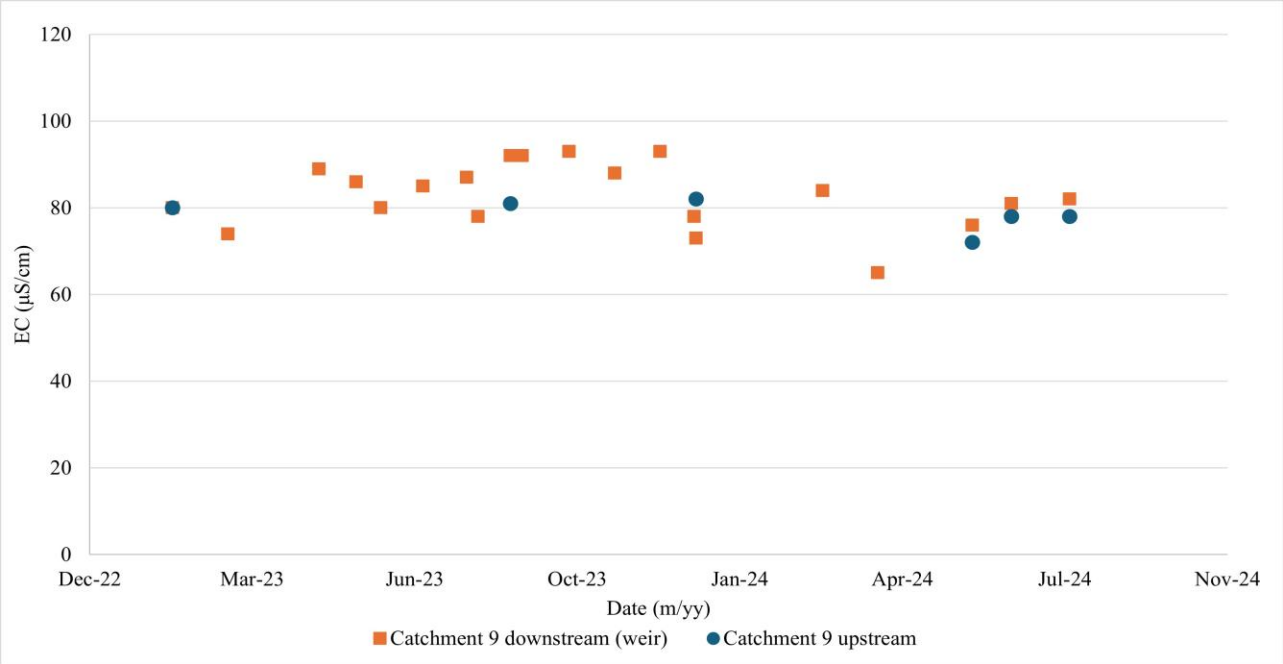

Figure 5.12: Comparison of EC between upstream and downstream of catchments 2,3,4,5,6,7 and 9

5.3.3.2 EC comparison of dry and wet seasons at the seven catchments

EC was measured during the wet (April) and dry seasons (June) across the Cathedral Peak catchments. **Figure 5.13** illustrates the seasonal variation in EC among these catchments. Throughout both seasons, Catchment 6 consistently exhibited the highest EC, indicating a strong influence of groundwater in this catchment and this high EC was contributed by the three groundwater tributaries. Similarly, Catchments 4 and 5 showed elevated EC levels, particularly in their downstream sections. In contrast, Catchment 2 displayed the lowest EC throughout both seasons.

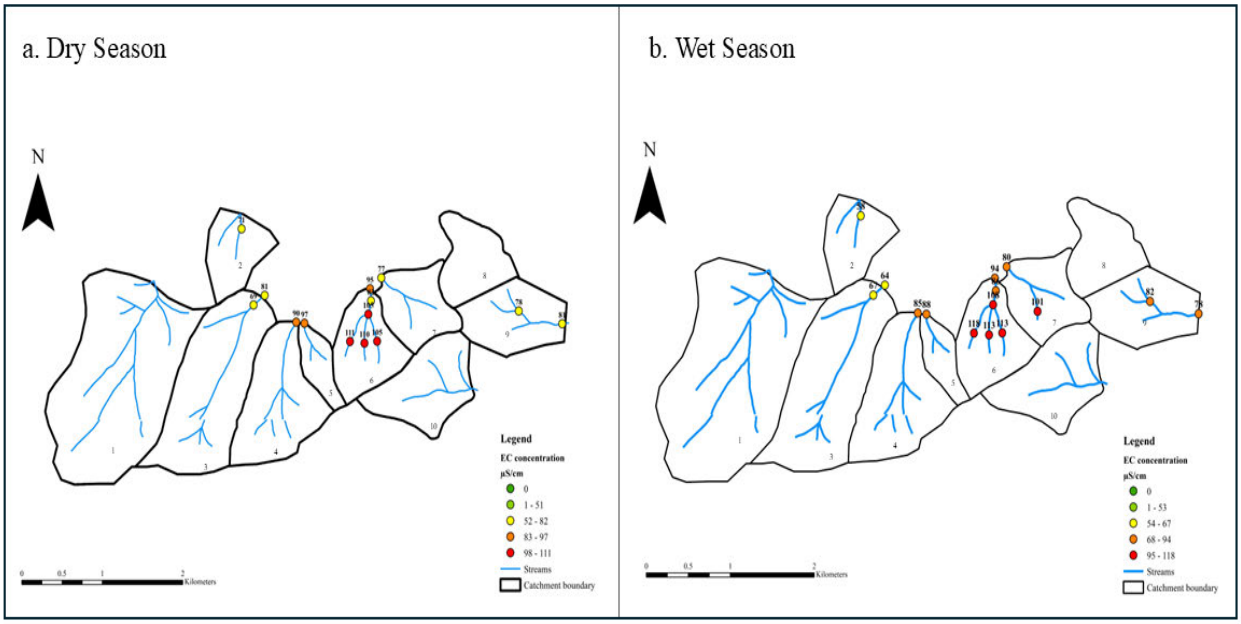

Figure 5.13: EC of Cathedral Peak catchments dry and wet season

5.3.3.3 $\delta^{18}O$ comparison for seven catchments at Cathedral Peak

A comparison of $\delta^{18}O$ values was conducted for upstream and downstream locations in the seven catchments of Cathedral Peak over a three-year period, from June 2022 to July 2023. This analysis aimed to determine the contribution of upstream water to downstream outlets in each catchment. In Catchment 2, the $\delta^{18}O$ signatures for downstream locations (-4.22‰ to -2.58‰) were isotopically similar to those upstream (-4.09‰ to -2.69‰). Similarly, in Catchment 3, the $\delta^{18}O$ signatures upstream (-5.41‰ to -3.34‰) were close to those downstream (-4.36‰ to -2.67‰) (**Figure 5.14b**). Catchments 4 (-3.93‰ to -3.2‰) and 5 (-5.9‰ to -2.37‰) displayed relatively stable $\delta^{18}O$ values over the sampling period; however, some values in Catchment 5 showed

enrichment and depletion, likely due to evaporation effects. In Catchment 6, the $\delta^{18}O$ values were isotopically similar to those in the three groundwater tributaries, suggesting that groundwater is the dominant source at the outlet (**Figure 5.14e**). Catchment 7 displayed similar characteristics to Catchment 6. Additionally, Catchment 9 showed comparable $\delta^{18}O$ values upstream (-3.89‰ to -3‰) and downstream (-3.86‰ to -2.89‰), indicating a consistent isotopic signature across both locations.

a. Catchment 2

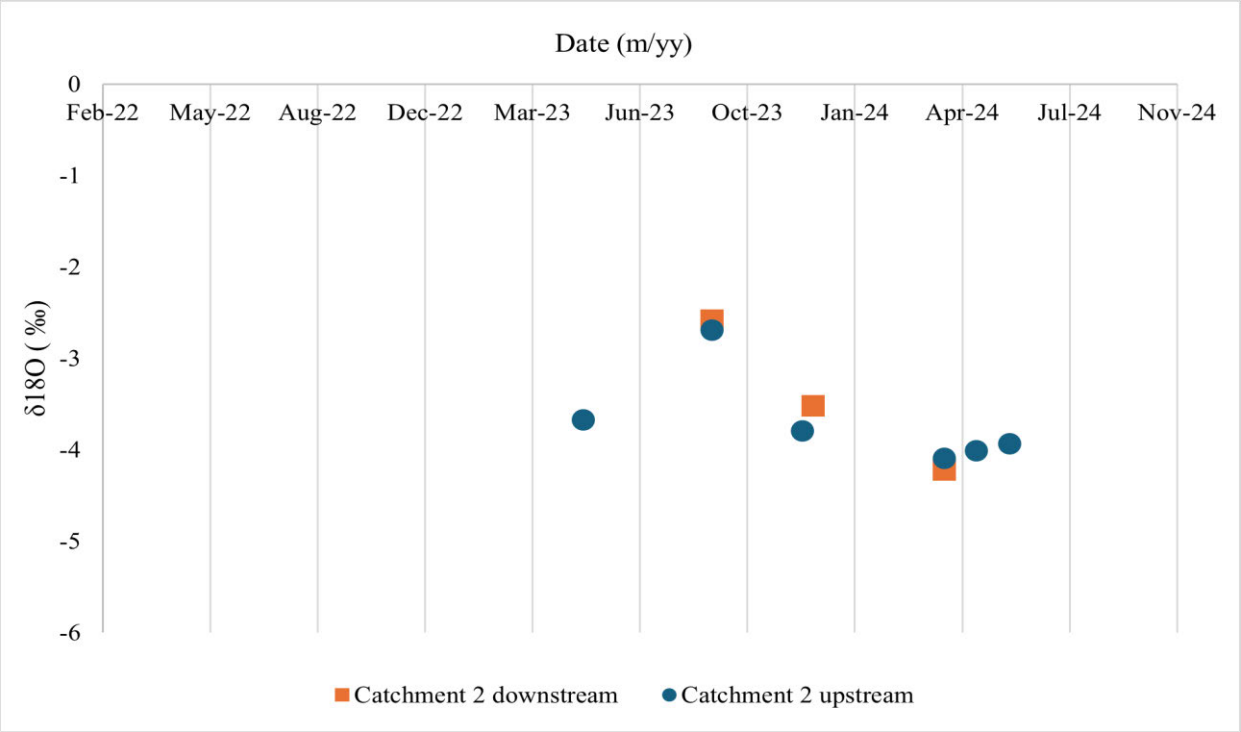

b. Catchment 3

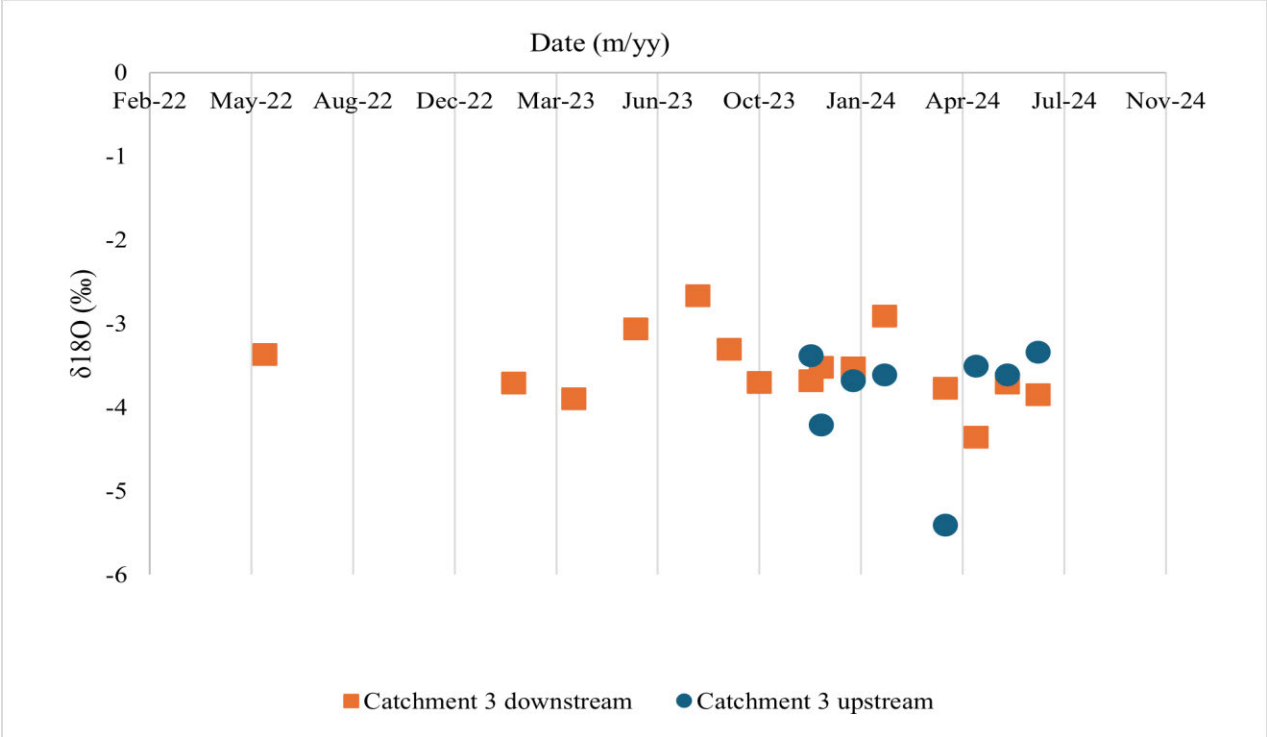

c. Catchment 4

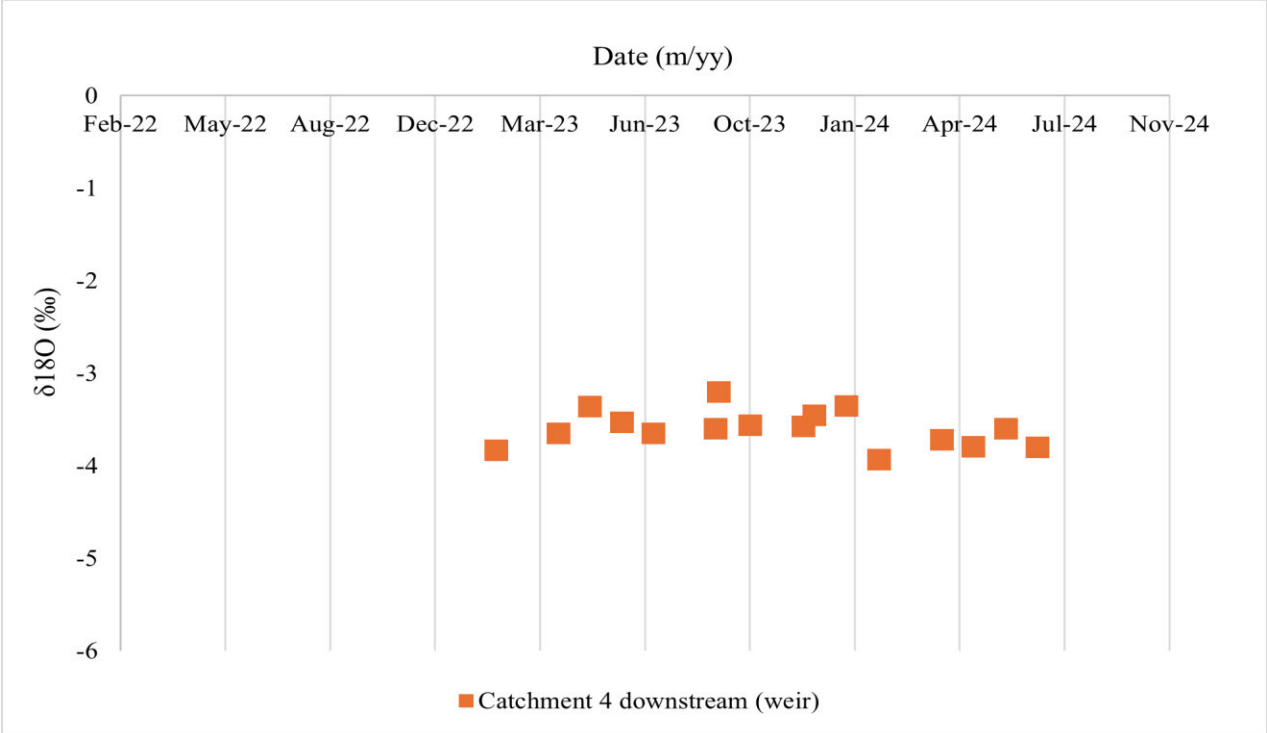

d. Catchment 5

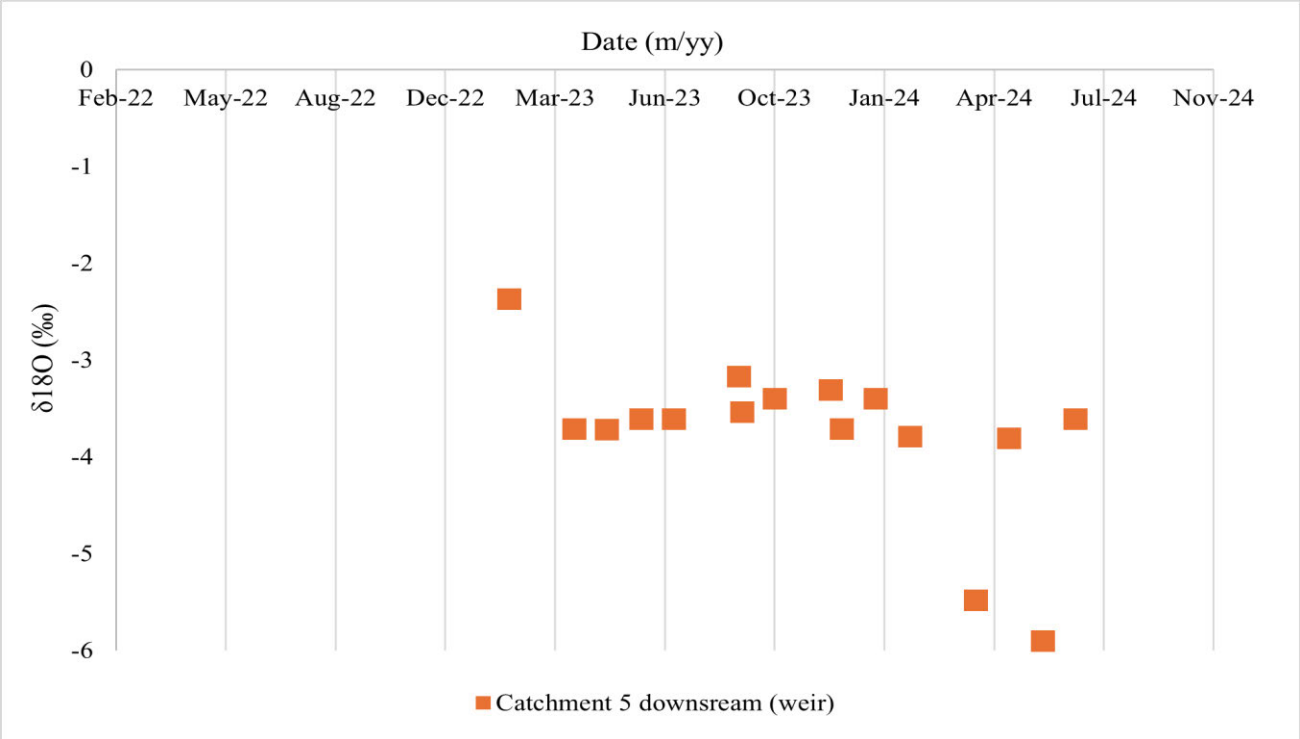

e. Catchment 6

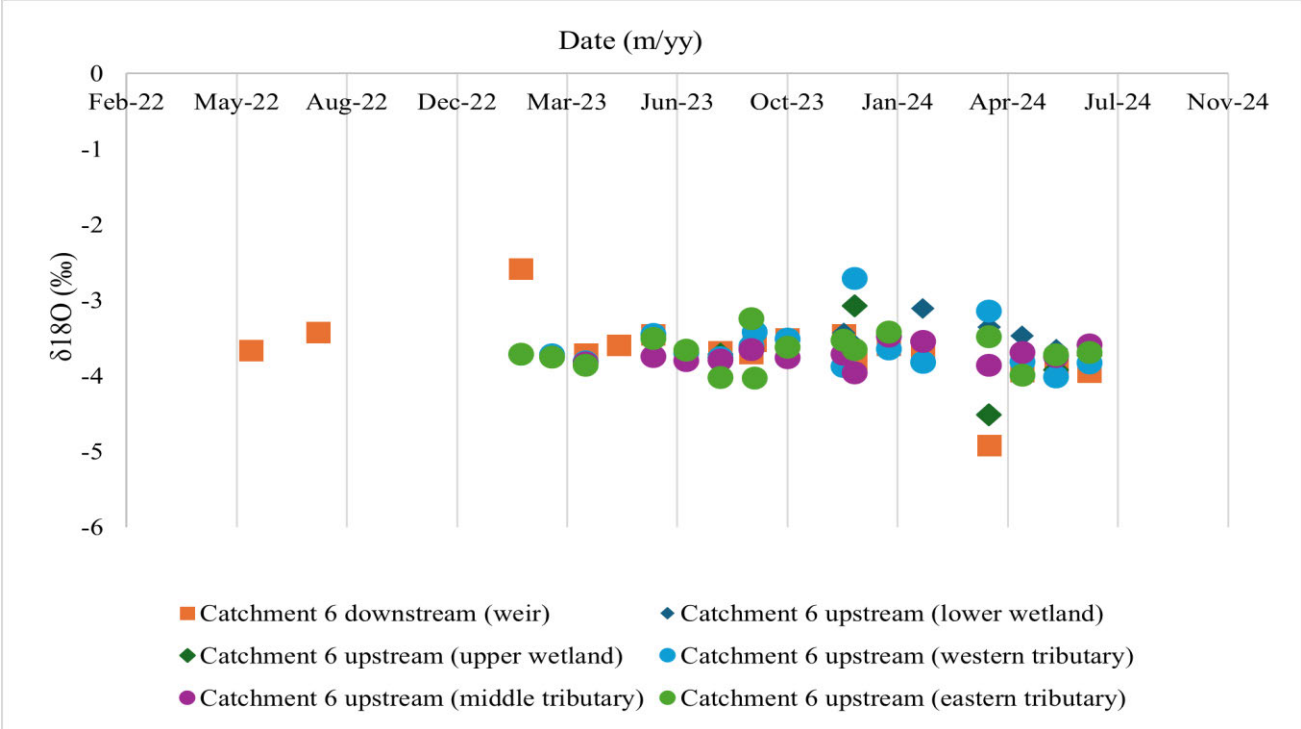

f. Catchment 7

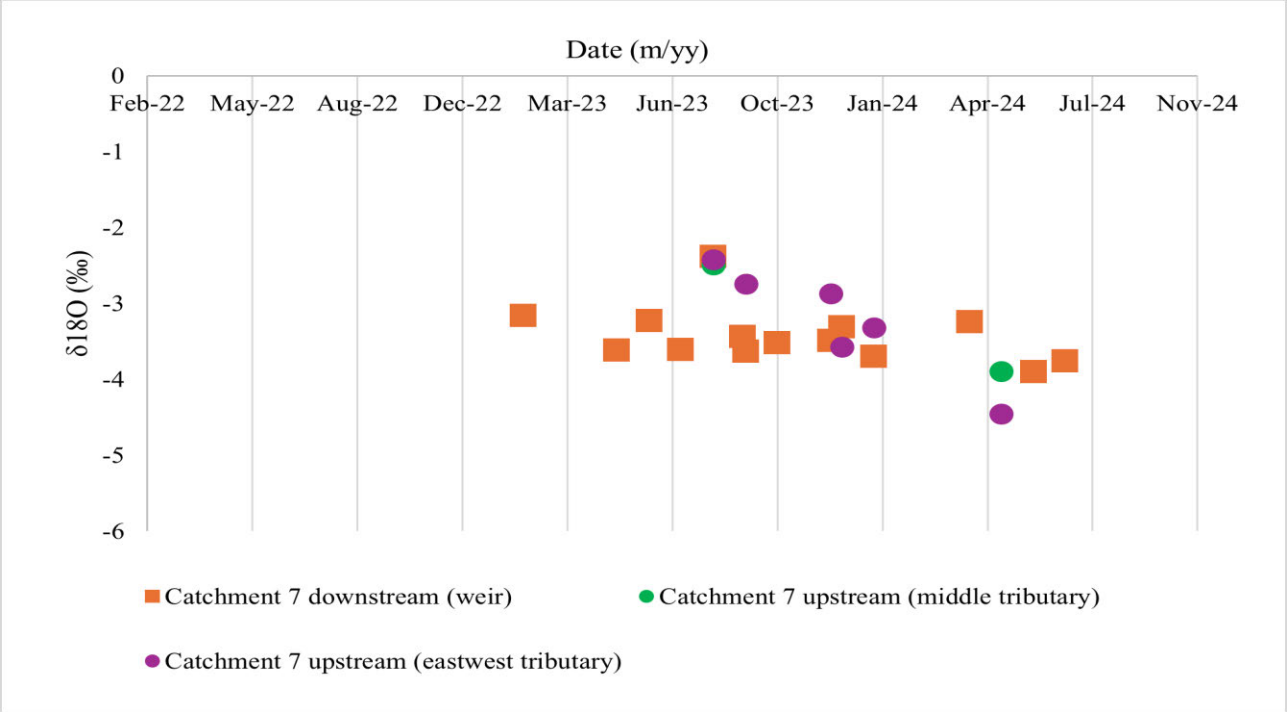

g. Catchment 9

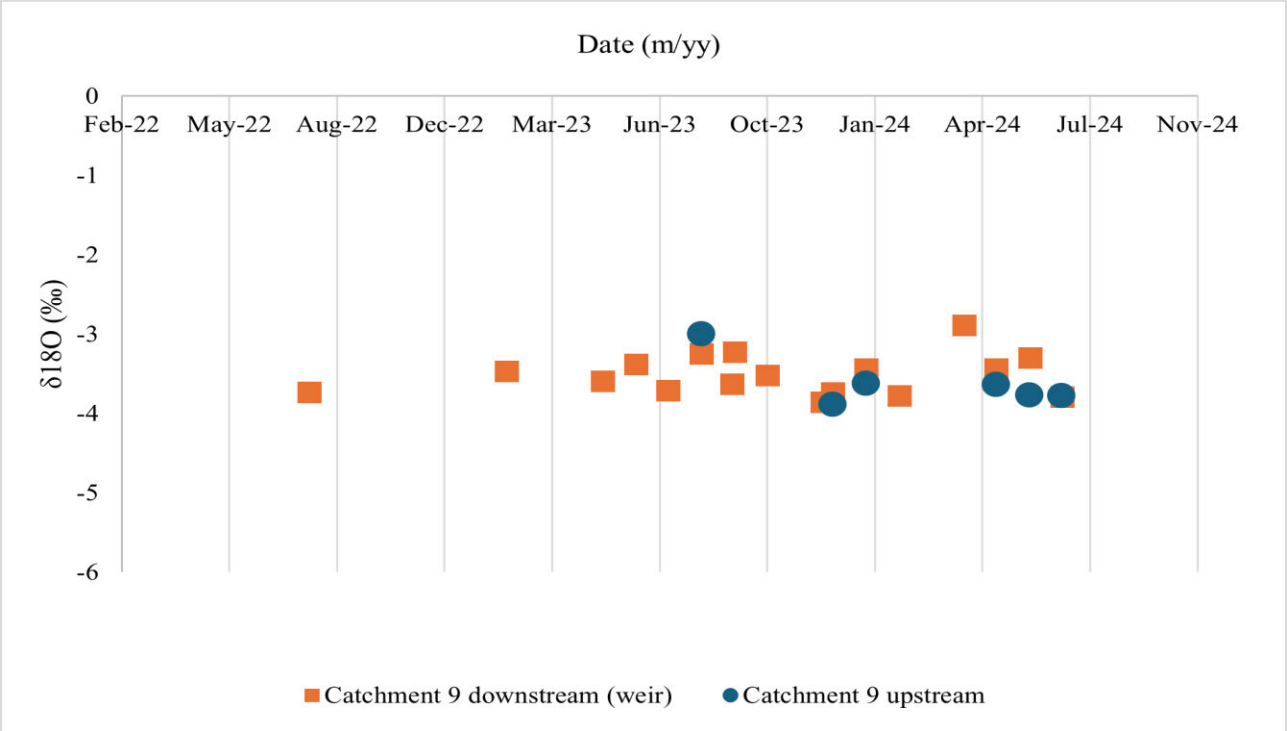

Figure 5.14: Comparison of $\delta^{18}O$ upstream and downstream of catchment 2,3,4,5,6,7 and 9

5.3.3.4 Isotope comparison of δ^2H and $\delta^{18}O$ for Cathedral Peak

All δ^2H and $\delta^{18}O$ values for the Cathedral Peak catchments were plotted against the Mike Pass LMWL ($\delta^2H = 6.43 * \delta^{18}O + 14.66$) (**Figure 5.15**). Most of the δ^2H and $\delta^{18}O$ values fall below the Mike Pass LMWL, suggesting that some of these surface waters may have been recharged by rainfall that experienced prior evaporation. A point from Catchment 6 upstream (upper wetland) (-4.51‰ for $\delta^{18}O$ and -16‰ for δ^2H) is closest to the LMWL, which could indicate recharge from recent rainfall during the wet season.

However, several points from different locations, such as Catchment 5 downstream (weir) (-5.48‰ for $\delta^{18}O$ and -17.5‰ for δ^2H, and -5.9‰ for $\delta^{18}O$ and -21‰ for δ^2H), Catchment 3 upstream (seepage) (-5.4‰ for $\delta^{18}O$ and -18.5‰ for δ^2H), Catchment 6 downstream (weir) (-4.42‰ for $\delta^{18}O$ and -15.6‰ for δ^2H), and Catchment 7 upstream (east-west tributary) (-4.45‰ for $\delta^{18}O$ and -13.6‰ for δ^2H), plot above the Mike Pass LMWL. This may indicate mixing between surface runoff and groundwater, each with distinct isotopic signatures. Notably, all points that plot above the Mike Pass LMWL were collected at the end of the wet season in April, suggesting a period of groundwater discharge and mixing with other water sources. This mixing likely minimises evaporation effects and increases $\delta^{18}O$ depletion (**Figure 5.15**).

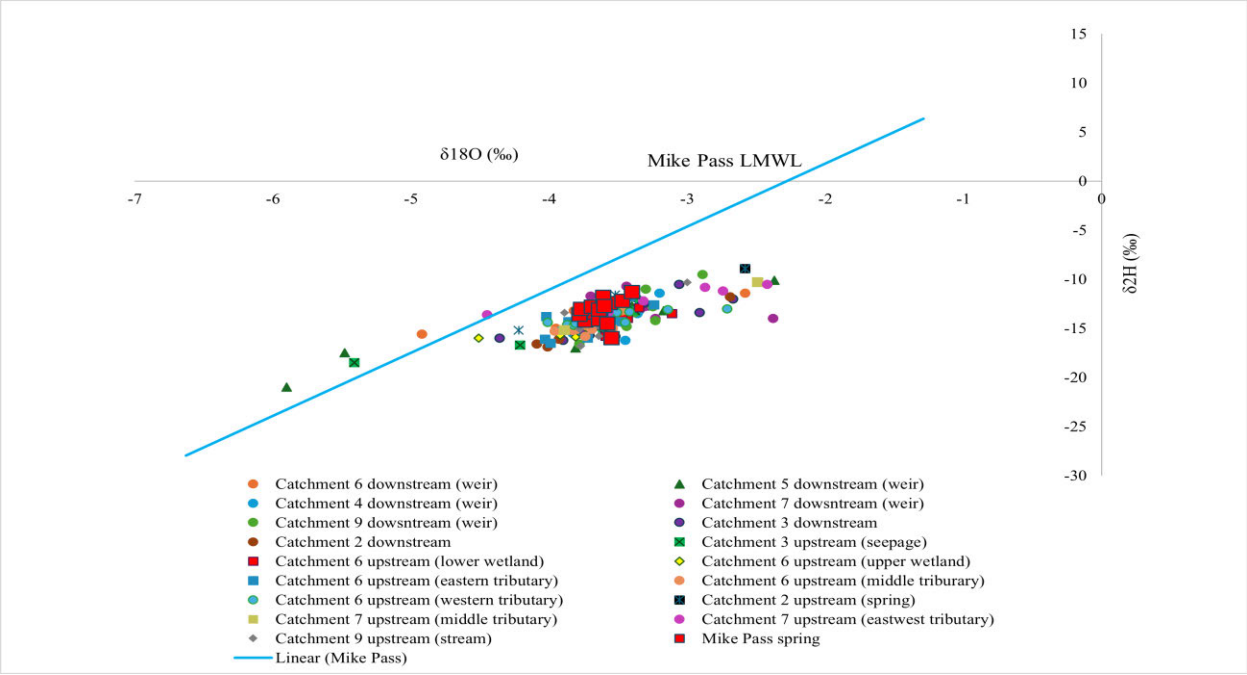

Figure 5.15: δ^2H and $\delta^{18}O$ for Cathedral Peak from February 2022 to July 2024

5.3.3.5 Isotope comparison of δ^2H and $\delta^{18}O$ for catchment 6,7 and 9 during dry and wet season

During the dry season, the isotopic values of δ^2H and $\delta^{18}O$ from catchments 6, 7, and 9 were plotted against the Mike Pass LMWL ($\delta^2H = 6.43 * \delta^{18}O + 14.66$). In catchment 6, the downstream weir recorded values of -4.92‰ for $\delta^{18}O$ and -15.6‰ for δ^2H, positioning them above the LMWL (**Figure 5.16**), which suggests mixing with other water sources. In contrast, the upstream upper wetland showed values of -4.51‰ for $\delta^{18}O$ and -16‰ for δ^2H, placing it directly below the LMWL, indicating potential recharge from recent rainfall. For catchment 7, both the downstream weir and the upstream east-west tributary exhibited closely aligned values, with the downstream weir at -3.24‰ for $\delta^{18}O$ and -12.3‰ for δ^2H and the upstream tributary at -3.32‰ for $\delta^{18}O$ and -12.2‰ for δ^2H. This proximity suggests that the upstream tributary may be recharging the weir. The remaining isotopic signatures from these catchments fell below the Mike Pass LMWL, indicating potential evaporation and mixing with contributions from other water sources.

In contrast, significant changes in isotopic signatures were observed during the wet season. The downstream weir in catchment 6 recorded values of -3.94‰ for $\delta^{18}O$ and -15.3‰ for δ^2H, positioning them below the LMWL alongside other catchment signals. This shift could be attributed to the evaporation and mixing of various water sources. Meanwhile, the upstream east-west tributary in catchment 7 showed values of -4.45‰ for $\delta^{18}O$ and -13.6‰ for δ^2H, aligning directly on the Mike Pass LMWL, suggesting a direct recharge from rainfall. These observations highlight the dynamic interactions between surface water and groundwater in response to seasonal changes.

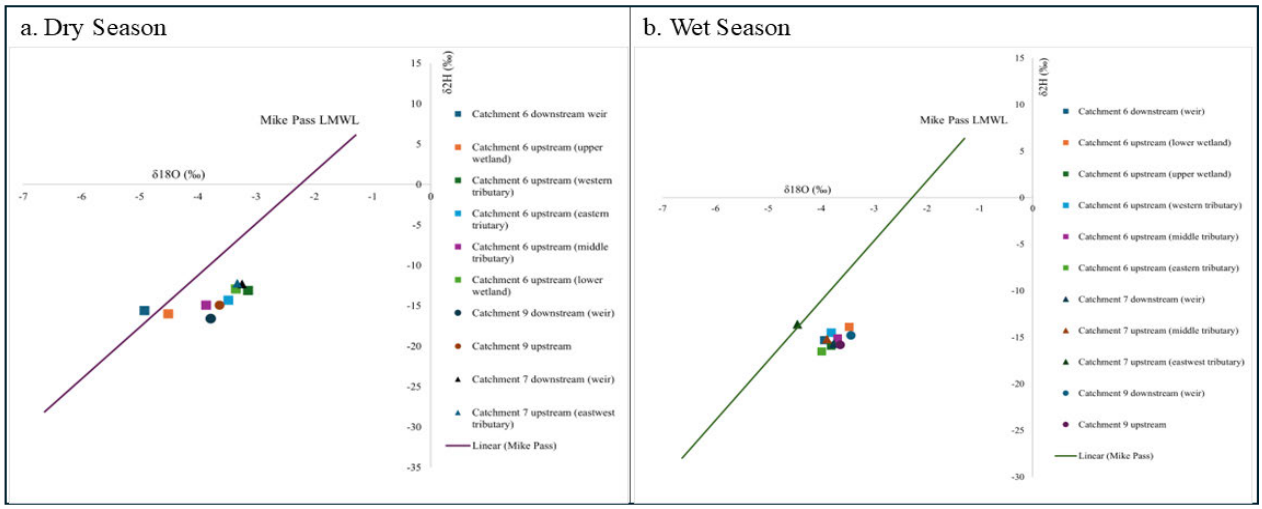

Figure 5.16: Isotope comparison of the wet and dry seasons for catchment 6,7 and 9

5.3.3.6 Catchment 6 event-based sampling EC

An event-based sampling was conducted during a rainfall event from December 12 to December 14, 2023, to investigate the role of groundwater in runoff generation. Catchment 6 was selected for this investigation, as previous results presented in this chapter indicated a high groundwater contribution. This was evident in the EC data (**Figure 5.12e**). Therefore, EC measurements were used to analyse groundwater contributions during a period of high rainfall. **Figure 5.17** illustrates the EC values recorded before (18:00 to 22:00), during (22:00 to 9:20), and after the rainfall event. Before the rainfall, the EC values of the three tributaries ranged from 113 µS/cm, 118 µS/cm, and 113 µS/cm, while the upper wetland had an EC of 108 µS/cm and the lower wetland measured 86 µS/cm. The EC for Catchment 6 was 96 µS/cm.

Additionally, the EC at the weir remained relatively constant before the rainfall, ranging between 96 and 95 µS/cm. However, as the rainfall began, the EC at the weir started to decrease, ranging between 93 and 81 µS/cm during the rainfall period. Following the rainfall, the EC at the weir gradually increased, stabilising at around 93 µS/cm. After the event, the EC values for the three tributaries were recorded as 112 µS/cm, 108 µS/cm, and 116 µS/cm, while the lower wetland had an EC of 82 µS/cm. The EC at the weir represents a mixture of contributions from the three tributaries and the two wetlands. During dry periods, the EC at the weir is relatively high, suggesting a greater contribution from the three tributaries compared to the nearby wetlands.

a.

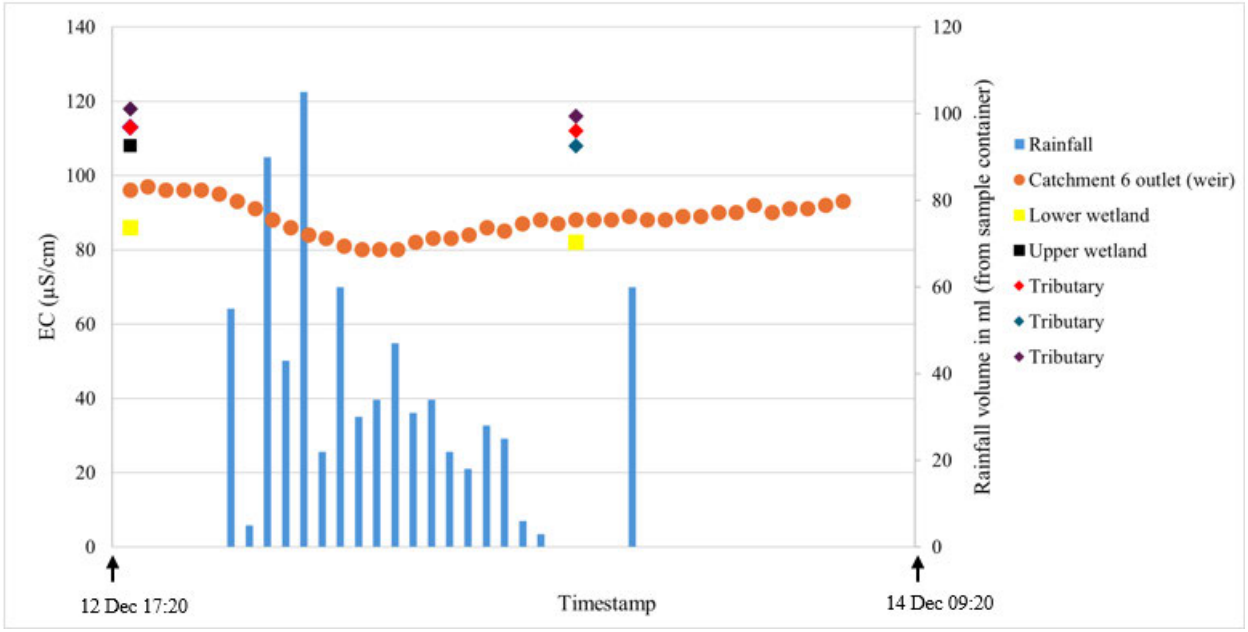

b.

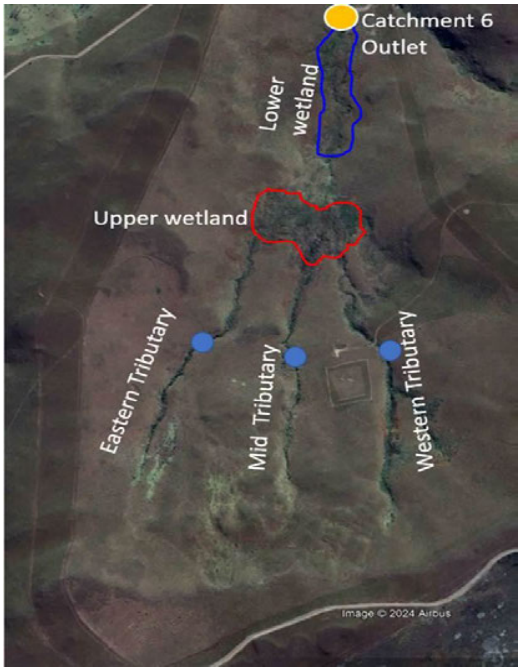

Figure 5.17: EC for event-based sampling at Catchment 6 from the 12 to 14 Dec

5.3.3.7 Catchment 6 event-based sampling for δ^2H and $\delta^{18}O$

The isotope composition of δ^2H and $\delta^{18}O$ from December 12 to December 14, 2023, is presented below (**Figure 5.18**). The isotope composition of rainfall ranged from -4.05 to -3‰ for $\delta^{18}O$ and from -11.6 to -6.4‰ for δ^2H. For the weir, the $\delta^{18}O$ values ranged from -4.05 to -2.76‰ and the δ^2H values ranged from -15.5 to -9.2‰. During the pre-event period, the water isotope signature of the weir was plotted closely to that of the tributaries and the wetland, indicating a strong connection among these water bodies. However, during the rain event, the isotope signature of the catchment outlet was plotted below that of the rainfall, suggesting that rainfall was contributing to the outlet's water composition. Notably, the outlet's isotope signatures were plotted below the LMWL, indicating evaporation effects.

Furthermore, these findings suggest that rainfall water could be mixing with nearby water bodies, such as wetlands, which may be contributing more significantly to the catchment outlet than tributaries during the rain event. Furthermore, this observation is supported by the EC data (**Figure 5.17**)**,** which showed a change in groundwater contribution from tributaries to the outlet before and during the rainfall event.in groundwater contributions from the tributaries to the outlet before and during the rainfall event.

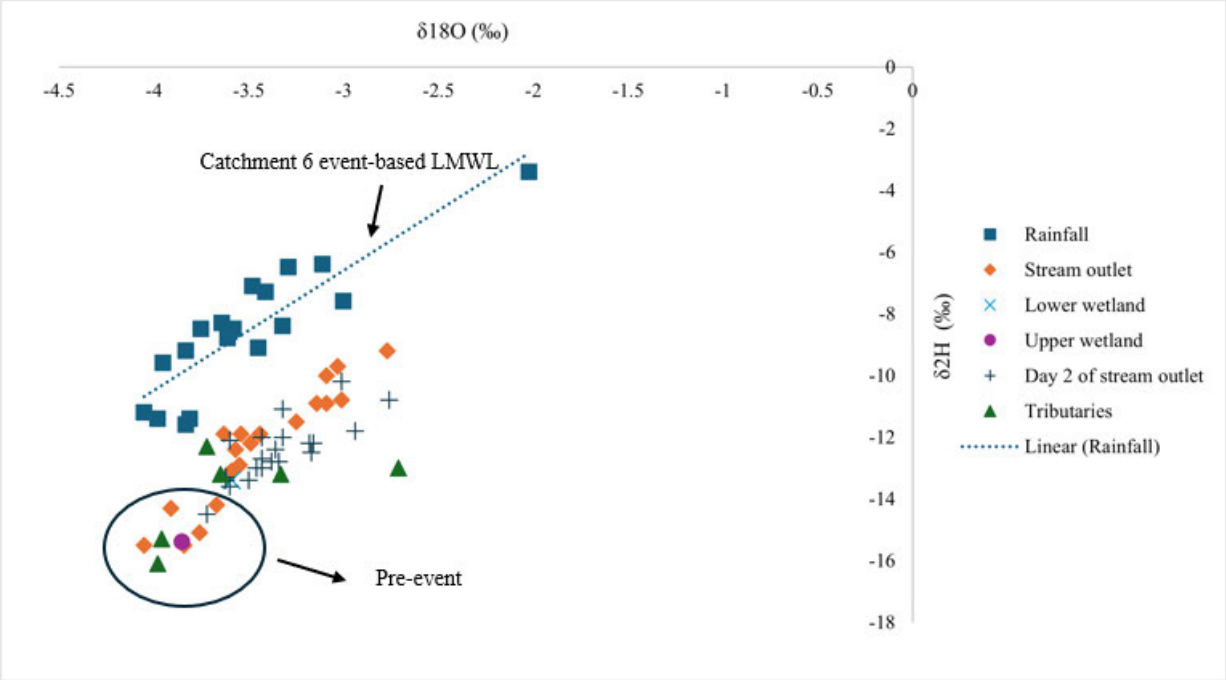

Figure 5.18: Isotope composition for event-based sampling at catchment 6 from 12 to 14 December

5.3.3.8 Catchment 6 second event-based sampling (EC)

A second event-based sampling was conducted from April 11 to April 12, 2024, at Catchment 6 (**Figure 5.19**) to investigate runoff generation on the hillslope. However, during this sampling period, only a small amount of rainfall was received, ranging from 4 to 15 mL (from the sampling bottle), which did not significantly affect groundwater contributions at the catchment outlet. The EC at the weir remained constant, ranging from 94 to 98 µS/cm. The EC was measured at 75 µS/cm in the lower wetland, while the upper wetland recorded an EC of 89 µS/cm. The three tributaries exhibited EC values of 121 µS/cm, 112 µS/cm, and 110 µS/cm, respectively. The lack of change in EC over the two-day sampling period suggests that the tributaries continued contributing to the catchment outlet.

a.

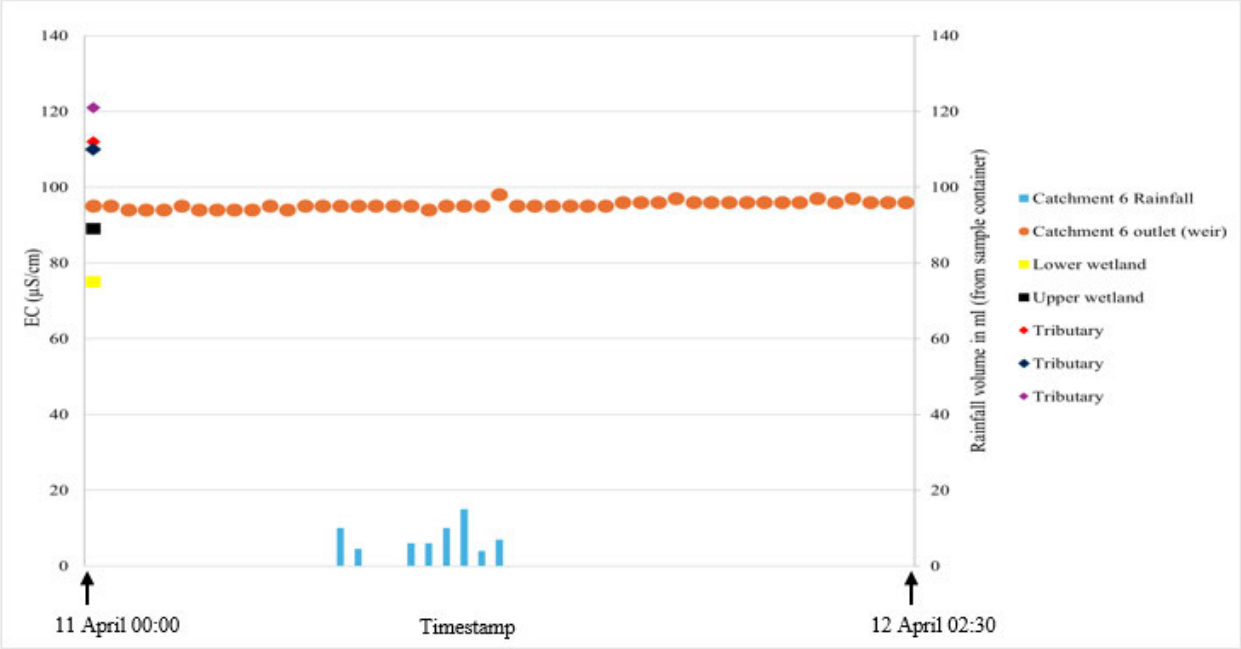

b.

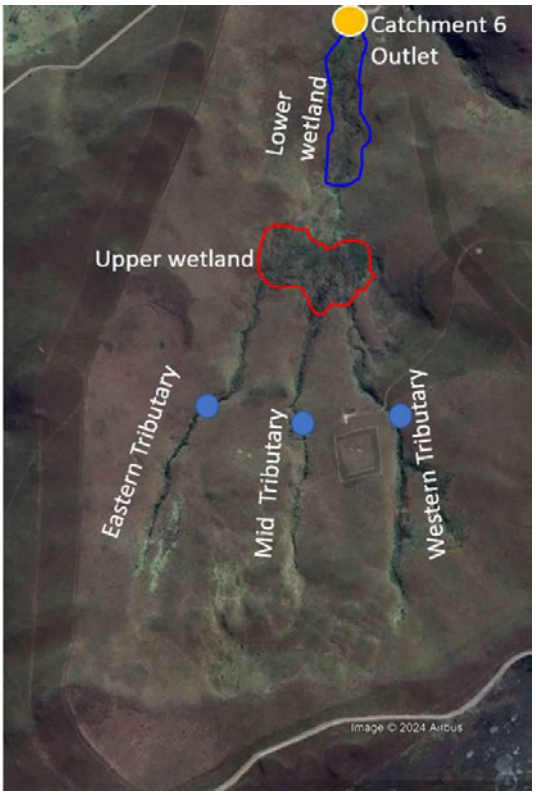

Figure 5.19: EC for event-based sampling at Catchment 6 from 11 to 12 April

5.3.3.9 Catchment 6 second event-based sampling (δ^2H and $\delta^{18}O$)

The isotope composition of δ^2H and $\delta^{18}O$ from April 11 to April 14, 2024, is presented in **Figure 5.20**. During this sampling period, there was insufficient rainfall, resulting in only a limited number of isotope samples being collected. The isotope composition for δ^2H ranged from -6.37 to -2.38‰, while $\delta^{18}O$ values varied from -29.8 to -5.9‰. This wide variation of isotope rainfall may be attributed to temperature effect in the Catchment 6, with the more enriched values corresponding to higher temperatures and the more depleted values due to cold temperature. In the lower wetland, the isotope values were -12.9‰ for δ^2H and -3.35‰ for $\delta^{18}O$. The upper wetland exhibited a range of -16‰ for δ^2H and -4.51‰ for $\delta^{18}O$. The three tributaries showed isotope values ranging from -14.9 to -13.1‰ for δ^2H and from -3.86 to -3.14‰ for $\delta^{18}O$. On the first day at the weir, the isotope signature varied from -16.6 to -12‰ for δ^2H and from -4.13 to -3.63‰ for $\delta^{18}O$. On the second day, the weir recorded an isotope value ranging between -19.1 to -11.3‰ for δ^2H and from -5.07 to -3.44‰ for $\delta^{18}O$.

Furthermore, **Figure 5.20** demonstrates that the weir falls within the event-based LMWL of Catchment 6, indicating that rainfall contributed to the recharge of the weir. Additionally, both the three tributaries and the lower wetland were plotted close to the weir on both days, suggesting that they also contributed to the flow at the weir during this period.

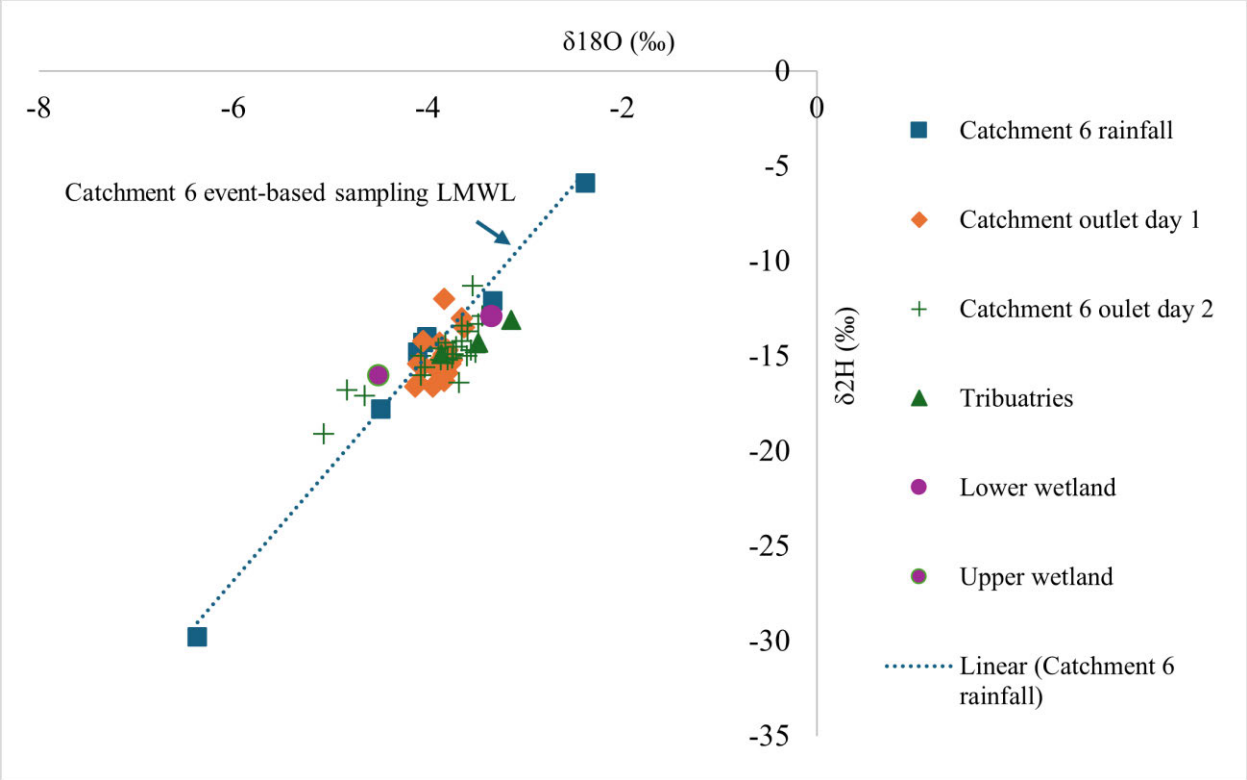

Figure 5.20: Isotope composition for event-based sampling at Catchment 6 (April 11-12, 2024)

CHAPTER 6: DISCUSSION

6.1 Introduction

The interaction between GW-SW at various spatial scales, such as hillslope, catchment, and regional levels, remains poorly understood, particularly in South Africa. This study seeks to address this knowledge gap by investigating the dynamics of GW-SW interactions across temporal and spatial scales, culminating in developing a conceptual model. This research represents the first comprehensive examination of groundwater's role at multiple spatial scales within the uThukela Catchment, using data collected at hourly, daily, and monthly intervals from five strategically placed rainfall collectors. This chapter presents key findings from this investigation, focusing on addressing the primary aim of developing a robust conceptual model. Additionally, results from chapter five are further explored and contextualised to enhance understanding and linkages with the study's overarching objectives.

6.2.1 Characterising rainfall isotope signals

This study constructed five LMWL (Pietermaritzburg; $\delta^2H = 7.37 * \delta^{18}O + 14.32$, Eshowe; $\delta^2H = 5.45*\delta^{18}O + 10.46$, Winterton; $\delta\delta^2H= 6.5*\delta^{18}O + 11.76$, Mike Pass; $\delta\delta^2H= 6.43*\delta^{18}O + 14.66$ and Catchment 6; $\delta\delta^2H= \delta2H = 5*\delta18O + 8.81$). The Pietermaritzburg LMWL had a slope of 7.37, which is closest to the GMWL of 8, suggesting that the conditions are close to equilibrium. The slight decrease in the slope could be attributed to evaporation from the falling rain that results in the enrichment of the heavy isotopes (δ^2H and $\delta^{18}O$) relative to the lighter ones (Gat, 1996). From the five LMWLs, Catchment 6 had the lowest slope (5); this slope does fall under the range of slopes (5–7) indicated by the Global Network of Isotopes in Precipitation (GNIP) on continental Africa (Cozma *et al.*, 2017; Wanke *et al.*, 2018). All the slopes of the LMWL of this study are low compared to other slopes of southern Africa from the GNIP stations in Uganda, the Democratic Republic of Congo (DRC), Zambia, Angola, Zimbabwe, Tanzania, and Namibia; which are between 7.05 to 7.96 (Wanke *et al.*, 2018). The slopes of this study are similar to other slopes in Cape Town, such as Cape Town (5.28) and Pretoria (6.55); this was determined based on the GNIP data from the International Atomic Energy Agency (IAEA) . The diverse local climate conditions and the potential impact of evaporation in this region could be the reason for the low slope.

In particular, Catchment 6 has the lowest slope in this study, which is due to the altitude effect, as precipitation at higher altitudes generally has more depleted values of heavy isotopes ($\delta^{2}H$ and $\delta^{18}O$) compared to the low lands. This due to the orographic lifting of moist air, which cools and condenses as it rises, leading to the rainout of heavier isotopes of $\delta^{2}H$ and $\delta^{18}O$, leading to a low LMWL slope. It is worth mentioning that Grab (2013) stated that the Drakensberg, where catchment 6 is located, acts as a barrier to air masses, forcing moist air from the warm Indian Ocean to ascend; as the air rises, it cools adiabatically and leads to cloud formation and precipitation.

As shown in **Table 5.2**, all the d-excess values in the uThukela were above 10‰ of the ocean moisture (Dansgaard, 1964); this implies that there is a higher proportion of moisture derived from local or continental sources rather than directly from the ocean. Winterton had the lowest d-excess (12.19‰), and this is different from the d-excess of the other stations located in the highlands of the uThukela, such as Mike Pass (20.07‰) and Catchment 6 (21.61‰). This low d-excess due to a local phenomenon of 'Rain shadow effect'. Dray *et al.* (1998) described the rain shadow effect as the difference in isotopic signatures observed between a mountainous massif's windward and leeward sides. This local phenomenon results in depleted isotopic values on the leeward slope (Winterton) compared to those on the windward side (Mike Pass and Catchment 6). According to Grujic *et al.* (2018), rain shadowing over the Shillong Plateau occurs as moist air from the Bay of Bengal rises over its southern slopes, cools, and releases heavy rainfall; the air then descends on the leeward side, warms, and becomes drier, creating a rain shadow with significantly reduced precipitation in regions like the Himalayan foothills of eastern Bhutan and this leads to depletion of isotope signature.

The d-excess of Mike Pass (20.07‰) and Catchment 6 (21.61‰) located in the Drakensberg escarpment were the highest, and this is attributed to the possibility of an additional supply of recycled moisture across the region. Thus, it was reported that the Drakensberg has variability and complexity in both spatial and temporal temperature trends, and this is attributed to the site-specific topographic controls, thus leading to different moisture sources and pathways. The Drakensberg escarpment acts as a barrier, dividing humid maritime air masses to the east (Indian Ocean) from the drier continental air masses to the west, and this influences the temperature and lapse rate trends in the escarpment and nearby regions.

The northeastern slopes of the Drakensberg experience stronger temperature inversions, occurring more frequently up to twice as often as the southeastern slopes, with the frequency of inversions varying depending on elevation. Additionally, it was highlighted that moisture from the Indian Ocean is uplifted along the eastern slope of the escarpment due to orographic forcing. This results in precipitation and the formation of clouds in high elevations. The clouds formed at higher altitudes may drift to the catchment's lowlands, suggesting that moisture sources are mixed along the uThukela.

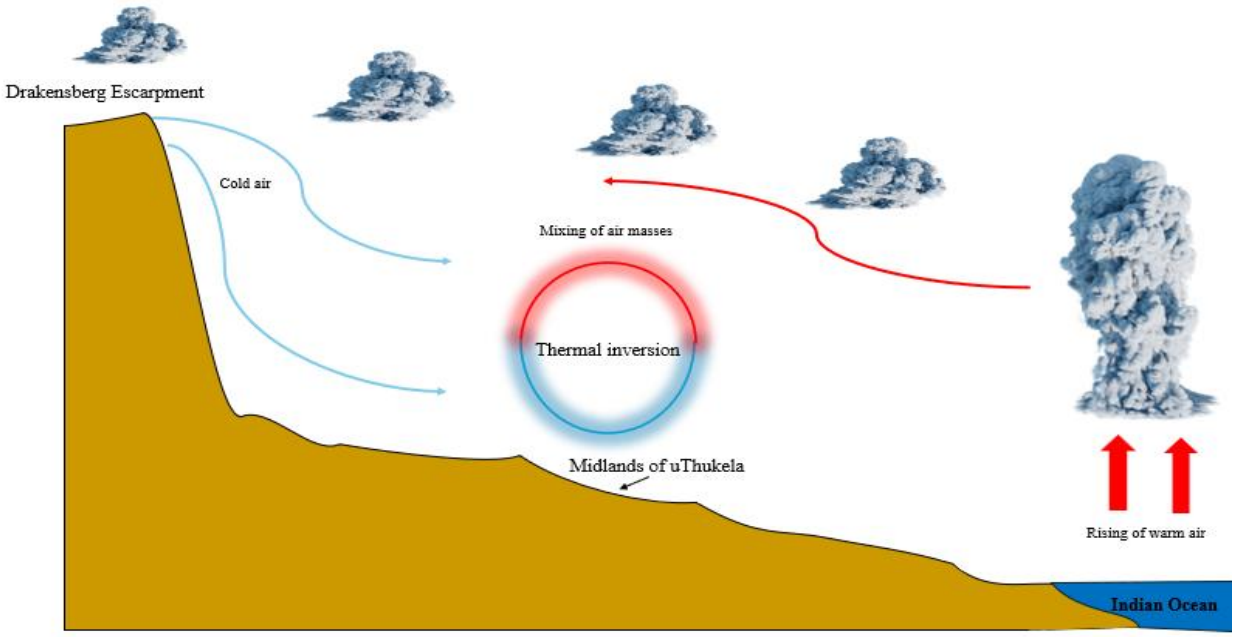

Figure 6.1: Air moisture trajectory of the uThukela

This study had a low altitude gradient of -0.06‰ for $\delta^{18}O$ per 100m; this low altitude effect is attributed to the strong mixing of moisture sources and the moisture trajectory from the Drakensberg escarpment and from the Indian Ocean. It was highlighted by Leketa and Abiye (2020) that the altitude effect is influenced by the altitude and moisture sources; the study demonstrated that moisture sources from the Atlantic and Indian Oceans can result in differences in isotope signature depending on where the moisture source originates. Additionally, the low altitude effect of the uThukela is attributed to thermal inversion in the Drakensberg escarpment and midlands of the uThukela Catchment (**Figure 6.1**), thermal inversions stabilise atmospheric layers, trapping the cooler air beneath a layer of warmer air. These inversions hinder vertical mixing, leading to a uniform isotopic composition across different elevations, hence the low

altitude effect. This phenomenon could be linked to the region's unique topography and weather systems.

Furthermore, this is linked to the findings of Harris and Diamond (2013) from Table Mountain, Western Cape Province in South Africa. The altitude gradient of the study was 0.085‰ for $\delta^{18}O$ per 100m. This low gradient is attributed to temperature variations with altitude; this could bring conditions higher up in the cloud to lower elevations, thereby suppressing the altitude effect. Grab (2013) indicated that the Drakensberg does not show a strong temperature lapse rate. Similarly to Table Mountain, this could bring conditions from higher up in the cloud to a lower elevation, weakening the altitudinal gradient.

Furthermore, a weak continentality effect of -0.04‰ for $\delta^{18}O$ per 100km was also demonstrated in this study. The lack of continentality effect is linked to the high d-excess caused by the mixing of moisture and its transport pathway from the Drakensberg escarpment and the Indian Ocean. Durowoju *et al.* (2019b) highlighted that the d-excess is useful for the determination of the relative contribution of inland moisture and oceanic moisture; it further stated that the depletion effect of the d-excess is called the 'continentality effect'.

The amount effect in this study is evident, especially in the Pietermarzitburg rainfall station. During periods of high rainfall, there was evidence of $\delta^{18}O$ depletion, and this finding was complemented by the existing literature in this study, which stated that heavy isotopes are depleted in rainfall, and this depletion is more noticeable in heavier rainfall events (Allen *et al.*, 2017). In Pietermarziburg, during the period of the intense storm (April 2022), which was attributed to the subtropical storm named 'Issa' that formed off the southeast coast of South Africa, the Pietermarziburg rainfall station recorded the most depleted isotope values during the period of the intense storm. These findings also supported other findings in South Africa, the Limpopo Province (Durowoju *et al.*, 2019a) and Johannesburg (Leketa and Abiye, 2020) that demonstrated that during periods of heavy rain, there is a depletion of heavy isotopes, which includes $\delta^{18}O$.

The seasonality effect provided in this study showed variability; this variability of the seasonality effect in Pietermaritzburg is due to the mixture of moisture sources across the seasons. The moisture sources originate from the Drakensberg escarpment and the Indian Ocean. This variation

of seasonality in Pietermaritzburg that is associated with the mixing of moisture sources necessitates further investigation of the trajectory and the mixing of moisture sources in South Africa.

6.2.2 GW-SW interactions

6.2.2.1 Regional scale

The study assessed GW-SW interaction at a regional scale, integrated methods of ^{222}Rn, BFI index, piezometric analysis and $\delta^{2}H$ and $\delta^{18}O$. The ^{222}Rn and BFI index data provided insight into groundwater discharging into the uThukela River. The ^{222}Rn and BFI index data varied upstream and downstream, with both results showing high concentrations of groundwater discharge in the upstream compared to the downstream. The high concentrations upstream of the catchment are closely linked to the geology and the presence of dykes and faults within the area (**Figure 5.6**).

The upstream, approximately southwest of the uThukela, shows a trend of faults and dykes, and that is the region where groundwater discharge is abundant. These findings complemented the literature provided, highlighting that high-permeable rocks have higher groundwater discharge than areas with low-permeable rocks (Kresic, 2006). Furthermore, it was also highlighted that the presence of dykes can act as a barrier or conduit to groundwater flow (Babiker and Gudmundsson, 2004).

However, compared to other studies in South Africa, the uThukela River ^{222}Rn concentration was relatively low compared to studies conducted in the Western Cape at the Gevonden and Molenaars rivers (Strydom *et al.*, 2021) and Gauteng in different rivers (Masevhe *et al.*, 2017). Additionally, these studies noted that this groundwater discharge is due to the underlying geology and the proximity of faults. Furthermore, it is indicated that there is an increase in ^{222}Rn concentration at rivers in immediate areas surrounding groundwater discharge points (Ellins *et al.*, 1990; Cook *et al.*, 2003). Therefore, BFI index and ^{222}Rn are useful methods of determining groundwater discharge into surface water bodies.

Furthermore, the deep regional groundwater discharge was assessed using $\delta^{2}H$ and $\delta^{18}O$ from Mike Pass and the Shu Shu thermal springs. The data revealed that the Shu Shu thermal springs are locally recharged from the nearby surface waters rather than meteoric waters from the highlands

of the uThukela Catchment. This lack of evidence of deep regional groundwater flow in the uThukela Catchment contradicts Gravelet-Blondin (2013), who highlighted that the springs are recharged approximately 130 km to the west towards the Drakensberg escarpment. The stable isotope data reveal that this recharge of the Shu Shu thermal springs is local, and this can thus be supported by the BFI index and ^{222}Rn that show low groundwater discharge at the lowlands of the catchment and this is mainly due to the geology and lithology of the Catchment. Additionally, the Shu Shu thermal springs emerge near the contact zone of the Karoo sediments and the basement rocks, which have low hydraulic conductivity (K) (Woodford and Chevallier, 2002). The Karoo sandstones have a hydraulic conductivity of 10−7 to 10−5 m/s, with shale acting as a confining layer (10^{-9} to 10^{-7} m/s). The low hydraulic conductivity of the lithologic units indicates low permeability, which restricts groundwater movement and connectivity throughout the catchment. This results in slow subsurface flow and minimal discharge to surface springs. Moreover, the absence of significant spring discharges from the sedimentary lithologies and basement rocks within the midlands of the uThukela Catchment highlights the limited influence of regional groundwater flow in this basin.

6.2.2.2 Catchment scale

The stable isotope data and EC in the catchment scale were used to determine the role of intermediate groundwater. However, in this study, it was observed that groundwater has the same isotopic signature as the streams, and this suggests that the streams contribute to recharging the groundwater. The Catchment scale is located in an area where the land use is mostly agricultural farming (**Figure 6.2**), and the farmers draw water from the surface waters and boreholes to irrigate the crops. There could be a possibility that this irrigation water can lead to surface runoff that recharges the groundwater and evaporates as it recharges.

IAEA (1996) highlighted that irrigation water can alter the isotope signature of groundwater because it can undergo prior evaporation, enriching or depletion of the isotopes before recharging the aquifers. Additionally, in South Africa, a study by Abiye *et al.* (2021) highlighted that high values of $\delta^{18}O$ in the groundwaters are believed to be from irrigation areas where evaporation enrichment occurred, which subsequently led to enriched $\delta^{18}O$ values for the groundwaters, and this was the impact of the land use. Moreover, El Mountassir *et al.* (2021) also highlighted the

influence of land use that recharge from irrigated water can cause enrichment on the isotopic composition of waters. However, there could also be a possibility that the streams are losing water to the ground. The isotope data are not clear as to which water is recharging the aquifers, but rivers are involved in recharging the aquifer; it could be direct leakage from the rivers recharging or its irrigation water from abstracted from groundwater that is returning.

The EC data further evident this relationship between the streams and the groundwater at the catchment scale (**Figure 5.11**). In the wet and dry seasons, the EC of the streams and the boreholes close to each other have more/less similar EC. This similarity in the EC of the streams and the boreholes indicates that there is a correlation between the surface water and groundwater in the catchment scale. Various studies globally have proven that EC can be used to investigate the interaction between GW-SW interactions, such as studies in Australia (Unland *et al.*, 2013), Germany (Kalbus *et al.*, 2006) and Taiwan (Tsai *et al.*, 2022). Furthermore, in South Africa, Welgus and Abiye (2022) highlighted the similarity in groundwater and river EC that are near each other, indicating an interaction between the two, meaning that groundwater recharge is localised.

Additionally, The findings of the stable isotope and the EC data suggest that the interactions of GW-SW in the catchment scale are localised, and in this data, no evidence of intermediate groundwater flow was found. It is mostly like the groundwaters within the catchment scale are gaining water from the streams instead of groundwater from the Drakensberg escarpment. The absence of intermediate groundwater flow in the Drakensberg region is primarily attributed to the low permeability of the geological formations within the Drakensberg Group. This group is predominantly composed of basalts, with minor occurrences of sandstones, tuffs, and agglomerates. The structural characteristics of these formations likely impede groundwater movement from the Drakensberg escarpment into the underlying mountain valleys.

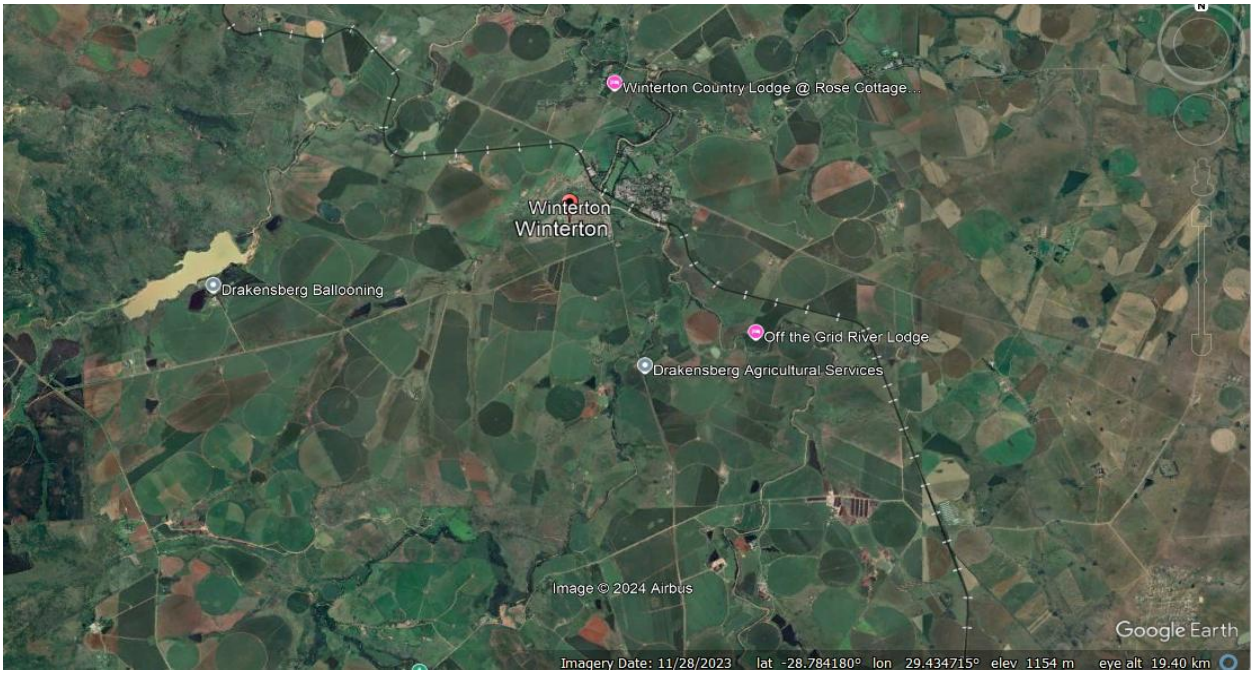

Figure 6.2: Image showing the landscape of the catchment scale (source: Google Earth Pro)

6.2.2.3 Hillslope scale

The stable isotope and EC data from the hillslope demonstrate the significance of each catchment in the hillslope. Catchment 3 stands out the most, with EC being the highest downstream compared to the catchments' upstream in almost all the months. This might be caused by the difference in topography, predominant contribution of shallow soil water and the absence of wetlands in this catchment. Catchment 3, compared to the other catchments, has a steep slope gradient at the top (**Figure 6.3**), which could suggest that it is surface water driven. Studies have shown that Mountain streams often have steep gradients, facilitating faster water movement (Grant, 1988; Gomi *et al.*, 2002; Mir and Patel, 2024). When it rains, water quickly travels down these slopes due to gravity, leading to rapid increases in streamflow downstream and this could limit groundwater recharge and discharge in this catchment.

This steep gradient facilitates more runoff from rainfall compared to a gentle plateau-like catchment 6 and 7. Furthermore, it was highlighted that the hydraulic gradient increases with slope steepness, which enhances drainage (Wang *et al.*, 2020). This means water on steep slopes drains more quickly than on gentler slopes, further contributing to surface runoff rather than groundwater recharge. In gentle terrains like Catchment 6 and 7, rainwater soaks inside the gentle plateau, contributing to groundwater recharge. However, it is worth noting that other factors, such as soil

property and vegetation, also contribute to runoff generation, especially in steep slope areas (Chen *et al.*, 2018).

Figure 6.3: Landscape terrain of catchment 3 (source: Google Earth Pro)

Additionally, the lack of wetlands in Catchment 3 further suggests that it is a surface water-driven catchment. In contrast to Catchment 3, the other catchments have higher EC upstream compared to downstream throughout the year, notably Catchments 6 and 7. This pattern points to a strong and persistent groundwater influence upstream of these catchments. Furthermore, downstream of these catchments, there is mixing and contribution from other sources that are downstream of these catchments, such as wetlands and seepages. The main factor for mixing water sources is called "groundwater ridging", a common process in hillslope hydrology (**Figure 6.5**). Zang *et al.* (2018) highlighted that groundwater ridging is a swift and rapid rise of the water table following recharge events in shallow groundwater systems. This phenomenon typically occurs where the capillary fringe reaches close to the surface, such as at the toe of a hillslope riparian zone with gently sloping topography.

In this context of catchments 6 and 7, there is a gentle slope topography upstream (**Figure 6.4**) compared to catchment 3. This suggests that during rainfall, the water seeps into the gentle plateau, further contributing to groundwater recharge. Flat areas or gentle slopes are highly effective for groundwater recharge because they promote high infiltration rates and generate less surface runoff

(Appels *et al.*, 2016). In contrast, steep slopes tend to have lower groundwater levels, with less time for stormwater infiltration. Consequently, rainfall quickly transforms into runoff and flows rapidly down the slope.

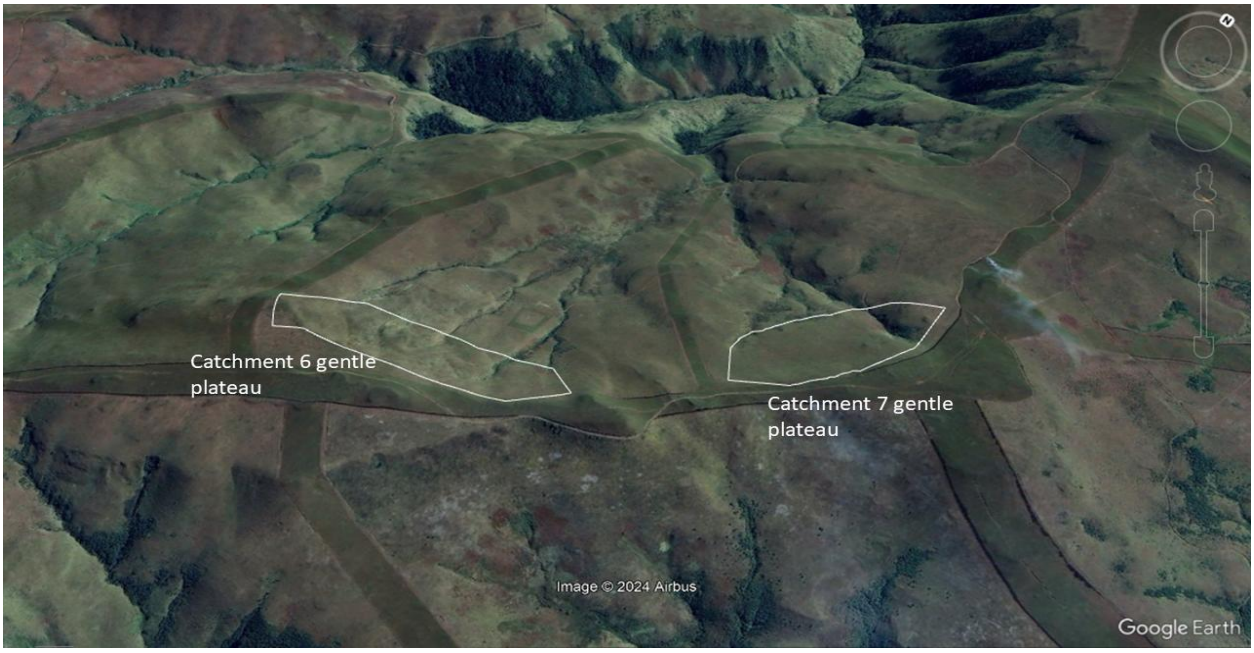

Figure 6.4: Catchment 6 and 7 plateau (source: Google Earth Pro)

Moreover, the change of the EC downstream of catchments 6 and 7 is a contribution from pre-existing water from the groundwater discharging into the stream and in the form of wetlands and seepages; this causes a change of EC in water flowing from the upstream, and as it mixes with the groundwater ridging water. A study conducted by Theron *et al.* (2022) in South Africa, the Western Cape Province highlighted that a small amount of rainfall is required to fill the capillary fringe, leading to an immediate rise in the water table; the steep hydraulic gradient is directed towards the lower stream and leads to the discharge of the pre-existing water into the stream (Zang *et al.*, 2018).

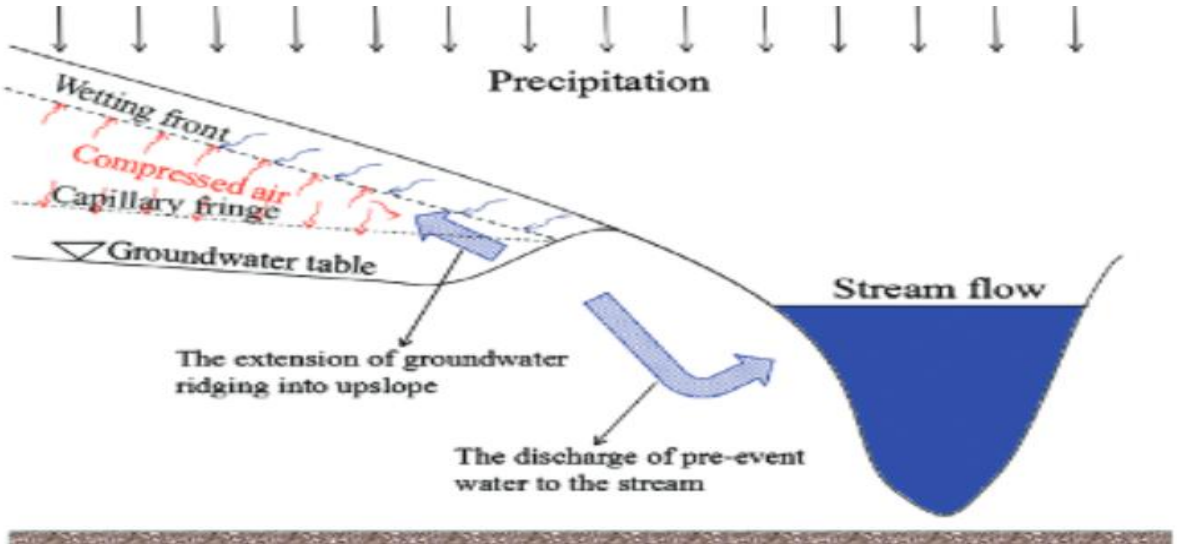

Figure 6.5: Schematic diagram of groundwater ridging in hillslope riparian zone (Zang et al., 2018)

Furthermore, during the dry and wet seasons, the catchments' downstream and upstream data varied. However, of all the catchments, catchment 6 demonstrated the most consistency in its stream outlet; the EC and the stable isotope findings from catchment 6 revealed that the catchment outlet resembled both the three groundwater-fed tributaries and the wetlands. However, during the dry months, the groundwater-fed tributaries contribute more to the stream's outlet than the wetlands. In contrast, during the wet months, the wetland significantly contributed to stream outlet, especially during periods of rain. These findings coincide with findings highlighted by Scheliga *et al.* (2019) during wetter conditions, wetlands connect and contribute more to the stream networks as they saturate more and lead to overland flow. However, during the dry conditions, groundwater seepage is more dominant (Lessels *et al.*, 2016).

To validate these findings further, the event-based sampling demonstrated that during a rainfall event, the wetland water contributes significantly to the stream outlet of catchment 6. This process between the rainfall and the wetland is noted as 'Fill and spill'. The fill and spill is a process that pertains to how wetlands respond to precipitation and runoff generation. The process of fill and spill has been documented in various research (Tromp-van Meerveld and McDonnell, 2006; Leibowitz *et al.*, 2016; McDonnell *et al.*, 2021). McDonnell *et al.* (2021) described the fill and spill as storage excess leading to pre-existing water spilling. Similarly, Scheliga *et al.* (2019) demonstrated fill and spill within wetlands act as temporary storage for water, buffering rainfall input. As rainfall continues, these fill up and start to spill into neighbouring channels, creating a

connection between them. In the context of catchment 6, the wetland quickly fills up immediately during a rainfall event and spills water to the stream outlet.

The findings reveal the intricate hydrologic dynamics of catchment 6, highlighting the dominance of bedrock groundwater during periods of low rainfall, which is supplemented by groundwater tributaries. During rain events, stable isotope data and EC measurements indicate a blend of water sources, with contributions from both the wetland and groundwater tributaries flowing into the stream outlet (**Figure 6.6**). Conversely, in dry periods, the stream outlet's composition closely mirrors that of the groundwater tributaries, showing minimal influence from the wetland.

Moreover, these observations underscore how topography, slope, and wetlands shape GW-SW dynamics. Catchments with gentle slopes and wetlands, like Catchment 6, promote effective groundwater recharge and release through the cyclical filling and emptying of the groundwater reservoir. This leads to a consistent predominance of groundwater in runoff throughout all seasons. In contrast, steep slopes, such as those found in Catchment 3, result in runoff generation that is primarily influenced by shallow regolith water.

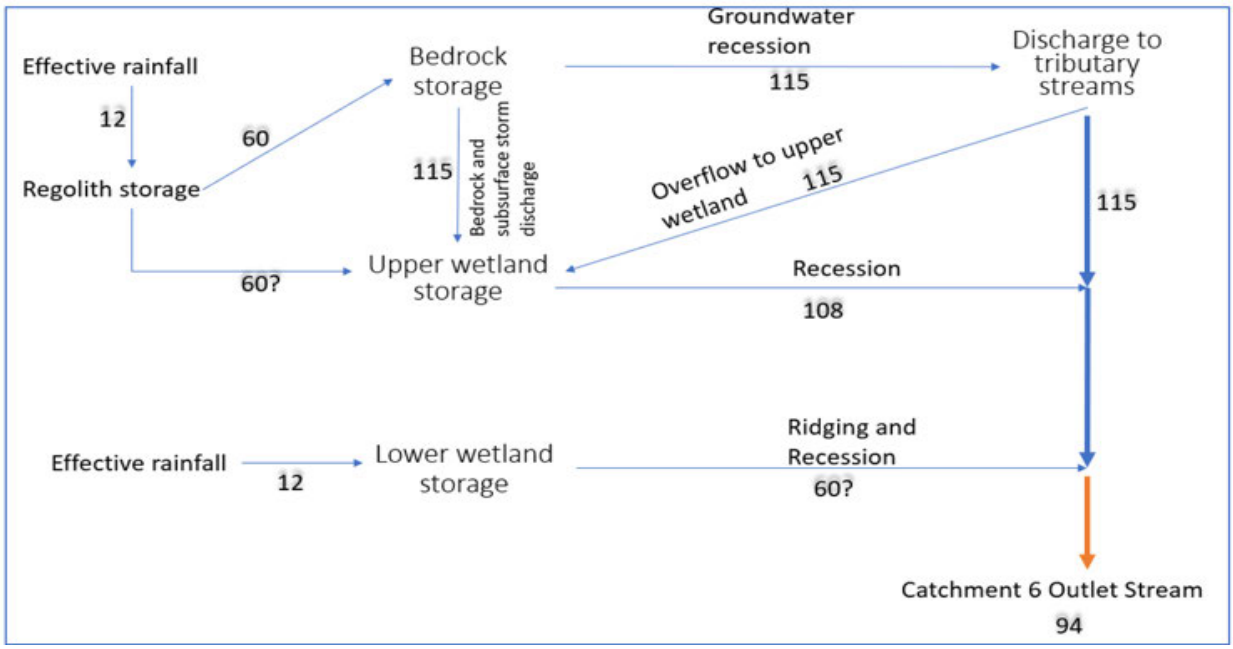

Figure 6.6: GW-SW interaction at Catchment 6, shaded numbers are EC (µS/cm) collected on the 12th of December 2023.

6.2.2.4 Conceptual model

GW and SW are intricately interconnected in many landscapes, so comprehending their relationship for effective water resource management is essential. Groundwater is crucial in sustaining surface water bodies, such as rivers and wetlands, particularly during dry periods. This hydraulic connection supports aquatic ecosystems and influences water availability for human use and environmental health. The study developed a conceptual model of GW-SW interactions based on observations of geology, lineaments, topography, seepages, groundwater levels, flow direction, and environmental isotopes (such as $\delta^{2}H$, $\delta^{18}O$, and ^{222}Rn), as well as hydrochemistry, baseflow separation, and piezometric analysis, as detailed in the preceding sections.

The aforementioned findings contributed to developing a conceptual model illustrating the interaction between GW and SW, encompassing groundwater recharge, discharge, flow processes, and their connections with surface waters. In this model, groundwater is depicted as moving from high-hydraulic head to low-hydraulic head areas, following a path of decreasing mechanical energy or potential, and ultimately discharging into surface depressions, wetlands, springs and rivers. This process is illustrated as it is crucial for sustaining river flows as baseflow during the dry season. Additionally, due to various topographic and hydraulic conditions, rivers and streams can also lose water along certain reaches, contributing to groundwater recharge.

Furthermore, other hydrological models that showed the interaction of GW and SW developed in South Africa, such as the Acru Model, do not fully capture the dynamics of GW-SW interactions due to insufficient data and a lack of comprehensive methodologies for assessing these interactions such as environmental isotopes used in this study. The conceptual model demonstrates the movement, recharge and discharge of groundwater at different scales (hillslope, catchment, regional). The hillslope dynamics reveal how shallow groundwater returns to stream outlets in the Drakensberg Mountains. At the catchment scale, data from ^{222}Rn indicates a significant discharge of groundwater into the streams. However, stable isotope analyses suggest that, in certain instances, stream waters also contribute to the recharge of groundwater. At the regional scale, there is no evidence of deep regional groundwater flow, but findings suggest that there is localised groundwater flow.

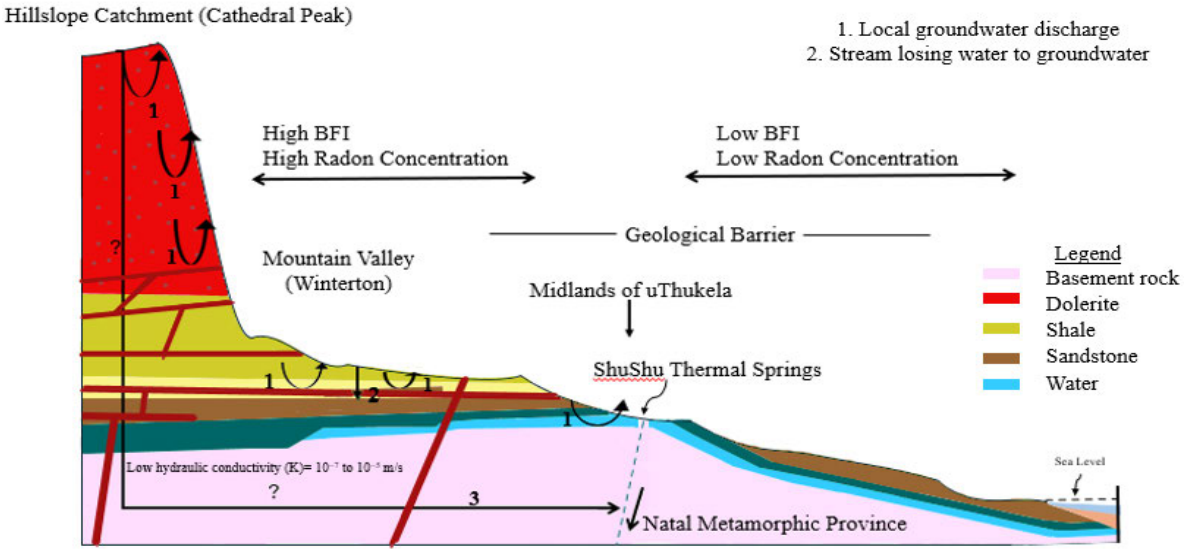

Figure 6.7: Conceptual Model of GW-SW interactions at uThukela Catchment

CHAPTER 7: CONCLUSION AND RECOMMENDATIONS

7.1 Conclusion

The various fields and secondary data collected, such as environmental isotopes, hydrochemistry, baseflow separation, and piezometric analysis data, were integrated and interpreted to understand and conceptualise GW-SW interactions of the uThukela Catchment. The conceptual model demonstrated how groundwater is recharged and discharged, its connection with surface water and its movement. The integrated methods that were used in this study coincided with each other to investigate the connection between GW and SW.

In characterising isotopes in rainfall , the findings regarding the altitude effect, amount effect, and seasonality effect could have significant implications for water resource management. The characterising rainfall isotope findings reveal complex interplay between local climatic conditions, topography, and moisture dynamics that shape rainfall isotopic signatures in the uThukela Catchment. Understanding these influences is crucial for conducting accurate hydrological assessments and implementating effective water resource management strategies.

In the regional scale, it was discovered that geology plays a dominant role in governing regional-scale groundwater dynamics. Groundwater flows originating from the higher elevations in the headwater regions is unlikely to pass through the very low-permeability basement rocks underlying the uThukela Catchment. These basement rocks, particularly at greater depths, demonstrate very low hydraulic conductivity, which creates barriers that restrict the flow of deep regional groundwater to downstream areas, such as the Shu Shu thermal springs. Consequently, this suggests that the groundwater is localised rather than part of a broader flow system. Furthermore, the lack of major springs at the interface of sedimentary lithologies and basement rocks in the middle reaches of the catchment highlights the limited influence of deep regional groundwater flow systems within the uThukela Catchment.

The catchment scale reveals aquifer recharge in the valleys of the Drakensberg Mountains primarily results from the vertical percolation of pre-evaporated surface waters. This process is likely linked to transmission losses from local streams or irrigation return flows from agricultural activities in the area. The findings suggest that aquifer recharge in the catchment scale is from local

sources. Additionally, Land use such as agriculture plays a vital role in the interaction of GW-SW within this scale. However, there is no evidence supporting the existence of intermediate groundwater flow discharge to the mountain valleys of the Drakensberg. This absence may be attributed to the low permeability of the geological formations, which restricts groundwater movement towards these valleys.

In the hillslope scale, the findings demonstrated that among the nine catchments at Cathedral Peak, Catchment 6 stands out as the most important due to its consistent predominance of groundwater across all seasons. In contrast, Catchment 3 is characterised as a surface water-driven catchment. Evidence indicates that groundwater plays a crucial role in runoff generation during both wet and dry seasons. Specifically, during dry periods, groundwater is the primary contributor to streamflow, providing essential baseflow to stream outlets. Conversely, during wet seasons and rainfall events, the phenomenon of groundwater ridging facilitates the rapid release of pre-event water into storm flows.

The role of groundwater and its factors controlling the interaction between GW and SW was well investigated in this study. Additionally, the integrated methods proved useful in investigating GW-SW interaction.

7.2 Recommendations

- Continuous rainfall isotope data collection is recommended to establish long-term trends.
- Future research should prioritise addressing the existing gaps in evidence regarding deep groundwater and regional flow dynamics. This can be achieved by focusing on the installation of deep wells, which will enable direct sampling and monitoring of groundwater at greater depths.
- Continuous monitoring of stream flow and installation of new gauging stations along the main rivers are recommended to improve the baseflow estimation of the catchment.
- The proposed conceptual model is not to scale and does not incorporate all local features. Further data can be gathered to enhance the conceptual model. Additionally, this model can serve as a foundation for improving water resource management and creating a regional numerical model.

- Future hydrology models should account for GW-SW interaction dynamics by employing integrated methods, such as environmental isotopes, to accurately determine their origins and flow patterns.

REFERENCES

Abiye, T, Mengistu, H, Masindi, K and Demlie, M. 2015. Surface water and groundwater interaction in the upper Crocodile River Basin, Johannesburg, South Africa: Environmental isotope approach. *South African Journal of Geology* 118 (2): 109-118.

Abiye, TA, Demlie, MB and Mengistu, H. 2021. An overview of aquifer physiognomies and the δ18O and δ2H distribution in the South African groundwaters. *Hydrology* 8 (2): 68.

Acocella, V, Korme, T and Salvini, F. 2003. Formation of normal faults along the axial zone of the Ethiopian Rift. *Journal of structural Geology* 25 (4): 503-513.

Adachi, I and Yamanaka, T. 2024. Isotopic evolutionary track of water due to interaction with rocks and its use for tracing water cycle through the lithosphere. *Journal of Hydrology* 628 130589.

Adams, JB, Taljaard, S and Van Niekerk, L. 2023. Water releases from dams improve ecological health and societal benefits in downstream estuaries. *Estuaries and Coasts* 46 (8): 2244-2258.

Ahmed, M, Chen, Y and Khalil, MM. 2022. Isotopic composition of groundwater resources in arid environments. *Journal of Hydrology* 609 127773.

Al-Nahmi, F, Alami, O, Baidder, L, Khanbari, K, Rhinane, H and Hilali, A. 2016. Using remote sensing for lineament extraction in Al Maghrabah area-Hajjah, Yemen. *The International Archives of the Photogrammetry, Remote Sensing and Spatial Information Sciences* 42 137-142.

Al Atawneh, D, Cartwright, N and Bertone, E. 2021. Climate change and its impact on the projected values of groundwater recharge: A review. *Journal of Hydrology* 601 126602.

Ala-aho, P, Rossi, PM, Isokangas, E and Kløve, B. 2015. Fully integrated surface–subsurface flow modelling of groundwater–lake interaction in an esker aquifer: Model verification with stable isotopes and airborne thermal imaging. *Journal of Hydrology* 522 391-406.

Allen, ST, Keim, RF, Barnard, HR, McDonnell, JJ and Renée Brooks, J. 2017. The role of stable isotopes in understanding rainfall interception processes: a review. *Wiley Interdisciplinary Reviews: Water* 4 (1): e1187.

Anderson Jr, WP and Emanuel, RE. 2010. Effect of interannual climate oscillations on rates of submarine groundwater discharge. *Water Resources Research* 46 (5).

Appels, WM, Bogaart, PW and van der Zee, SE. 2016. Surface runoff in flat terrain: How field topography and runoff generating processes control hydrological connectivity. *Journal of Hydrology* 534 493-504.

Baalousha, HM. 2016. Groundwater pumping versus surface-water take. *Modeling Earth Systems and Environment* 2 1-6.

Babiker, M and Gudmundsson, A. 2004. The effects of dykes and faults on groundwater flow in an arid land: the Red Sea Hills, Sudan. *Journal of Hydrology* 297 (1-4): 256-273.

Baker, MA, Valett, HM and Dahm, CN. 2000. Organic carbon supply and metabolism in a shallow groundwater ecosystem. *Ecology* 81 (11): 3133-3148.

Banerjee, D and Ganguly, S. 2023. A review on the research advances in groundwater–surface water interaction with an overview of the phenomenon. *Water* 15 (8): 1552.

Baskaran, S, Ransley, T, Brodie, R and Baker, P. 2009. Investigating groundwater–river interactions using environmental tracers. *Australian Journal of Earth Sciences* 56 (1): 13-19.

Batista, LV, Gastmans, D, Sánchez-Murillo, R, Farinha, BS, dos Santos, SMR and Kiang, CH. 2018. Groundwater and surface water connectivity within the recharge area of Guarani aquifer system during El Niño 2014–2016. *Hydrological Processes* 32 (16): 2483-2495.

Benetti, M, Reverdin, G, Pierre, C, Merlivat, L, Risi, C, Steen-Larsen, HC and Vimeux, F. 2014. Deuterium excess in marine water vapor: Dependency on relative humidity and surface wind speed during evaporation. *Journal of Geophysical Research: Atmospheres* 119 (2): 584-593.

Benjmel, K, Amraoui, F, Boutaleb, S, Ouchchen, M, Tahiri, A and Touab, A. 2020. Mapping of groundwater potential zones in crystalline terrain using remote sensing, GIS techniques, and multicriteria data analysis (Case of the Ighrem Region, Western Anti-Atlas, Morocco). *Water* 12 (2): 471.

Bertrand, G, Siergieiev, D, Ala-Aho, P and Rossi, P. 2014. Environmental tracers and indicators bringing together groundwater, surface water and groundwater-dependent ecosystems: importance of scale in choosing relevant tools. *Environmental earth sciences* 72 813-827.

Bhagwat, A, Ojha, CSP, Kumar, S and Kumar, B. 2024. Use of environmental isotopes in leachate studies through multiple isotopic analysis–a review. *Environmental Technology Reviews* 13 (1): 214-234.

Bhat, NA and Jeelani, G. 2018. Quantification of groundwater–surface water interactions using environmental isotopes: A case study of Bringi Watershed, Kashmir Himalayas, India. *Journal of Earth System Science* 127 (5): 63.

Booth, EG, Zipper, SC, Loheide II, SP and Kucharik, CJ. 2016. Is groundwater recharge always serving us well? Water supply provisioning, crop production, and flood attenuation in conflict in Wisconsin, USA. *Ecosystem Services* 21 153-165.

Braun, K, Bar-Matthews, M, Ayalon, A, Zilberman, T and Matthews, A. 2017. Rainfall isotopic variability at the intersection between winter and summer rainfall regimes in coastal South Africa (Mossel Bay, Western Cape Province). *South African Journal of Geology 2017* 120 (3): 323-340.

Breña-Naranjo, JA, Pedrozo-Acuña, A, Pozos-Estrada, O, Jiménez-López, SA and López-López, MR. 2015. The contribution of tropical cyclones to rainfall in Mexico. *Physics and Chemistry of the Earth, Parts A/B/C* 83 111-122.

Bresciani, E, Goderniaux, P and Batelaan, O. 2016. Hydrogeological controls of water table-land surface interactions. *Geophysical Research Letters* 43 (18): 9653-9661.

Calver, A, Kirkby, M and Weyman, D. 2019. Modelling hillslope and channel flows. *Spatial analysis in geomorphology* 197-218.

Caponera, F. 1989. Remote sensing image interpretation for ground-water surveying. *RSC Series (FAO)*.

Cartwright, I, Weaver, TR and Tweed, SO. 2008. Integrating physical hydrogeology, hydrochemistry, and environmental isotopes to constrain regional groundwater flow: Southern Riverine Province, Murray Basin, Australia. In: *Groundwater Flow Understanding*. CRC Press.

Chabalala, DT, Ndambuki, JM, Salim, RW and Rwanga, SS.2019. Impact of climate change on the rainfall pattern of Klip River catchment in Ladysmith, KwaZulu Natal, South Africa. *IOP Conference Series: Materials Science and Engineering*, 012088. IOP Publishing.

Chen, H, Zhang, X, Abla, M, Lü, D, Yan, R, Ren, Q, Ren, Z, Yang, Y, Zhao, W and Lin, P. 2018. Effects of vegetation and rainfall types on surface runoff and soil erosion on steep slopes on the Loess Plateau, China. *Catena* 170 141-149.

Chen, X, Zhang, Z, Chen, X and Shi, P. 2009. The impact of land use and land cover changes on soil moisture and hydraulic conductivity along the karst hillslopes of southwest China. *Environmental Earth Sciences* 59 811-820.

Chidambaram, S, Prasanna, MV, Ramanathan, A, Vasu, K, Hameed, S, Warrier, U, Srinivasamoorthy, K, Manivannan, R, Tirumalesh, K and Anandhan, P. 2009. A study on the factors affecting the stable isotopic composition in precipitation of Tamil Nadu, India. *Hydrological Processes: An International Journal* 23 (12): 1792-1800.

Chizhova, J, Kireeva, M, Rets, E, Ekaykin, A, Kozachek, A, Veres, A, Zolina, O, Varentsova, N, Gorbarenko, A and Povalyaev, N. 2022. Stable isotope (δ 18 O, δ 2 H) signature of river runoff, groundwater, and precipitation in three river basins in the center of East European Plain. *Earth System Science Data Discussions* 1-14.

Clark, ID and Fritz, P. 2013. *Environmental isotopes in hydrogeology*. CRC press.

Cluett, A, Thomas, E, Evans, S and Keys, P. 2021. Seasonal variations in moisture origin explain spatial contrast in precipitation isotope seasonality on coastal western Greenland. *Journal of Geophysical Research: Atmospheres* 126 (11): e2020JD033543.

Condon, LE and Maxwell, RM. 2015. Evaluating the relationship between topography and groundwater using outputs from a continental-scale integrated hydrology model. *Water Resources Research* 51 (8): 6602-6621.

Cook, P, Favreau, G, Dighton, J and Tickell, S. 2003. Determining natural groundwater influx to a tropical river using radon, chlorofluorocarbons and ionic environmental tracers. *Journal of Hydrology* 277 (1-2): 74-88.

Costa, D, Zhang, H and Levison, J. 2021. Impacts of climate change on groundwater in the Great Lakes Basin: A review. *Journal of Great Lakes Research* 47 (6): 1613-1625.

Cozma, AI, Baciu, C, Papp, D, Roşian, G and Pop, C-I. 2017. Isotopic composition of precipitation in western Transylvania (Romania) reflected by two local meteoric water lines. *Carpathian journal of earth and environmental sciences* 12 (2): 357-364.

Craig, H. 1961. Isotopic variations in meteoric waters. *Science* 133 (3465): 1702-1703.

Dansgaard, W. 1964. Stable isotopes in precipitation. *tellus* 16 (4): 436-468.

Dar, T, Rai, N, Kumar, S and Bhat, A. 2024. Spatiotemporal dynamics of stable isotopes of different water sources in Western Himalayas: Insights into regional hydrological processes. *Applied Geochemistry* 106038.

Deshpande, R, Maurya, AS, Kumar, B, Sarkar, A and Gupta, S. 2013. Kinetic fractionation of water isotopes during liquid condensation under super-saturated condition. *Geochimica et Cosmochimica Acta* 100 60-72.

Dray, M, Jusserand, C, Novel, J and Zuppi, G.1998. Air mass circulation and the isotopic "shadow effect" in precipitation in the French and Italian Alps. *Isotope techniques in the study of environmental change: Proceedings of an International Symposium of Past and Current Environmental Changes in the Hydrosphere and Lithosphere: Vienna, International Atomic Energy Agency*, 107-117.

Durowoju, OS, Butler, M, Ekosse, G-IE and Odiyo, JO. 2019a. Hydrochemical processes and isotopic study of geothermal springs within Soutpansberg, Limpopo Province, South Africa. *Applied Sciences* 9 (8): 1688.

Durowoju, OS, Ekosse, G-IE and Odiyo, JO. 2019b. Determination of isotopic composition of rainwater to generate local meteoric water line in Thohoyandou, Limpopo Province, South Africa. *Water SA* 45 (2): 183-189.

Durridge Company Inc. 2022. BIG BOTTLE SYSTEM [Internet]. DURRIDGE Company Inc. Available from: https://durridge.com/documentation/RAD7%20Manual.pdf. [Accessed: 12 November 2023].

Earman, S and Dettinger, M. 2011. Potential impacts of climate change on groundwater resources–a global review. *Journal of water and climate change* 2 (4): 213-229.

El Mountassir, O, Ouazar, D, Bahir, M, Chehbouni, A and Carreira, PM. 2021. GIS-based assessment of aquifer vulnerability using DRASTIC model and stable isotope: a case study on Essaouira basin. *Arabian Journal of Geosciences* 14 1-21.

Ellins, KK, Roman-Mas, A and Lee, R. 1990. Using 222Rn to examine groundwater/surface discharge interaction in the Rio Grande de Manati, Puerto Rico. *Journal of Hydrology* 115 (1-4): 319-341.

Fan, Y, Miguez-Macho, G, Weaver, CP, Walko, R and Robock, A. 2007. Incorporating water table dynamics in climate modeling: 1. Water table observations and equilibrium water table simulations. *Journal of Geophysical Research: Atmospheres* 112 (D10).

Ferronsky, V, Polyakov, V, Ferronsky, V and Polyakov, V. 2012. Isotopic Composition of Formation Waters. *Isotopes of the Earth's Hydrosphere* 129-153.

Freeze, RA. 1969. The mechanism of natural ground-water recharge and discharge: 1. One-dimensional, vertical, unsteady, unsaturated flow above a recharging or discharging ground-water flow system. *Water Resources Research* 5 (1): 153-171.

Garcia-Fresca, B and Sharp, JM. 2005. Hydrogeologic considerations of urban development: Urban-induced recharge.

Gat, JR. 1971. Comments on the stable isotope method in regional groundwater investigations. *Water resources research* 7 (4): 980-993.

Gat, JR. 1996. Oxygen and hydrogen isotopes in the hydrologic cycle. *Annual Review of Earth and Planetary Sciences* 24 (1): 225-262.

Geris, J, Comte, J-C, Franchi, F, Petros, AK, Tirivarombo, S, Selepeng, AT and Villholth, KG. 2022. Surface water-groundwater interactions and local land use control water quality impacts of extreme rainfall and flooding in a vulnerable semi-arid region of Sub-Saharan Africa. *Journal of Hydrology* 609 127834.

Gomi, T, Sidle, RC and Richardson, JS. 2002. Understanding processes and downstream linkages of headwater systems: headwaters differ from downstream reaches by their close coupling to hillslope processes, more temporal and spatial variation, and their need for different means of protection from land use. *BioScience* 52 (10): 905-916.

Gonfiantini, R, Fröhlich, K, Araguás-Araguás, L and Rozanski, K. 1998. Isotopes in groundwater hydrology. In: *Isotope tracers in catchment hydrology*. Elsevier.

Grab, SW. 2013. Fine-scale variations of near-surface-temperature lapse rates in the high Drakensberg Escarpment, South Africa: environmental implications. *Arctic, antarctic, and alpine research* 45 (4): 500-514.

Grant, GE.1988. Morphology of high gradient streams at different spatial scales, western Cascades, Oregon. *Workshop on "Channel geomorphological change and sediment control at Devastated River*, 13-14.

Gravelet-Blondin, KR. 2013. A geological and hydrogeological study of the Shu Shu thermal springs, KwaZulu-Natal. Unpublished thesis.

Green, TR. 2016. Linking climate change and groundwater. *Integrated groundwater management: Concepts, approaches and challenges* 97-141.

Grujic, D, Govin, G, Barrier, L, Bookhagen, B, Coutand, I, Cowan, B, Hren, MT and Najman, Y. 2018. Formation of a rain shadow: O and H stable isotope records in authigenic clays from the Siwalik Group in eastern Bhutan. *Geochemistry, Geophysics, Geosystems* 19 (9): 3430-3447.

Guggenmos, M, Jackson, B and Daughney, C. 2011. Investigation of groundwater-surface water interaction using hydrochemical sampling with high temporal resolution, Mangatarere catchment, New Zealand. *Hydrology and Earth System Sciences Discussions* 8 (6): 10225-10273.

Hall, F, Donahue, P and Eldridge, A.1985. Radon gas in ground water of New Hampshire. *The Second Annual Eastern Regional Ground Water Conference July 16-18, 1985, Portland, Maine. 1985. p 86-101, 6 fig, 1 tab, 19 ref.*

Han, D, Currell, MJ, Cao, G and Hall, B. 2017. Alterations to groundwater recharge due to anthropogenic landscape change. *Journal of Hydrology* 554 545-557.

Hardie, MA, Doyle, RB, Cotching, WE and Lisson, S. 2012. Subsurface lateral flow in texture-contrast (duplex) soils and catchments with shallow bedrock. *Applied and Environmental Soil Science* 2012 (1): 861358.

Harris, C. 2023. O-and H-isotope record of Cape Town rainfall from 1996 to 2022: the effect of increasing temperature, and the 'water crisis' of 2015 to 2018. *South African Journal of Geology* 126 (4): 515-528.

Harris, C, Burgers, C, Miller, J and Rawoot, F. 2010. O-and H-isotope record of Cape Town rainfall from 1996 to 2008, and its application to recharge studies of Table Mountain groundwater, South Africa. *South African Journal of Geology* 113 (1): 33-56.

Harris, C and Diamond, R. 2013. Oxygen and hydrogen isotopes record of cape town rainfall and its application to recharge studies of Table Mountain groundwater. *The Use of Isotope Hydrology to Characterize and Assess Water Resources in South (ern) Africa* 38-52.

Harrison, R, van Tol, J and Amiotte Suchet, P. 2022. Hydropedological Characteristics of the Cathedral Peak Research Catchments. *Hydrology* 9 (11): 189.

Hashemi, H, Uvo, CB and Berndtsson, R. 2015. Coupled modeling approach to assess climate change impacts on groundwater recharge and adaptation in arid areas. *Hydrology and Earth System Sciences* 19 (10): 4165-4181.

Healy, RW. 2010. *Estimating groundwater recharge*. Cambridge university press.

Hemond, HF and Fechner, EJ. 2022. *Chemical fate and transport in the environment*. academic press.

Hencher, S. 2010. Preferential flow paths through soil and rock and their association with landslides. *Hydrological processes* 24 (12): 1610-1630.

Herrera-Pantoja, M and Hiscock, K. 2008. The effects of climate change on potential groundwater recharge in Great Britain. *Hydrological Processes: An International Journal* 22 (1): 73-86.

Hokanson, K, Mendoza, C and Devito, K. 2019. Interactions between regional climate, surficial geology, and topography: characterizing shallow groundwater systems in subhumid, low-relief landscapes. *Water Resources Research* 55 (1): 284-297.

Hughes, A, Mansour, M, Ward, R, Kieboom, N, Allen, S, Seccombe, D, Charlton, M and Prudhomme, C. 2021. The impact of climate change on groundwater recharge: National-scale assessment for the British mainland. *Journal of Hydrology* 598 126336.

Hund, SV, Grossmann, I, Steyn, DG, Allen, DM and Johnson, MS. 2021. Changing water resources under El Niño, climate change, and growing water demands in seasonally dry tropical watersheds. *Water Resources Research* 57 (11): e2020WR028535.

Huntington, JL and Niswonger, RG. 2012. Role of surface-water and groundwater interactions on projected summertime streamflow in snow dominated regions: An integrated modeling approach. *Water Resources Research* 48 (11).

IAEA. 1996. *Isotope Field Applications for Groundwater Studies in the Middle East*. International Atomic Energy Agency (IAEA), Vienna, Austria.

Ichiyanagi, K, Numaguti, A and Kato, K. 2002. Interannual variation of stable isotopes in Antarctic precipitation in response to El Niño-Southern Oscillation. *Geophysical research letters* 29 (1): 1-1-1-4.

Ingraham, NL. 1998. Isotopic variations in precipitation. In: *Isotope tracers in catchment hydrology*. Elsevier.

Ingrid Dennis and Rainer Dennis. 2009. Reserve Determination Study in the Thukela Catchment: Groundwater Component.

Jasechko, S and Taylor, RG. 2015. Intensive rainfall recharges tropical groundwaters. *Environmental Research Letters* 10 (12): 124015.

Jiao, Y, Liu, C, Liu, Z, Ding, Y and Xu, Q. 2020. Impacts of moisture sources on the temporal and spatial heterogeneity of monsoon precipitation isotopic altitude effects. *Journal of hydrology* 583 124576.

Jing, Z, Yu, W, Lewis, S, Thompson, LG, Xu, J, Zhang, J, Xu, B, Wu, G, Ma, Y and Wang, Y. 2022. Inverse altitude effect disputes the theoretical foundation of stable isotope paleoaltimetry. *Nature Communications* 13 (1): 4371.

Joseph, A, Frangi, JP and Aranyossy, JF. 1992. Isotope characteristics of meteoric water and groundwater in the Sahelo-Sudanese zone. *Journal of Geophysical Research: Atmospheres* 97 (D7): 7543-7551.

Jouzel, J, Hoffmann, G, Koster, R and Masson, V. 2000. Water isotopes in precipitation:: data/model comparison for present-day and past climates. *Quaternary Science Reviews* 19 (1-5): 363-379.

Kalbus, E, Reinstorf, F and Schirmer, M. 2006. Measuring methods for groundwater–surface water interactions: a review. *Hydrology and Earth System Sciences* 10 (6): 873-887.

Kasenow, M. 2001. *Applied ground-water hydrology and well hydraulics*. Water Resources Publication.

Kebede, S, Abdalla, O, Sefelnasr, A, Tindimugaya, C and Mustafa, O. 2017. Interaction of surface water and groundwater in the Nile River basin: isotopic and piezometric evidence. *Hydrogeology Journal* 25 (3): 707.

Kebede, S, Charles, K, Godfrey, S, MacDonald, A and Taylor, RG. 2021. Regional-scale interactions between groundwater and surface water under changing aridity: evidence from the River Awash Basin, Ethiopia. *Hydrological Sciences Journal* 66 (3): 450-463.

Kebede, S and Travi, Y. 2012. Origin of the δ18O and δ2H composition of meteoric waters in Ethiopia. *Quaternary International* 257 4-12.

Kebede, S, Travi, Y, Alemayehu, T and Ayenew, T. 2005. Groundwater recharge, circulation and geochemical evolution in the source region of the Blue Nile River, Ethiopia. *Applied Geochemistry* 20 (9): 1658-1676.

Kendall, C and McDonnell, JJ. 2012. *Isotope tracers in catchment hydrology*. Elsevier.

Kern, Z, Hatvani, IG, Czuppon, G, Fórizs, I, Erdélyi, D, Kanduč, T, Palcsu, L and Vreča, P. 2020. Isotopic 'altitude'and 'continental'effects in modern precipitation across the Adriatic–Pannonian Region. *Water* 12 (6): 1797.

Kern, Z, Kohán, B and Leuenberger, M. 2014. Precipitation isoscape of high reliefs: interpolation scheme designed and tested for monthly resolved precipitation oxygen isotope records of an Alpine domain. *Atmospheric chemistry and physics* 14 (4): 1897-1907.

Khan, HH and Khan, A. 2019. Groundwater-surface water interaction along river Kali, near Aligarh, India. *HydroResearch* 2 119-128.

Kim, K and Lee, X. 2011. Isotopic enrichment of liquid water during evaporation from water surfaces. *Journal of hydrology* 399 (3-4): 364-375.

Kirchner, JW and Allen, ST. 2019. Seasonal partitioning of precipitation between streamflow and evapotranspiration, inferred from end-member splitting analysis.

Kirkby, M. 2019. Infiltration, throughflow, and overland flow. In: *Introduction to Fluvial Processes*. Routledge.

Kolusu, SR, Shamsudduha, M, Todd, MC, Taylor, RG, Seddon, D, Kashaigili, JJ, Ebrahim, GY, Cuthbert, MO, Sorensen, JP and Villholth, KG. 2019. The El Niño event of 2015–2016: climate anomalies and their impact on groundwater resources in East and Southern Africa. *Hydrology and Earth System Sciences* 23 (3): 1751-1762.

Kong, Y and Pang, Z. 2016. A positive altitude gradient of isotopes in the precipitation over the Tianshan Mountains: Effects of moisture recycling and sub-cloud evaporation. *Journal of Hydrology* 542 222-230.

Kresic, N. 2006. *Hydrogeology and groundwater modeling*. CRC press.

Kuenene, B, Van Huyssteen, C and Le Roux, P. 2013. Selected soil properties as indicators of soil water regime in the Cathedral Peak VI catchment of KwaZulu-Natal, South Africa. *South African Journal of Plant and Soil* 30 (1): 1-6.

Le Maitre, DC and Colvin, CA. 2008. Assessment of the contribution of groundwater discharges to rivers using monthly flow statistics and flow seasonality. *Water SA* 34 (5): 549-564.

Leibowitz, SG, Mushet, DM and Newton, WE. 2016. Intermittent surface water connectivity: fill and spill vs. fill and merge dynamics. *Wetlands* 36 (Suppl 2): 323-342.

Leketa, K and Abiye, T. 2020. Investigating stable isotope effects and moisture trajectories for rainfall events in Johannesburg, South Africa. *Water Sa* 46 (3): 429-437.

Leketa, K, Abiye, T, Zondi, S and Butler, M. 2019. Assessing groundwater recharge in crystalline and karstic aquifers of the Upper Crocodile River Basin, Johannesburg, South Africa. *Groundwater for Sustainable Development* 8 31-40.

Lessels, JS, Tetzlaff, D, Birkel, C, Dick, J and Soulsby, C. 2016. Water sources and mixing in riparian wetlands revealed by tracers and geospatial analysis. *Water Resources Research* 52 (1): 456-470.

Levy, J and Xu, Y. 2011. Groundwater management and groundwater/surface-water interaction in the context of South African water policy.

Li, B, Yang, L, Song, X and Diamantopoulos, E. 2023. Identifying surface water and groundwater interactions using multiple experimental methods in the riparian zone of the polluted and disturbed Shaying River, China. *Science of The Total Environment* 875 162616.

Li, X, Chang, SX and Salifu, KF. 2014. Soil texture and layering effects on water and salt dynamics in the presence of a water table: a review. *Environmental reviews* 22 (1): 41-50.

Liu, Y and Yamanaka, T. 2012. Tracing groundwater recharge sources in a mountain–plain transitional area using stable isotopes and hydrochemistry. *Journal of Hydrology* 464 116-126.

Lorentz, S, Bursey, K, Idowu, O, Pretorius, C and Ngeleka, K. 2007. Definition and upscaling of key hydrological processes for application in models. *Water Research Commission, Pretoria. WRC Report* (1320/1): 07.

Mahlangu, S, Lorentz, S, Diamond, R and Dippenaar, M. 2020. Surface water-groundwater interaction using tritium and stable water isotopes: A case study of Middelburg, South Africa. *Journal of African Earth Sciences* 171 103886.

Margat, J and Van der Gun, J. 2013. *Groundwater around the world: a geographic synopsis*. Crc Press.

Markovich, KH, Manning, AH, Condon, LE and McIntosh, JC. 2019. Mountain-block recharge: A review of current understanding. *Water Resources Research* 55 (11): 8278-8304.

Martinez, JL, Raiber, M and Cox, ME. 2015. Assessment of groundwater–surface water interaction using long-term hydrochemical data and isotope hydrology: Headwaters of the Condamine River, Southeast Queensland, Australia. *Science of the Total Environment* 536 499-516.

Masevhe, L, MAVUNDA, R and Connell, S. 2017. A general survey of radon concentration in water from rivers in Gauteng, South Africa using a solid-state α-detector. *J. Environ. Anal. Toxicol* 7 (04): 2161-0525.1000472.

Mathew, BP and Samant, HP. 2012. Influence of dykes on regional hydraulic gradient-A Case study around Nandurbar, Nandurbar District, Maharashtra, India. *The Xavier's Research Journal* 3 (1).

Mathinya, NV, Clark, VR, van Tol, JJ and Franke, AC. 2022. Resilience and sustainability of the Maloti-Drakensberg Mountain System: A case study on the Upper uThukela catchment. In: *Human-Nature Interactions: Exploring Nature's Values Across Landscapes*. Springer International Publishing Cham.

McDonnell, J, Rowe, L and Stewart, M. 1999. A combined tracer-hydrometric approach to assess the effect of catchment scale on water flow path, source and age. *IAHS-AISH publication* 265-273.

McDonnell, JJ, Spence, C, Karran, DJ, Van Meerveld, H and Harman, CJ. 2021. Fill-and-spill: A process description of runoff generation at the scale of the beholder. *Water Resources Research* 57 (5): e2020WR027514.

McIntosh, JC and Ferguson, G. 2021. Deep meteoric water circulation in Earth's crust. *Geophysical Research Letters* 48 (5): e2020GL090461.

Mensah, JK, Ofosu, EA, Yidana, SM, Akpoti, K and Kabo-bah, AT. 2022. Integrated modeling of hydrological processes and groundwater recharge based on land use land cover, and climate changes: A systematic review. *Environmental Advances* 8 100224.

Mihret, B and Wuletaw, A. 2025. The Impact of Geological Structures on Groundwater Potential Assessment in Volcanic Rocks of the Northwestern Ethiopian Plateau: A Review. *EGUsphere* 2025 1-14.

Mileham, L, Taylor, RG, Todd, M, Tindimugaya, C and Thompson, J. 2009. The impact of climate change on groundwater recharge and runoff in a humid, equatorial catchment: sensitivity of projections to rainfall intensity. *Hydrological Sciences Journal* 54 (4): 727-738.

Mir, AA and Patel, M. 2024. A Comprehensive Review on Sediment Transport, Flow Dynamics, and Hazards in Steep Channels. *Journal of Water Management Modeling*.

Mitra, S, Srivastava, P, Singh, S and Yates, D. 2014. Effect of ENSO-induced climate variability on groundwater levels in the lower Apalachicola-Chattahoochee-Flint River Basin. *Transactions of the ASABE* 57 (5): 1393-1403.

Moodley, K, Toucher, ML and Lottering, RT. 2023. Simulating future land-use within the uThukela and uMngeni catchments in KwaZulu-Natal. *Scientific African* 20 e01666.

Moseki, MC. 2013. Surface water-Groundwater interactions: Development of methodologies suitable for South African conditions. Unpublished thesis, University of the Free State.

Muhammad, S and Sadiq, U. 2014. Analysis of stable isotopic composition of precipitation in Katsina state in Nigeria as an indication of water cycle. *Adv. Phys. Theor. Appl* 33 28-34.

Naganna, SR, Deka, PC, Ch, S and Hansen, WF. 2017. Factors influencing streambed hydraulic conductivity and their implications on stream–aquifer interaction: a conceptual review. *Environmental Science and Pollution Research* 24 24765-24789.

Ndlovu, M and Demlie, M. 2018. Statistical analysis of groundwater level variability across KwaZulu-Natal Province, South Africa. *Environmental Earth Sciences* 77 (21): 739.

Ngubo, CZ. 2019. An investigation of the impacts of Acacia Mearnsii plantations on secondary aquifer systems within the Two Streams catchment, KwaZulu-Natal, South Africa. Unpublished thesis.

Niewodnizański, J, Grabczak, J, Barański, L and Rzepka, J. 1981. The altitude effect on the isotopic composition of snow in high mountains. *Journal of Glaciology* 27 (95): 99-111.

Nilsen, K, Sydnes, M, Gudmundsson, A and Larsen, B.2003. How dykes affect groundwater transport in the northern part of the Oslo Graben. *EGS-AGU-EUG Joint Assembly*, 9684.

Nimmo, JR. 2016. Quantitative framework for preferential flow initiation and partitioning. *Vadose Zone Journal* 15 (2): 1-12.

Ntanganedzeni, B, Elumalai, V and Rajmohan, N. 2018. Coastal aquifer contamination and geochemical processes evaluation in Tugela catchment, South Africa—Geochemical and statistical approaches. *Water* 10 (6): 687.

Olivarius, M, Weibel, R, Hjuler, ML, Kristensen, L, Mathiesen, A, Nielsen, LH and Kjøller, C. 2015. Diagenetic effects on porosity–permeability relationships in red beds of the Lower Triassic Bunter Sandstone Formation in the North German Basin. *Sedimentary Geology* 321 139-153.

Otte, I, Detsch, F, Gütlein, A, Scholl, M, Kiese, R, Appelhans, T and Nauss, T. 2017. Seasonality of stable isotope composition of atmospheric water input at the southern slopes of Mt. Kilimanjaro, Tanzania. *Hydrological Processes* 31 (22): 3932-3947.

Ouyang, Y, Grace, JM, Parajuli, PB and Caldwell, PV. 2022. Impacts of multiple hurricanes and tropical storms on watershed hydrological processes in the Florida panhandle. *Climate* 10 (3): 42.

Owuor, SO, Butterbach-Bahl, K, Guzha, AC, Rufino, MC, Pelster, DE, Díaz-Pinés, E and Breuer, L. 2016. Groundwater recharge rates and surface runoff response to land use and land cover changes in semi-arid environments. *Ecological Processes* 5 1-21.

Paces, JB and Wurster, FC. 2014. Natural uranium and strontium isotope tracers of water sources and surface water–groundwater interactions in arid wetlands–Pahranagat Valley, Nevada, USA. *Journal of hydrology* 517 213-225.

Parsons, R. 2004. *Surface Water: Groundwater Interaction in a Southern African Context*. Water Research Commission Pretoria, South Africa.

Partington, D, Brunner, P, Simmons, C, Werner, A, Therrien, R, Maier, H and Dandy, G. 2012. Evaluation of outputs from automated baseflow separation methods against simulated baseflow from a physically based, surface water-groundwater flow model. *Journal of Hydrology* 458 28-39.

Peel, M, Kipfer, R, Hunkeler, D and Brunner, P. 2022. Variable 222Rn emanation rates in an alluvial aquifer: Limits on using 222Rn as a tracer of surface water–Groundwater interactions. *Chemical Geology* 599 120829.

PLAN, BS. 2015. UThukela District Municipality: Biodiversity Sector Plan.

Poage, MA and Chamberlain, CP. 2001. Empirical relationships between elevation and the stable isotope composition of precipitation and surface waters: considerations for studies of paleoelevation change. *American Journal of Science* 301 (1): 1-15.

Prabu, P and Rajagopalan, B. 2013. Mapping of lineaments for groundwater targeting and sustainable water resource management in hard rock hydrogeological environment using RS-GIS. *Climate change and regional/local responses* 235-247.

Putman, AL, Fiorella, RP, Bowen, GJ and Cai, Z. 2019. A global perspective on local meteoric water lines: Meta-analytic insight into fundamental controls and practical constraints. *Water Resources Research* 55 (8): 6896-6910.

Qin, W, Han, D, Song, X and Liu, S. 2021. Environmental isotopes (δ18O, δ2H, 222Rn) and hydrochemical evidence for understanding rainfall-surface water-groundwater transformations in a polluted karst area. *Journal of Hydrology* 592 125748.

Rahman, A. 2008. A GIS based DRASTIC model for assessing groundwater vulnerability in shallow aquifer in Aligarh, India. *Applied geography* 28 (1): 32-53.

Rempe, DM and Dietrich, WE. 2014. A bottom-up control on fresh-bedrock topography under landscapes. *Proceedings of the National Academy of Sciences* 111 (18): 6576-6581.

Rishma, C and Katpatal, YB. 2019. ENSO modulated groundwater variations in a river basin of Central India. *Hydrology Research* 50 (2): 793-806.

Rodgers, P, Soulsby, C, Waldron, S and Tetzlaff, D. 2005. Using stable isotope tracers to assess hydrological flow paths, residence times and landscape influences in a nested mesoscale catchment. *Hydrology and Earth System Sciences* 9 (3): 139-155.

Roets, W, Xu, Y, Raitt, L, El-Kahloun, M, Meire, P, Calitz, F, Batelaan, O, Anibas, C, Paridaens, K and Vandenbroucke, T. 2008. Determining discharges from the Table Mountain Group (TMG) aquifer to wetlands in the Southern Cape, South Africa. *Hydrobiologia* 607 175-186.

Rumsey, CA, Miller, MP, Susong, DD, Tillman, FD and Anning, DW. 2015. Regional scale estimates of baseflow and factors influencing baseflow in the Upper Colorado River Basin. *Journal of Hydrology: Regional Studies* 4 91-107.

Salati, E, Dall'Olio, A, Matsui, E and Gat, JR. 1979. Recycling of water in the Amazon basin: an isotopic study. *Water resources research* 15 (5): 1250-1258.

Salem, A, Abduljaleel, Y, Dezső, J and Lóczy, D. 2023. Integrated assessment of the impact of land use changes on groundwater recharge and groundwater level in the Drava floodplain, Hungary. *Scientific Reports* 13 (1): 5061.

Samie, SGAE. 2020. Enhancing the Use of Isotope Hydrology in Planning, Management, and Development of Water Resources.

Scanlon, BR, Jolly, I, Sophocleous, M and Zhang, L. 2007. Global impacts of conversions from natural to agricultural ecosystems on water resources: Quantity versus quality. *Water resources research* 43 (3).

Scheliga, B, Tetzlaff, D, Nuetzmann, G and Soulsby, C. 2019. Assessing runoff generation in riparian wetlands: monitoring groundwater–surface water dynamics at the micro-catchment scale. *Environmental monitoring and assessment* 191 (2): 116.

Schneeberger, R, Egli, D, Lanyon, GW, Mäder, UK, Berger, A, Kober, F and Herwegh, M. 2018. Structural-permeability favorability in crystalline rocks and implications for groundwater flow paths: a case study from the Aar Massif (central Switzerland). *Hydrogeology Journal* 26 (8): 2725-2738.

Schubert, M, Schmidt, A, Paschke, A, Lopez, A and Balcazar, M. 2008. In situ determination of radon in surface water bodies by means of a hydrophobic membrane tubing. *Radiation Measurements* 43 (1): 111-120.

Schwartz, FW and Zhang, H. 2024. *Fundamentals of groundwater*. John Wiley & Sons.

Seiler, K-P and Gat, JR. 2007. *Groundwater recharge from run-off, infiltration and percolation*. Springer Science & Business Media.

Shanafield, M and Cook, PG. 2014. Transmission losses, infiltration and groundwater recharge through ephemeral and intermittent streambeds: A review of applied methods. *Journal of Hydrology* 511 518-529.

Siddik, MS, Tulip, SS, Rahman, A, Islam, MN, Haghighi, AT and Mustafa, SMT. 2022. The impact of land use and land cover change on groundwater recharge in northwestern Bangladesh. *Journal of Environmental Management* 315 115130.

Simmers, I. 2003. *Understanding water in a dry environment: IAH International Contributions to Hydrogeology 23*. CRC Press.

Singh, KP. 1968. Some factors affecting baseflow. *Water Resources Research* 4 (5): 985-999.

Singh, R and Jamal, A. 2002. Dykes as groundwater loci in parts of Nashik District, Maharashtra. *Geological Society of India* 59 (2): 143-146.

Singh, TD, Prakash, S and Manohar, S. 2023. Assessment of the performance and compatibility of acrylic polymer and silane based consolidants on deteriorated heritage masonry units subjected to salt weathering. *Journal of Building Engineering* 77 107490.

Skeppström, K and Olofsson, B. 2007. Uranium and radon in groundwater. *European water* 17 (18): 51-62.

Somers, LD and McKenzie, JM. 2020. A review of groundwater in high mountain environments. *Wiley Interdisciplinary Reviews: Water* 7 (6): e1475.

Sophocleous, M. 2002. Interactions between groundwater and surface water: the state of the science. *Hydrogeology journal* 10 52-67.

Stevanović, Z. 2015. Characterization of karst aquifer. *Karst aquifers—characterization and engineering* 47-125.

Strydom, T, Nel, J, Nel, M, Petersen, R and Ramjukadh, C. 2021. The use of Radon (Rn222) isotopes to detect groundwater discharge in streams draining Table Mountain Group (TMG) aquifers. *Water SA* 47 (2): 194-199.

Stueck, H, Koch, R and Siegesmund, S. 2013. Petrographical and petrophysical properties of sandstones: statistical analysis as an approach to predict material behaviour and construction suitability. *Environmental earth sciences* 69 1299-1332.

Sun, C, Tian, L, Shanahan, TM, Partin, JW, Gao, Y, Piatrunia, N and Banner, J. 2022. Isotopic variability in tropical cyclone precipitation is controlled by Rayleigh distillation and cloud microphysics. *Communications Earth & Environment* 3 (1): 50.

Tadesse, E, Azagegn, T and Alemayehu, T. 2023. Characterizing groundwater and surface water interaction using geological, environmental tracers (222Rn, EC, δ18O, and δ2H) and baseflow index methods for part of the Upper Awash and the adjacent Blue Nile Basin, Ethiopia. *Journal of African Earth Sciences* 104992.

Tang, M, Yu, S, You, S and Jiang, P. 2024. The Characteristics and Application of Deuterium and Oxygen Isotopes to Karst Groundwater, Southwest China. *Water* 16 (13): 1812.

Taupin, JD, Coudrain-Ribstein, A, Gallaire, R, Zuppi, GM and Filly, A. 2000. Rainfall characteristics (δ18O, δ2 H, ΔT and ΔH r) in western Africa: Regional scale and influence of irrigated areas. *Journal of Geophysical Research: Atmospheres* 105 (D9): 11911-11924.

Terzer-Wassmuth, S, Araguás-Araguás, LJ, Wassenaar, LI and Stumpp, C. 2023. Global and local meteoric water lines for δ 17O/δ 18O and the spatiotemporal distribution of Δ′ 17O in Earth's precipitation. *Scientific Reports* 13 (1): 19056.

Tetzlaff, D, Birkel, C, Dick, J, Geris, J and Soulsby, C. 2014. Storage dynamics in hydropedological units control hillslope connectivity, runoff generation, and the evolution of catchment transit time distributions. *Water resources research* 50 (2): 969-985.

Theron, C, Lorentz, S and Xu, Y. 2022. Rainfall-induced groundwater ridging and the Lisse effect on tailings storage facilities: A literature review. *Journal of the Southern African Institute of Mining and Metallurgy* 122 (2): 37-44.

Toucher, M, Lawrence, K, van Rensburg, SJ and Gordijn, P. 2020. A unique data set from southern Africa's mesic high-altitude fire climax grasslands: The Cathedral Peak experimental catchments from 1948 onwards. *Authorea Preprints*.

Travaglia, C. 1984. Groundwater assessment in hard rocks, case histories: Upper Volta and the People's Democratic Republic of Yemen.

Treble, P, Budd, W, Hope, P and Rustomji, P. 2005. Synoptic-scale climate patterns associated with rainfall δ18O in southern Australia. *Journal of Hydrology* 302 (1-4): 270-282.

Trenberth, KE. 1999. Conceptual framework for changes of extremes of the hydrological cycle with climate change. *Climatic change* 42 (1): 327-339.

Trenberth, KE. 2011. Attribution of climate variations and trends to human influences and natural variability. *Wiley Interdisciplinary Reviews: Climate Change* 2 (6): 925-930.

Trinh, DA, Luu, MTN and Le, QTP. 2017. Use of stable isotopes to understand run-off generation processes in the R ed R iver D elta. *Hydrological Processes* 31 (22): 3827-3843.

Tromp-van Meerveld, H and McDonnell, J. 2006. Threshold relations in subsurface stormflow: 2. The fill and spill hypothesis. *Water resources research* 42 (2).

Tsai, YJ, Chen, YJ, Weng, CH, Syu, FT, Hsu, K-A and Lee, WL. 2022. Application of Stream Conductivity to Activity of Potential Large-Scale Landslide. *Frontiers in Earth Science* 10 759556.

Tyler, S, Chapman, J, Conrad, S, Hammermeister, D, Blout, D, Miller, J, Sully, M and Ginanni, J. 1996. Soil-water flux in the southern Great Basin, United States: Temporal and spatial variations over the last 120,000 years. *Water Resources Research* 32 (6): 1481-1499.

UMgeni-UThukela Water. 2021. ENVIRONMENTAL SUSTAINABILITY, INCLUDING WATER RESOURCES ADEQUACY. [Internet]. Available from: https://www.umgeni.co.za/environment/. [Accessed: 11 November 2023].

Unland, N, Cartwright, I, Andersen, MS, Rau, GC, Reed, J, Gilfedder, BS, Atkinson, AP and Hofmann, H. 2013. Investigating the spatio-temporal variability in groundwater and surface water interactions: a multi-technique approach. *Hydrology and Earth System Sciences* 17 (9): 3437-3453.

van Beek, R, Cammeraat, E, Andreu, V, Mickovski, SB and Dorren, L. 2008. Hillslope processes: Mass wasting, slope stability and erosion. *Slope stability and erosion control: Ecotechnological solutions* 17-64.

Vogel, J, JC, L and WG, M. 1975. Natural isotopes in surface and groundwater from Argentina.

VonVeh, M and Andersen, N. 1990. Normal-slip faulting in the coastal areas of northern Natal and Zululand, South Africa. *South African journal of geology* 93 (4): 574.

Wade, M, O'Brien, GC, Wepener, V and Jewitt, G. 2021. Risk assessment of water quantity and quality stressors to balance the use and protection of vulnerable water resources. *Integrated Environmental Assessment and Management* 17 (1): 110-130.

Wakode, HB, Baier, K, Jha, R and Azzam, R. 2018. Impact of urbanization on groundwater recharge and urban water balance for the city of Hyderabad, India. *International Soil and Water Conservation Research* 6 (1): 51-62.

Wang, C, Wang, B, Wang, Y, Wang, Y, Zhang, W and Yan, Y. 2020. Impact of near-surface hydraulic gradient on the interrill erosion process. *European Journal of Soil Science* 71 (4): 598-614.

Wang, C, Zhao, C, Xu, Z, Wang, Y and Peng, H. 2013a. Effect of vegetation on soil water retention and storage in a semi-arid alpine forest catchment. *Journal of arid land* 5 207-219.

Wang, P, Yu, J, Zhang, Y and Liu, C. 2013b. Groundwater recharge and hydrogeochemical evolution in the Ejina Basin, northwest China. *Journal of Hydrology* 476 72-86.

Wanke, H, Gaj, M, Beyer, M, Koeniger, P and Hamutoko, JT. 2018. Stable isotope signatures of meteoric water in the Cuvelai-Etosha Basin, Namibia: Seasonal characteristics, trends and relations to southern African patterns. *Isotopes in environmental and health studies* 54 (6): 588-607.

Warku, F, Korme, T, Wedajo, GK and Nedow, D. 2022. Impacts of land use/cover change and climate variability on groundwater recharge for upper Gibe watershed, Ethiopia. *Sustainable Water Resources Management* 8 1-16.

Weitz, J and Demlie, M. 2014. Conceptual modelling of groundwater–surface water interactions in the Lake Sibayi Catchment, Eastern South Africa. *Journal of African Earth Sciences* 99 613-624.

Welgus, MN and Abiye, TA. 2022. Surface water and groundwater interaction in the Vredefort Dome, South Africa: a stable isotope and multivariate statistical approach. *Environmental Monitoring and Assessment* 194 (10): 672.

Whipple, KX. 2004. Bedrock rivers and the geomorphology of active orogens. *Annu. Rev. Earth Planet. Sci.* 32 (1): 151-185.

Winter, TC. 1999. Relation of streams, lakes, and wetlands to groundwater flow systems. *Hydrogeology Journal* 7 28-45.

Winter, TC. 2000. *Ground water and surface water: a single resource*. Diane Publishing.

Winter, TC. 2007. The role of ground water in generating streamflow in headwater areas and in maintaining base flow 1. *JAWRA Journal of the American Water Resources Association* 43 (1): 15-25.

Wirmvem, MJ, Ohba, T, Fantong, WY, Ayonghe, SN, Suila, JY, Asaah, ANE, Asai, K, Tanyileke, G and Hell, JV. 2014. Monthly δ18O, δD and Cl− characteristics of precipitation in the Ndop plain, Northwest Cameroon: Baseline data. *Quaternary International* 338 35-41.

Wirmvem, MJ, Ohba, T, Kamtchueng, BT, Taylor, ET, Fantong, WY and Ako, AA. 2017. Variation in stable isotope ratios of monthly rainfall in the Douala and Yaounde cities, Cameroon: local meteoric lines and relationship to regional precipitation cycle. *Applied Water Science* 7 2343-2356.

Wirth, SB, Carlier, C, Cochand, F, Hunkeler, D and Brunner, P. 2020. Lithological and tectonic control on groundwater contribution to stream discharge during low-flow conditions. *Water* 12 (3): 821.

Woodford, A and Chevallier, L. 2002. Hydrogeology of the Main Karoo Basin: Current knowledge and future research needs. *Water Research Commission Report No. TT* 179 (02): 482.

Wu, N, Ding, X, Wen, Z, Chen, G, Meng, Z, Lin, L and Min, J. 2020. Contrasting frontal and warm-sector heavy rainfalls over South China during the early-summer rainy season. *Atmospheric Research* 235 104693.

Wu, Y, Wen, X and Zhang, Y. 2004. Analysis of the exchange of groundwater and river water by using Radon-222 in the middle Heihe Basin of northwestern China. *Environmental geology* 45 647-653.

Xiao, X, Zhang, X, Xiao, Z, Rao, Z, He, X and Zhang, C. 2023. Seasonal variation and influence factors of river water isotopes in the East Asian monsoon region: a case study in the Xiangjiang River basin spanning 13 hydrological years. *Hydrology and Earth System Sciences* 27 (20): 3783-3802.

Xie, R, Zhen, L, Wu, X and Li, J. 2023. Isotopic compositions (δD, δ18O) and end-member mixing for the control interface in a complex tidal region. *Science of The Total Environment* 866 161438.

Yadav, SK. 2023. Land Cover Change and Its Impact on Groundwater Resources: Findings and Recommendations.

Yang, X, Hu, J, Ma, R and Sun, Z. 2021. Integrated hydrologic modelling of groundwater-surface water interactions in cold regions. *Frontiers in Earth Science* 9 721009.

You, Y, Qu, S, Wang, Y, Yang, Q, Shi, P, Jiang, Y and Yang, X. 2021. Applicability of Difference in Oxygen-18 and Deuterium of Water Sources and Isotopic Hydrograph Separation in a Bamboo Catchment during Different Rainfall Types. *Water* 13 (24): 3531.

Zang, YG, Sun, DM, Feng, P and Semprich, S. 2018. Numerical analysis of groundwater ridging processes considering water-air flow in a Hillslope. *Groundwater* 56 (4): 594-609.

Zega, B, He, S and Lubis, A. 2020. Characteristics of Stable Isotope Compositions (δ 18 O and δ 2 H) of Surface Water in Bengkulu City. *Atom Indonesia* 46 (2): 85-90.

Zeng, Y, Xie, Z, Liu, S, Xie, J, Jia, B, Qin, P and Gao, J. 2018. Global land surface modeling including lateral groundwater flow. *Journal of Advances in Modeling Earth Systems* 10 (8): 1882-1900.

Zhang, F, Huang, T, Man, W, Hu, H, Long, Y, Li, Z and Pang, Z. 2021. Contribution of recycled moisture to precipitation: A modified D-excess-based model. *Geophysical Research Letters* 48 (21): e2021GL095909.

Zhu, Y, Zhai, Y, Teng, Y, Wang, G, Du, Q, Wang, J and Yang, G. 2020. Water supply safety of riverbank filtration wells under the impact of surface water-groundwater interaction: Evidence from long-term field pumping tests. *Science of the Total Environment* 711 135141.